

INVESTIGATION OF THE KINETIC MECHANISM OF GLUTAMINE- AND
AMMONIA-DEPENDENT REACTIONS OF *E. coli* ASPARAGINE SYNTHETASE
B USING ISOTOPE PARTITIONING AND STEADY-STATE KINETICS

By

POURAN HABIBZADEGAH-TARI

A DISSERTATION PRESENTED TO THE GRADUATE SCHOOL
OF THE UNIVERSITY OF FLORIDA IN PARTIAL FULFILLMENT
OF THE REQUIREMENTS FOR THE DEGREE OF
DOCTOR OF PHILOSOPHY

UNIVERSITY OF FLORIDA

1996

ACKNOWLEDGMENTS

I would like to thank the members of my committee, Dr cain, Dr Cohen, Dr Dunn, and Dr Richards for their guidance and suggestions. I would like to thank my advisor Dr Schuster for giving me the chance to do reseacrch in his laboratory. Although he was always busy with a lot of other things, the very limited time I had with him was filled with new ideas to solve problems. I would very much like to thank Dr Alison helping me with my research, and for being there for me always.

I would like to thank all the friends I met in and out of Dr Schuster's laboratory for their support and encouragement.

I thank my husband, Esfandiar, for being my friend for the past eighteen years, specially during this period of my life. I am grateful for his ongoing support and for lifting my spirit when it was down.

I am specially grateful to my mom for coming to this country and taking care of my daughter while I was busy with school. I know how hard it was for her to stay in this country for ten months and not be able to communicate with anyone. I want thank her with all my heart and say how sorry I am for not being able to spend enough time with her.

Finally, I want thank my daughter, Maryam, for being who she is, my love. I hope I can make it up to her after I finish school.

TABLE OF CONTENTS

	<u>page</u>
AKNOWLEDGEMENTS	ii
LIST OF TABLES	vi
LIST OF FIGURES	vii
ABSTRACT	xii
CHAPTERS	
1 INTRODUCTION.....	1
2 INVESTIGATION OF THE MECHANISM OF E. COLI ASPARAGINE SYNTHETASE USING ISOTOPE PARTITIONING.....	26
Introduction	26
Materials and Methods	29
Chemicals and Reagents	29
Expression of the Protein and Purification	30
Protein Concentration Determination	31
Isotope Partitioning Experiments with Radioactive L-Aspartate, Glutamine- and Ammonia-Dependent Reactions	31
Determination of K _d for L-Aspartate	34
Isotope Partitioning Experiments with Radioactive ATP, Glutamine- and Ammonia- Dependent Reactions	34
Aspartate-Dependent ATP Hydrolysis	36
Theory	37
Results	39
Isotope Partitioning Experiments with Radioactive L-Aspartate, Glutamine- and Ammonia-Dependent Reactions	39
Isotope Partitioning Experiments with Radioactive ATP, Glutamine- and Ammonia- Dependent Reactions	40
Aspartate-Dependent ATP Hydrolysis	41
Discussion	47
3 SUBSTRATE BINDING AND PRODUCT RELEASE OF ASPARAGINE SYNTHETASE B STUDIED BY STEADY STATE KINETICS.....	55
Introduction	55

Materials and Methods	56
Chemicals and Reagents	56
Expression of the Protein and Purification	57
Protein Concentration Determination	57
Enzyme Assays	57
Stoichiometry of PP _i and L-Glutamate	59
Results	60
Initial Rate Studies	60
Inhibition by Substrate Analogs	65
Stoichiometry of Glutamine-Dependent Reaction	67
Product Inhibition Studies	68
Discussion	74
4 EFFECT OF TEMPERATURE ON THE ASPARAGINE SYNTHETASE B....	146
Introduction	146
Materials and Methods	146
Chemicals and Reagents	146
Expression of the Protein and Purification	147
Protein Concentration Determination	147
Enzyme Assays	147
Thermodynamic of Activation	148
Results and Discussion	149
5 SUMMARY AND CONCLUSIONS	157
LIST OF REFERENCES	166
BIOGRAPHICAL SKETCH	172

LIST OF TABLES

<u>Table</u>	<u>page</u>
2.1 Trapping of L-aspartate from Complexes in the Steady State, Using (¹⁴ C) L-aspartate, Ammonia- and Glutamine- Dependent Reactions	43
2.2 Trapping of ATP from Complexes in the Steady State, Using (³ H) ATP, Ammonia- and Glutamine- Dependent Reactions.	44
3.1 Inhibition patterns for ASB obtained with β -methyl aspartate, AMP-PNP and L-glutamic acid γ -methyl ester with respect to L-aspartate, ATP and L-glutamine. .	142
3.2 Product inhibition data for ammonia-dependent reaction of ASB	143
3.3 Product inhibition data for glutamine-dependent reaction of ASB.	144
4.1 Thermodynamic properties for ammonia- and glutamine-dependent reactions of ASB.	156

LIST OF FIGURES

<u>Figure</u>	<u>page</u>
1.1	(a) Currently accepted mechanism for the hydrolysis of L-glutamine to yield ammonia and an acylenzyme 1 by analogy with purF enzyme, GPA. (b) Synthesis of L-asparagine by reaction of ammonia with activated aspartyl derivative 2. (c) Hydrolysis reaction to yield L-glutamate from the acylenzyme 1.23
1.2	Sequence alignment of the N-terminal domains of E. coli ASB and human AS as deduced from oligonucleotide sequencing.24
1.3	Proposed mechanism for the synthesis of L-asparagine by E. coli ASB, via an imide intermediate 3.25
2.1	Determination of K _d for Aspartate.45
2.2	Rate of AMP formation as a function of time.46
3.1A	Double-reciprocal plot of initial velocity versus L-aspartate concentration at various fixed concentrations of ATP.96
3.1B	Replots of the reciprocal-fixed variable substrate ATP vs slope (plus) and intercept (square) from Fig.3.1A.97
3.2A	Double-reciprocal plot of initial velocity versus L-glutamine concentration at various concentrations of ATP.98
3.2B	Replots of the reciprocal-fixed variable substrate ATP vs slope (plus) and intercept (cross) from Fig.3.2A.99
3.3A	Double-reciprocal plot of initial velocity versus L-aspartate concentration at various fixed concentrations of L-glutamine.100
3.3B	Replots of the reciprocal-fixed variable substrate L-glutamine vs slope (plus) and intercept (cross) from Fig. 3.3A.101

3.4A	Double-reciprocal plot of initial velocity <i>versus</i> ATP concentration at various fixed concentrations of L-aspartate.	102
3.4B	Replots of the reciprocal-fixed variable substrate L-aspartate <i>vs</i> slope (plus) and intercept (cross) from Fig. 3.4A.	103
3.5A	Double-reciprocal plot of initial velocity <i>versus</i> ATP concentration at various fixed concentrations of NH ₃	104
3.5B	Replots of the reciprocal-fixed variable substrate NH ₃ <i>vs</i> slope (plus) and intercept (cross) from Fig. 3.5A.	105
3.6A	Double-reciprocal plot of initial velocity <i>versus</i> L-aspartate concentration at various fixed concentrations of NH ₃	106
3.6B	Replots of the reciprocal-fixed variable substrate NH ₃ <i>vs</i> slope (plus) and intercept (cross) from Fig. 3.6A.	107
3.7	Double-reciprocal plot of initial velocity <i>versus</i> L-glutamine concentration at fixed concentration of LGH.	108
3.8	Double-reciprocal plot of initial velocity <i>versus</i> ATP concentration at fixed concentration of L-glutamine (plus) and LGH (cross) (0.2 mM).	109
3.9	Double-reciprocal plot of initial velocity <i>versus</i> L-aspartate concentration at various fixed concentrations of ATP.	110
3.10	Double-reciprocal plot of initial velocity <i>versus</i> L-glutamine concentration at various concentrations of ATP.	111
3.11	The ratio of L-glutamate produced/PPi produced <i>versus</i> concentration of L-glutamine.	112
3.12	Double-reciprocal plot of initial velocity <i>versus</i> NH ₃ concentration at various fixed concentrations of L-asparagine.	113
3.13	Double-reciprocal plot of initial velocity <i>versus</i> ATP concentration at various fixed concentrations of L-asparagine.	114

3.14	Double-reciprocal plot of initial velocity versus L-aspartate concentration at various fixed concentrations of L-asparagine.	115
3.15	Double-reciprocal plot of initial velocity versus ATP concentration at various fixed concentrations of AMP.	116
3.16	Double-reciprocal plot of initial velocity versus L-aspartate concentration at various fixed concentrations of AMP.	117
3.17	Double-reciprocal plot of initial velocity versus NH ₃ concentration at various fixed concentrations of AMP.	118
3.18	Double-reciprocal plot of initial velocity versus L-glutamine concentration at various fixed concentrations of L-asparagine.	119
3.19	Double-reciprocal plot of initial velocity versus ATP at various fixed concentrations of L-asparagine. ..	120
3.20	Double-reciprocal plot of initial velocity versus L-aspartate concentration at various fixed concentrations of L-asparagine.	121
3.21	Double-reciprocal plot of initial velocity versus ATP concentration at various fixed concentrations of PP _i	122
3.22	Double-reciprocal plot of initial velocity versus L-aspartate concentration at various fixed concentrations of PP _i	123
3.23	Double-reciprocal plot of initial velocity versus ATP concentration at various fixed concentrations of L-glutamate.	124
3.24	Double-reciprocal plot of initial velocity versus L-aspartate concentration at various fixed concentrations of L-glutamate.	125
3.25	Double-reciprocal plot of initial velocity versus L-glutamine concentration at various fixed concentrations of L-glutamate.	126
3.26	Double-reciprocal plot of initial velocity versus L-glutamine concentration at various fixed concentrations of AMP.	127

3.27	Double-reciprocal plot of initial velocity versus L-aspartate concentration at various fixed concentrations of AMP.	128
3.28	Double-reciprocal plot of initial velocity versus ATP concentration at various fixed concentrations of AMP.	129
3.29	Double-reciprocal plot of initial velocity versus L-aspartate concentration at various fixed concentrations of L-glutamine in the presence of L-glutamate (50 mM).	130
3.30	Double-reciprocal plot of initial velocity versus L-aspartate concentration at various fixed concentrations of L-glutamine in the presence of PP_i (0.4 mM).	131
3.31	Double inhibition studies plot of L-asparagine concentration <i>versus</i> reciprocal initial velocity at various fixed concentrations of AMP.	132
3.32	Double inhibition studies plot of L-glutamate concentration <i>versus</i> reciprocal initial velocity at various fixed concentrations of AMP.	133
3.33	Double inhibition studies plot of L-glutamate concentration <i>versus</i> reciprocal initial velocity at various fixed concentrations of L-asparagine.	134
3.34	Double-reciprocal plot of initial velocity versus L-aspartate concentration at fixed varied concentrations of L-glutamate and AMP in a constant ratio ($[L\text{-glutamate}] = 5 [AMP]$).	135
3.35	Double-reciprocal plot of initial velocity versus ATP concentration at fixed varied concentrations of L-aspartate.	136
3.36	Double-reciprocal plot of initial velocity versus ATP concentration at fixed varied concentrations of L-aspartate.	137
3.37	Double-reciprocal plot of initial velocity versus ATP concentration at fixed varied concentrations of L-aspartate.	138
3.38	Double-reciprocal plot of initial velocity versus ATP concentration at fixed varied concentrations of L-aspartate.	139

3.39	Double-reciprocal plot of initial velocity versus ATP concentration at fixed varied concentrations of L-aspartate.	140
3.40	Double-reciprocal plot of initial velocity versus ATP concentration at fixed varied concentrations of L-aspartate.	141
3.41	Double-reciprocal plot of initial velocity versus ATP concentration at fixed varied concentrations of L-aspartate.	142
4.1	Arrhenius plot of the Vmax values for the ammonia-dependent reaction, varying NH ₃ concentration.	152
4.2	Arrhenius plot of the Vmax values for the ammonia-dependent reaction, varying ATP concentration.	153
4.3	Arrhenius plot of the Vmax values for the ammonia-dependent reaction, varying L-aspartate concentration.	154
4.4	Arrhenius plot of the Vmax values for the glutamine-dependent reaction, varying L-glutamine concentration.	155

Abstract of Dissertation Presented to the Graduate School
of the University of Florida in Partial Fulfillment of the
Requirements for the Degree of Doctor of Philosophy

INVESTIGATION OF THE KINETIC MECHANISM OF GLUTAMINE- AND
AMMONIA-DEPENDENT REACTIONS OF *E. coli* ASPARAGINE SYNTHETASE
B USING ISOTOPE PARTITIONING AND STEADY-STATE KINETICS

By

POURAN HABIBZADEGAH-TARI

August, 1996

Chairman: Dr. Sheldon M. Schuster
Major Department: Biochemistry and Molecular Biology

The kinetic mechanism of the *Escherichia coli* asparagine synthetase B was deduced from initial velocity studies. In addition to varying substrate concentrations in a variety of ratios, products and substrate analogs were used as inhibitors in additional studies. While these studies provided limitations to the possible kinetic mechanisms, the results were equivocal. The data were consistent with a ping pong mechanism with either inorganic pyrophosphate or L-glutamate released prior to addition of other substrates. Therefore, from these data, two ter-quad mechanisms, bi-uni-uni-ter ping-pong and uni-uni-bi-ter ping-pong, were possible. In order to resolve this dilemma, a series of isotope partitioning studies of both the glutamine- and

ammonia-dependent reactions of ASB were carried out as well. Major conclusions derived from the isotope partitioning experiments regarding the kinetic mechanism of ASB are as follows: 1) The enzyme catalyzes aspartate-dependent ATP hydrolysis, which requires no nitrogen source. 2) The binding and hydrolysis of L-glutamine or the binding of ammonia is not required prior to ATP and L-aspartate binding for the synthesis reaction. These results together clearly support an ordered bi-uni-uni-ter ping-pong mechanism for the ammonia- and the glutamine-dependent reactions of *E. coli* ASB, with ATP binding first and L-aspartate second. This is followed by release of PP_i and subsequent addition of L-glutamine or ammonia.

The information obtained from product inhibition studies was also consistent with the existence of an isomerization step following the release of the last product. Another very important observation made in this work was that the glutaminase reaction was shown to be occurring at the same time as the synthetase reaction, and in fact increasing with increasing concentrations of L-glutamine

These observations resulted in a complete model for the glutamine-dependent AS reaction, and computer modeling was used to stimulate the proposed mechanism. According to the proposed model the reaction mechanism is quite complex, and is an ordered bi-uni-uni-ter ping-pong mechanism with a side reaction, glutaminase, for the *E. coli* ASB enzyme.

CHAPTER 1 INTRODUCTION

Vauquelin and Robiquet (1806) were the first to report the isolation of L-asparagine, which was the first amino acid ever identified. The metabolic importance of this amino acid has emerged from numerous studies that have appeared describing both the anabolic and catabolic pathways from numerous organisms. Early on it was shown that L-asparagine can be hydrolyzed by L-asparaginase to yield L-aspartate and ammonia (Broome, 1963), and for many years this was thought to be the major use of L-asparagine. However, a study by Meister et al. (1952) had suggested that L-asparagine can also be degraded via asparagine transamination followed by amide hydrolysis. Later, Moraga et al. (1989) described the mode of L-asparagine catabolism via asparagine transaminase and α -amidase in rat liver mitochondria. In addition, evidence was presented that suggested the existence of an as yet uncharacterized pathway for asparagine catabolism in mitochondria. L-asparagine has also been shown to be involved in providing the residue necessary for linkage of oligosaccharides to glycoproteins (Spiro, 1969), so that possibly the most important fate of L-asparagine is its incorporation into protein (Coony and Handschumacher, 1970).

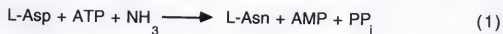
The interest in asparagine metabolism was intensified from the finding by Kidd (1953) that a factor in guinea pig

serum had antitumor activity. Later, Broome related the antitumor properties of guinea pig serum to its L-asparaginase activity (1963 and 1968). Since that time, L-asparaginase, which catalyzes the hydrolysis of L-asparagine, has been used clinically to treat patients with lymphomas (Oettgen et al., 1970 and Ertel et al., 1979). When used on patients with acute lymphoblastic leukemia (ALL), L-asparaginase resulted in complete remission for 40% of the patients (Uren et al., 1977). When L-asparaginase was used in combination with prednisone and vincristine, it resulted in 95% complete remission for ALL previously untreated patients (Uren et al., 1977). Although L-asparaginase is a potent chemotherapeutic agent, several side effects have been reported that would limit its general utility. These side effects include chills, fever, nausea, life-threatening serum ammonia concentrations, liver dysfunction (Oettgen et al., 1970 and Terebello et al., 1986), central nervous dysfunction (Land et al., 1972), and tumor resistance (Uren et al., 1977).

The effectiveness of L-asparaginase is due to its ability to lower the circulating level of asparagine (Broome, 1968). This suggests the possibility that a highly specific and potent inhibitor of the enzyme responsible for synthesis of L-asparagine, namely asparagine synthetase (AS), might be effective in treating tumors. A great deal of the early work on AS was directed at this goal which involved screening of a broad range of inhibitors. Several hundreds of randomly selected compounds and a host of available and newly

synthesized substrate analogs have been tested as AS inhibitors. Few compounds inhibited AS, and those that did, exhibited weak inhibition. The most promising inhibitor of asparagine synthetase, β -aspartyl methylamide, increased life span from 31 to 79 percent when administered to mice bearing L-asparaginase resistant tumors (Uren et al., 1977). However, this compound was proven to be a better inhibitor of the L-asparaginase than of AS. No other compounds have been found to possess sufficient potency to warrant further study. Therefore, detailed structural, chemical and mechanistic information is essential in order to design effective inhibitors of AS. For example, given the success in the discovery of drugs based upon transition state analogs (Barlett and Marlowe, 1983), elucidation of the mechanistic details underlying the AS reaction mechanism may prove an alternate approach to obtaining potent AS inhibitors. Therefore, we have chosen to study in detail the mechanism of AS.

Asparagine synthetase was demonstrated for the first time in *Lactobacillus arabinosus* (Ravel et al., 1962). The bacterial enzyme was shown to catalyze conversion of L-aspartate to β -aspartylhydroxamate in the presence of hydroxylamine and ATP, and alternatively to L-asparagine in the presence of ammonia and ATP.



Along with the adenosine triphosphate (ATP) a divalent metal ion, either Mn^{2+} or Mg^{2+} , was required. Adenosine 5'-phosphate and inorganic pyrophosphate (PPi) were shown to be products along with L-asparagine. The production of asparagine synthetase decreased more than 10-fold when the cells were grown in the presence of L-asparagine. In addition, the activity *in vitro* of the enzyme was inhibited by L-asparagine (Ravel et al., 1962).

Following the partial purification (10-fold), the initial velocity and other properties were determined. The K_m for ATP, L-aspartate and Mg^{2+} were 0.2 mM, 4.2 mM and 3.5 mM, respectively. The pH optimum for the formation of β -aspartylhydroxamate was between 6.0 and 6.5, and for the synthesis of L-asparagine was 8.2. The enzyme was also shown to catalyze an aspartate-dependent exchange of ATP and PPi which was inhibited by L-asparagine. L-glutamine did not serve as a nitrogen source.

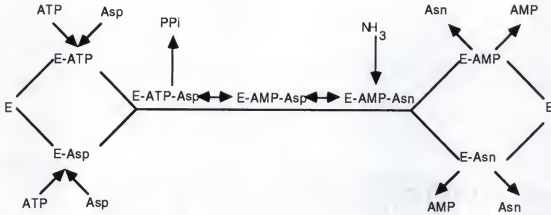
Asparagine synthetase from *Streptococcus bovis* was studied by Burchall et al. in 1964. The bacterial extract was shown to catalyze the formation of a hydroxamate of L-aspartate in the presence of ATP and Mg^{+2} . The AS from *Streptococcus bovis* was partially purified from the extract (21-fold) and characterized. The bacterial enzyme was shown to catalyze the conversion of L-aspartate to β -aspartylhydroxamate in the presence of hydroxylamine, ATP and Mg^{+2} . Ammonia could also be used to replace hydroxylamine, forming L-asparagine, but L-glutamine could not. ATP was

converted to AMP and PP_i , and no ADP was detected. The K_m 's for ATP, L-aspartate, NH_4^+ and Mg^{2+} were 4 mM, 26 mM and 4 mM and 45 mM, respectively. Fifty percent of the enzyme activity was lost when AS was incubated with iodoacetate (10 mM), p-hydroxymercuribenzoate (10 mM) and silver nitrate (10 mM). L-asparagine, which inhibited the enzyme activity at a concentration of 2 mM, was found to be a competitive inhibitor with respect to L-aspartate. Curiously, however, the enzyme synthesis was not repressed when bacterial cells were grown in the presence of L-asparagine.

The presence of AS in *E. coli* was demonstrated by Ceder and Schwartz (1969a). AS was purified 370-fold from a mutant of *E. coli* that was either deficient in L-asparaginase II or else its activity was inhibited by 5-diazo-4-oxo-L-norvaline (DONV). The molecular weight of the enzyme was determined to be 80,000 by gel filtration and was shown to be stabilized by 2-mercaptoethanol and by 10% glycerol. The asparagine synthesis reaction required L-aspartate, an ATP- Mg^{2+} complex, and ammonia, with stoichiometric production of PP_i and AMP. L-glutamine did not serve as a nitrogen source, but hydroxylamine could be substituted for ammonia, forming β -aspartylhydroxamate instead of L-asparagine. The pH optimum was found to be 8.4. The enzyme, in the absence of ammonia, was shown to catalyze an aspartate-dependent exchange of ATP and PP_i , which was inhibited by L-asparagine.

Kinetic studies were performed to obtain the mechanism of the *E. coli* AS enzyme (Ceder and Schwartz, 1969b). Initial

velocities of AS activity were determined when the concentration of two of the three substrates, L-aspartate, ATP, and ammonia were varied, keeping the third substrate constant. When either L-aspartate and ammonia, or ATP and ammonia was varied, a parallel initial velocity pattern was seen, characteristic of a ping-pong mechanism where a product (PPi) is released before ammonia binds the enzyme. The initial velocity pattern was intersecting when L-aspartate and ATP were the variable substrates, suggesting that these two substrates are added in a sequential manner to the enzyme. The enzyme was also shown to catalyze the transfer of ^{18}O from the β -carbonyl group of aspartate to the phosphate of AMP, suggesting a β aspartyl-adenylate intermediate. The product inhibition studies indicated that the order of addition of ATP and L-aspartate is random, which was confirmed by kinetic studies of the PPi-ATP exchange. Initial rates of the ^{32}P -PPi exchange reaction were determined with varying concentrations of ATP and substrate, while maintaining the concentration of PPi constant. An intersecting pattern was observed. In both, the point of intersection was situated to the left of the ordinate. These results were consistent with the rapid equilibrium random mechanism, for which a general rate equation was presented. The mechanism of *E. coli* AS was reported to be bi-uni-uni-bi Ping-Pong, with random ATP and L-aspartate addition and random AMP and L-asparagine release as shown below.



Later, Felton et al. (1980) showed that *E. coli* contains two genes coding for asparagine synthetase, which were renamed *asnA* and *asnB*. Their studies showed that these genes are located at two points in the chromosome and that both must be mutated to produce an auxotroph.

Biochemical and genetic studies were performed by Humbert and Simoni (1980) to determine if the *E. coli* genes were distinct or the if they were products of gene duplication. Two strains, *asnA*⁺ *asnB* and *asnA* *asnB*⁺, were constructed, and the asparagine synthetic reaction of their extracts was characterized. Their studies showed that *asnA* gene codes for the enzyme previously characterized by Ceder and Schwartz (1969). The *asnB* gene coded for an enzyme (ASB) that was different from ASA. Dialyzed extracts containing ASB enzyme had a lower specific activity for asparagine synthesis. ASB was able to use L-glutamine or ammonia as the nitrogen source. ASB was also distinguished from ASA by its

greater lability at low temperatures and greater stability at high temperatures.

The *E. coli* ASA, an ammonia-dependent AS, is composed of 330 amino acids (Nakamura et al., 1981), while the *E. coli* ASB, a glutamine-dependent AS, is composed of 554 amino acids (Scofield et al., 1990). No similarity can be detected between the amino acid sequence of *E. coli* ASA and *E. coli* ASB, indicating that although the two AS synthesize the same product, they have evolved from different sources. A highly conserved protein motif characteristic of Class II aminoacyl tRNA synthetase was found to align with a region of *E. coli* ASA. Site directed mutagenesis of some of the conserved residues in the motif resulted in an inactive enzyme, suggesting the possibility that *E. coli* ASA evolved from an ancestral aminoacyl tRNA synthetase (Hinchman et al., 1992). The *E. coli* ASB was aligned with the protein sequence of human asparagine synthetase that can use both glutamine and ammonia as substrates. Interestingly, the two proteins were shown to be quite homologous (37%) with regard to their amino acid sequence. This indicated that the two genes may have evolved from a common ancestral gene (Scofield et al. 1990). The significant amount of similarity between the human and *E. coli* glutamine-dependent gene products might suggest that these highly conserved regions are critical for the enzymatic activity or structure in both enzymes.

Cloning, overexpression and characterization of ASB was reported by Scofield et al. (1990) and Boehlein et al.

(1994). The recombinant ASB possessed a molecular mass of about 63 KDa. Addition of chloride (10 mM) to the assay medium increased glutamine-dependent activity ASB by a factor of 2 but did not affect the ammonia-dependent reaction. Magnesium ion (Mg^{2+}) gave the highest activity. Co^{2+} , the only ion that could replace Mg^{2+} , supported 80 and 50% of the Mg^{2+} -dependent ASB activity when either L-glutamine or ammonia was the nitrogen source, respectively. A number of nucleotides were also assayed as substrates for ASB. dATP and ATP were utilized in both reactions at a similar rate, whereas GTP utilization was only 15% that of ATP. The pH optima were determined to be 6.5-8 for the glutamine- and ammonia-dependent activities of ASB.

Asparagine synthetase was also purified and characterized from *Klebsiella aerogenes* (Reitzer and Magasanik, 1982) and *Saccharomyces cerevisiae* (Ramos and Wiame, 1979 & 1980). Asparagine synthetase has also been isolated and characterized from higher organisms such as chick embryo liver (Arfin, 1967), beef pancreas (Luehr and Schuster, 1985), and rat liver (Hongo et al., 1978). Asparagine synthetase from mammalian sources was shown to catalyze the conversion of L-aspartate to L-asparagine in the presence of L-glutamine with concomitant cleavage of ATP to AMP and PP_i as shown below.



Ammonia was also shown to serve as a nitrogen source in the absence of glutamine. When glutamine is used, a glutaminase activity is associated with the asparagine synthetase activity. This glutaminase activity was shown to occur in the



absence and in the presence of all substrates of the asparagine synthetase.

Underlying all of these previous studies of AS is the concept that any potent and specific inhibitor of AS could become a very useful chemotherapeutic agent. The failure of previous attempts to inhibit AS specifically is due to a deficiency of our understanding of the chemical and kinetic mechanism of the enzyme. Although very little information is available regarding the chemical mechanism of AS, there is a general agreement that aspartyl-AMP, an activated form of L-aspartate, is the reaction intermediate (Luehr and Schuster, 1985, Horowitz and Meister, 1972). Nevertheless, the pathway by which the amide nitrogen is transferred from the L-glutamine to this activated complex in AS needs further characterization.

The ability to use ammonia or L-glutamine as the nitrogen source is also found in other amidotransferases such as such as glutamine phosphoribosylpyrophosphate amidotransferase, GPA, (Mei and Zalkin, 1989), CTP synthetase (Weng et al., 1986), and GMP synthetase (Zalkin and Truit,

1977). Two types of glutamine amide transfer domains (GAT domains) have been identified in glutamine amidotransferase enzymes. The first type shows homology to the GAT domain derived from the *purF* gene and is called a *purF*-type GAT domain. This amidotransferase subfamily includes glutamine phosphoribosylpyrophosphate amidotransferase, GPA, (Mei and Zalkin, 1982), AS (Andrulis et al., 1987 & Scofield et al., 1990) and glucosamine-6-P synthase (Walker et al., 1984). The N-terminal four amino acids in these enzymes are highly conserved. The second type shows homology to the GAT domain derived from the *trpG* gene which includes CTP synthetase (Weng et al., 1986), carbamyl-phosphate synthetase (Piette et al., 1984) and GMP synthetase (Zalkin and Truit, 1977). A *trpG*-type GAT domain is characterized by three internal regions of conserved amino acids (Mei and Zalkin, 1987).

In 1989, Mei and Zalkin reported the chemical pathway by which nitrogen is transferred from L-glutamine in related glutamine-dependent enzymes. In *purF*-type enzymes, most notably GPA (Mei and Zalkin, 1989), the N-terminal cysteine (Cys-1) residue appears critical for the formation of a covalent glutaminyll intermediate. In this family, the Cys-1 was shown to be critical for glutamine-dependent, but not ammonia-dependent, activity because covalent modification of this residue with diazo-oxo-norleucine (DON) resulted only in the elimination of glutamine-dependent activity. In GPA a 'catalytic triad' composed of Cys-1, His-101 and Asp-29 was proposed. Mutagenesis of these residues in GPA resulted in

the loss of glutamine-, but not ammonia-dependent activity. The cysteine-histidine interaction of amidotransferases resembles that in papain. In papain, His-159 functions as a general base to increase the nucleophilicity of Cys-25; an acidic residue is not involved in the proton shuttle (see Zalkin et al., 1989). Rather, the side chain of Asn-175 is hydrogen bonded with imidazole N-3 of His-159 to fix its position, whereas imidazole N-1 accepts a proton from Cys-25. (see Zalkin et al., 1989). In GPA, in analogy to papain, it was proposed that Cys-1 participates in an amide hydrolysis reaction to release ammonia, and His and Asp act as general bases in the reaction. On the basis of the chemical modification and site directed mutagenesis, it was proposed that glutamine is converted to an acylenzyme intermediate by the nucleophilic attack of the Cys-1 thiolate anion on the primary amide. Such a reaction would release ammonia which, if protected from protonation, can undergo nucleophilic reaction.

The human AS, also a member of the "*purF*" type of glutamine amide transfer enzyme, is characterized by the presence of an N-terminal cysteine followed by conserved glycine and isoleucine residues (See Mei and Zalkin, 1989 and Richards and Schuster, 1992). Site-specific mutagenesis was used to replace the N-terminal cysteine (Cys-1) by alanine in human AS. The mutation resulted in the loss of the glutamine-dependent AS activity, while the ammonia-dependent activity remained unaffected (Van Heeke and Schuster, 1989). Because

of the fact that human AS has the conserved residues defining the proposed catalytic triad, it was suggested (Mei and Zalkin, 1989) that the hydrolysis of L-glutamine to yield free ammonia is the basis of the glutamine-dependent activity in this enzyme (Fig. 1.1). Due to the lack of structural information concerning the location of the L-glutamine and ammonia binding pockets in human AS, the support for enzymatic generation of 'free' ammonia as a reaction intermediate is circumstantial. Further, the molecular mechanism by which ammonia is sequestered from solvent and retained in its unprotonated form remains an open question (Richards and Schuster, 1992). On the other hand, it is true that all asparagine synthetases, and other *purF* enzymes as well, can utilize ammonia as a nitrogen source in the absence of L-glutamine, showing that free ammonia not only binds within the enzyme active site, but also remains sufficiently nucleophilic to release L-asparagine from aspartyl-AMP (Richards and Schuster, 1992). By contrast, the *E.coli* ASB lacks the conserved histidine residue, necessary for the nitrogen transfer if the reaction proceeds by the accepted pathway in other glutamine amidotransferases (Fig. 1.2), but still retains the ability to synthesize L-asparagine and exhibits similar specificity to human AS (Richards and Schuster, 1992). Based on these findings it was suggested that at least for the ASB enzyme, the proposed mechanism for nitrogen transfer in the glutamine-dependent synthesis of asparagine, may not occur (Richards and Schuster, 1992). This

led to an alternative chemical pathway for the nitrogen transfer reaction, proposed by Richards and Schuster (1992), which does not require the generation of free ammonia (Fig. 1.3). According to this mechanism L-glutamine reacts directly with aspartyl-AMP to form an imide intermediate. Cys-1 is still essential for the glutamine-dependent activity because hydrolysis of the imide is required to produce L-asparagine and the acylenzyme derivative of L-glutamate. One of the important features of the intermediate is that the nitrogen retains amide character and therefore possesses little basicity. The imide can interact with the protein through the same functional groups used for interaction with L-glutamine and L-aspartate. In addition, the anionic form of L-asparagine is the leaving group which relieves the need for general acid catalysis by a histidine residue. Finally, such a reaction mechanism eliminates the possibility of diffusion of ammonia from the active site during the reaction and removes the need for additional structural features for maintaining ammonia in its unprotonated form (Richards and Schuster, 1992). The two catalytic mechanisms described here are fundamentally different, and efforts have been underway to address the differences posed by the two proposed mechanisms.

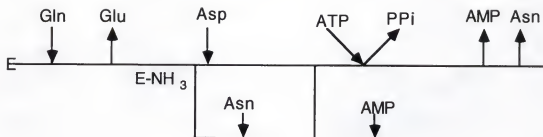
Studying the kinetic mechanism, which is the focus of this dissertation, would allow us to draw certain conclusions about the order of the binding of the substrates and release of products. For example, if L-glutamate release occurs prior

to the binding of either ATP or L-aspartate, it would be very difficult to justify the mechanistic hypothesis involving the imide intermediate (Richards and Schuster, 1992). Based on their proposal for the nitrogen transfer mechanism, L-glutamine reacts directly with aspartyl-AMP to form an asymmetric imide intermediate. Therefore, L-glutamate release can not happen prior to ATP and L-aspartate binding. The kinetic mechanism of AS has been proposed for several forms of AS: e.g., ASA from *E. coli* (Ceder and Schwartz, 1969, 1969), 6C3HED-RG1 tumor (Chou, 1970), mouse pancreas (Milman et al., 1980), beef pancreas (Markin et al., 1981), and rat liver (Hongo and Sato, 1985), and as discussed below, considerable controversy exists.

On the basis of initial velocity and product inhibition studies, Chou (1970) suggested that the reaction catalyzed by AS from 6C3HED-RG1 tumor is ping-pong. He observed double reciprocal plots which showed parallel lines when either L-glutamine was varied *versus* ATP or when L-glutamine was varied *versus* L-aspartate. Double reciprocal plots of parallel lines were also observed when L-aspartate was varied *versus* ATP. Inhibition studies showed L-asparagine was a competitive inhibitor with respect to L-glutamine, and PP_i was a competitive inhibitor with respect to ATP. Based on these observations, the following penta-uni-bi ping-pong mechanism was proposed for the 6C3HED-RG1 tumor line AS.



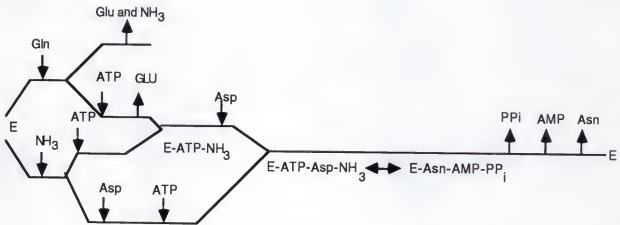
Using steady-state kinetic methods, Milman et al. (1980) proposed a uni-uni-bi-ter ping-pong Theorell-Chance mechanism for the glutamine-dependent reaction of mouse AS. Initial velocity and product inhibition studies were conducted with the glutamine-dependent reaction of the AS from mouse pancreas. Parallel double reciprocal plots were observed with L-glutamine *versus* either L-aspartate or ATP, while intersecting patterns were observed with L-aspartate *versus* ATP. These patterns were reported to be indicative of a hybrid ping-pong mechanism consisting of a glutaminase partial reaction and a sequential catalysis involving L-aspartate and ATP. Product inhibition studies involving the four products, L-glutamate, AMP, PPI and L-asparagine, were carried out to delineate further the kinetic mechanism. The patterns from these experiments were reported to be consistent with a hybrid uni-uni-bi-ter ping-pong Theroll-Chance mechanism where the glutaminase reaction occurs first. In other words, L-glutamine binds first followed by the



release of L-glutamate. L-aspartate is the second substrate to bind followed by a Theorell-Chance step, (ATP on/PP_i off). AMP and L-asparagine are subsequently released in an ordered fashion. However, there was disagreement between the predicted patterns and the experimental results for AMP *versus* ATP and L-asparagine *versus* all three substrates. These discrepancies were rationalized to suggest the formation E.NH₃.Asn and E.NH₃.AMP abortive complexes.

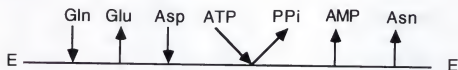
The kinetic mechanism of bovine pancreatic AS was deduced from initial velocity studies and product inhibition studies, of both the ammonia- and glutamine-dependent reactions (Markin et al., 1981). For the glutamine-dependent reaction, parallel lines were observed in the double reciprocal plots of 1/V *versus* 1/[L-glutamine] at varied L-aspartate concentrations, and in the plot of 1/V *versus* 1/[ATP] at varied L-aspartate concentrations. Intersecting lines were found for the plot of 1/V *versus* 1/[ATP] at varied glutamine concentrations. For further clarification of the order of substrate addition and product release, the product inhibition of the initial velocity, including a dual

inhibition study, was done for the glutamine-dependent AS. The results supported an ordered bi-uni-uni-ter ping-pong mechanism. According to the proposed mechanism, L-glutamine and ATP sequentially bind followed by the release of L-glutamate and the addition of L-aspartate and the release of PP_i , AMP, and L-asparagine. The mechanism was found to be significantly different for the ammonia-dependent reaction. NH_3 bound first followed by a random addition of ATP and L-aspartate. PP_i , AMP, and L-asparagine are then sequentially released. From these studies, a comprehensive mechanism has been proposed through which either glutamine or NH_3 can provide nitrogen for L-asparagine production from L-aspartate as shown below.

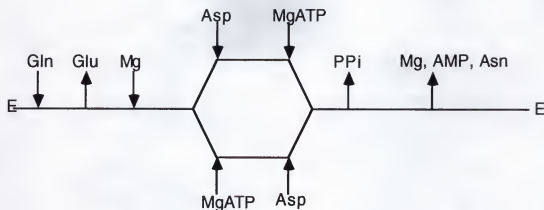


The kinetic mechanism of rat liver AS was studied by Hongo and Sato (1985). The initial velocity studies, with L-glutamine as a varied substrate and L-aspartate as a varied

changing fixed substrate, showed a series of parallel lines in the form of a double reciprocal plot. A parallel double reciprocal plot was also observed between L-glutamine and ATP. On the other hand, intersecting lines were obtained between L-aspartate and ATP. Product inhibition studies were also conducted. These studies were performed with a high concentration of Mg^{2+} . The mechanism of the reaction was suggested to be uni-uni-bi-ter ping-pong Theorell-Chance. According to their mechanism, L-glutamine binds first followed by L-glutamate release, and L-aspartate and ATP bind in an ordered manner followed by ordered release of PPi , AMP, L-asparagine.



When the Mg^{2+} concentration was kept 0.5-2.0 mM over the ATP concentration, the binding of substrates after the release of L-glutamate was in rapid equilibrium with ordered Mg^{2+} and random L-aspartate-ATP.



Clearly there are dramatic differences in the mechanisms presented, and the sources of these differences are unclear. The differences regarding the order of substrate binding and product release could be due to the different enzyme sources used. Another potential cause for differing results may be the presence of certain contaminants. While it is accepted that the degree of enzymatic purity will not alter a kinetic mechanism, the presence of any contaminant that breaks down the substrates or the measured product could have substantially contributed to the discrepancies. This is especially important because the presence of a contaminating glutaminase or asparaginase activity could potentially alter the observations. Further, the differences between the results could be due to the single experimental approach utilized. All studies in the past relied solely on steady state kinetic methods, and no other technique, such as isotope partitioning, was employed.

The kinetic mechanism of *E. coli* ASB, for both the L-glutamine-dependent and ammonia-dependent reactions, using an overexpressed, stable and pure enzyme has been investigated. Although the techniques employed are basically those used in the past, the enzyme is far more pure, and highly stable. These studies provide us with information regarding the kinetic mechanism and relevant rate constants. In addition, the ability to use techniques such as isotope partitioning (trapping), pioneered by Meister and Rose and their co-workers (Krishnaswamy et al., 1962; Rose et al., 1974), allows us to address problems such as substrate inhibition and/or abortive complex formation observed with steady state analyses, and will provide us with information about catalytic competency of the enzyme-substrate complexes. The data presented will show that no decision could be made on any one mechanism proposed for glutamine-dependent reaction of ASB, if we were to rely only on steady state kinetics. But together with the help of isotope partitioning experiments, support is provided for an ordered bi-uni-uni-ter ping-pong mechanism for the glutamine-dependent reaction of *E. coli* ASB. ATP binds first and L-aspartate second. This is followed by release of PP_i and subsequent addition of L-glutamine. The L-glutamate release is not required prior to the binding of ATP and L-aspartate. However, further studies suggest that the simple ordered bi-uni-uni-ter ping-pong mechanism is not applicable to *E. coli* ASB enzyme. From these data a comprehensive mechanism was proposed for the glutamine-

dependent AS reaction of ASB, which was examined through computer modeling.

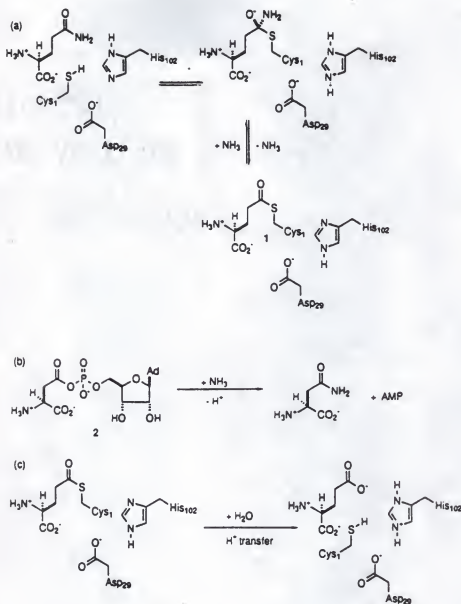


Fig. 1.1 (a) Currently accepted mechanism for the hydrolysis of L-glutamine to yield ammonia and an acyl-enzyme 1 by analogy with purF enzyme, GPA. (b) Synthesis of L-asparagine by reaction of ammonia with activated aspartyl derivative 2. (c) Hydrolysis reaction to yield L-glutamate from the acyl-enzyme 1. Residue numbering to that of human AS. This diagram was taken from Richards and Schuster, 1992).

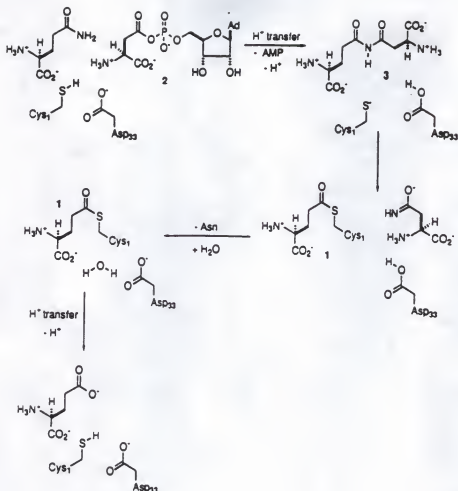
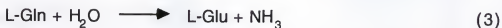
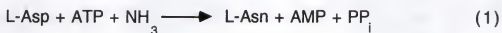


Fig. 1.3 Proposed mechanism for the synthesis of L-asparagine by *E. coli* ASB, via an imide intermediate 3. attack of the primary amide occurs directly upon activated L-aspartate 2. Cys-1 and asp-33 are then involved in the hydrolysis of the imide to yield L-glutamate and L-asparagine in subsequent steps. residues numbering corresponds to that of the Asn B gene product. This was taken from Richards and Schuster, 1992.

CHAPTER 2
INVESTIGATION OF THE MECHANISM OF *E. COLI* ASPARAGINE
SYNTHETASE USING ISOTOPE PARTITIONING

Introduction

Asparagine synthetase B from *E. coli* catalyzes the following reactions.



The *E. coli* ASA which catalyzes strictly the ammonia-dependent synthesis of L-asparagine is the most extensively characterized in terms of kinetic and chemical mechanism. The order of substrate addition and product release has been determined, and evidence for the existence of an aspartyl-AMP intermediate has also been provided (Ceder and Schwartz, 1969a & 1969b).

Studies on the mammalian AS also indicated that the enzyme produces an aspartyl-AMP intermediate (Luehr and Schuster, 1985, Horowitz and Meister, 1972). Using steady state kinetics, the kinetic mechanism of the glutamine-dependent synthesis of AS was deduced for enzymes from different mammalian tissues (Chou, 1970, Milman et al., 1980,

Markin et al., 1981 and Hongo and Sato, 1985). However, there were disagreements in the conclusions presented as discussed in chapter 1. The differences regarding the order of substrate binding and product release could be due to different enzyme sources used. In addition, none of the studies used a pure enzyme preparation. Although it is generally accepted that the degree of enzymatic purity will not alter a kinetic mechanism, the presence of any contaminants that break down the substrates or the measured product could have contributed to the variety of results obtained. This is especially a potential problem with asparaginase and glutaminase activities. The differences between the studies could also be due to a limited experimental approach, relying solely on steady state kinetic methods. No other technique was used. For example, the isotope trapping method, isotope exchange and pre-steady-state kinetic methods were not used.

The kinetic mechanism of *E. coli* ASB, a member of the *purF* family of glutamine-dependent amidotransferase, has not been studied. Cloning, overexpression and characterization of ASB was performed by Scofield et al. (1990) and Boehlein et al. (1994). The overexpression of the enzyme allows us to obtain a large quantity of highly pure and stable enzyme which in turn offers a unique opportunity to determine accurately the reaction mechanism of ASB.

This chapter describes isotope partitioning experiments that were performed to obtain information on the mechanism of

ASB. The isotope trapping methodology has been used in studies of glutamine synthetase (Meister et al., 1962), argininosuccinate synthetase (Rochovansky and Ratner, 1967) phosphofructokinase (Uyeda, 1970), hexokinase (Rose et al., 1974, 1979, 1981) and CTP synthetase (Lewis and Villafranca, 1989). Meister and his co-workers used the technique to show if an activated form of L-glutamate (glutamyl-P) was an intermediate in glutamine synthetase. Other investigators used the technique to determine the order of addition of substrates (Rochovansky and Ratner, 1967, Uyeda, 1970 and Lewis, Rose et al., 1974, 1979, 1981 and Villafranca, 1989). In this technique, enzyme and one radioactive substrate are incubated (pulse), followed by the simultaneous addition of a solution (chase) containing any other substrates necessary for reaction, as well as a large excess of unlabelled substrate to dilute the radioactive substrate with the carrier substrate, therefore diminishing the effect of additional catalytic turnovers. The reaction is also terminated as soon as possible after mixing to avoid utilization of free labelled substrate. The formation of a labelled product establishes the catalytic competency of the initial enzyme-substrate complex. We applied the isotope partitioning technique to determine the sequence of addition of substrates for both the glutamine- and ammonia-dependent reactions of AS. The technique was also employed to obtain the K_d for L-aspartate and ATP.

Materials and Methods

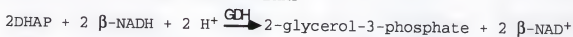
Chemicals and Reagents

L-[$^{14}\text{C}(\text{U})$]Aspartate (224.8 mCi/mmol) was purchased from NEN Research Products (Boston, MA). [2,8- ^3H] Adenosine 5'-Triphosphate (30.0 Ci/mmol) was bought from Amersham Life Science (England). Scintillation Liquid ScintiVersTM II and trichloroacetic acid (TCA) were purchased from Fisher Scientific (Orlando, FL). The ion exchange mono Q columns were obtained from Bio-Rad. The pyrophosphate reagent, containing fructose-6-phosphate kinase pyrophosphate dependent (PPi-PFK), aldolase, triosephosphate isomerase (TPI), and glycerophosphate dehydrogenase (GDH), for following PPi production, MgCl_2 , ATP, L-aspartate, L-asparagine, L-glutamine, AMP, ammonium acetate, ninhydrin, ethylenediaminetetraacetic acid (EDTA), Tris(hydroxymethyl)aminomethane (Tris-HCl), Bis(2-hydroxyethyl)iminotris(hydroxymethyl)methane (Bis Tris), isopropyl-1-thio- β -D-galactopyranoside (IPTG), and glycerol were all purchased from Sigma. DE-81 anion-exchange chromatography paper was supplied by Whatman (Hillsboro, OR). Dithiothreitol (DTT) was obtained from Promega Corporation (Madison, Wisconsin).

Expression of the Protein and Purification

An overexpression vector for *E. coli* ASB, pET-B, has been constructed by Hinchman and Schuster (1994). The *E. coli* B strain, BL21DE3plys S (F^- , ompT, rb^- , mb^-) was transformed with pET-B plasmid. Protein expression, cell culture and enzyme purification was carried out as described before (Boehlein et al., 1994). Transformed cells were plated onto Luria Broth agar plates supplemented with bacto-tryptone (10 g/Liter), bacto yeast extract (5 g/Liter), NaCl (5 g/Liter), pH 7.0, ampicillin (100 μ g/ml), and chloroamphenicol (30 μ g/ml). Plates were incubated at 37°C overnight. Single colonies were used to inoculate fresh minimal media supplemented with tryptone (10 g/ liter), ampicillin (100 μ g/ml), chloroamphenical (30 μ g/ml), and D-glucose (0.75%). The cultures were grown in an environmental shaker at 37°C. When they reached an absorbance ($\lambda=600$ nm) of 0.7-1.0, the cultures were induced by adding IPTG to a final concentration of 1 mM. Cells were harvested after 2.5-hours by centrifugation at 15,000 rpm for 5 min in a Beckman Model J2-21 centrifuge. The supernatant fluid was discarded and the pellets were stored at -70°C until needed. Cells were lysed by vortexing the pellets in enzyme buffer (50 mM Bis-Tris pH 6.5, 1 mM DTT, 0.5 mM EDTA, and 10% glycerol) using one-tenth of the original cell culture volume. DNase was added and cells were left on ice for 0.5 hr. The cell debris was

removed by centrifugation at 15,000 rpm for 20 min in Beckman centrifuge. The soluble cell extract containing L-asparagine synthetase B was purified by ion-exchange chromatography, as described previously (Boehlein et al., 1994). Glycerol was then added to a final concentration of 10%. The activity of L-asparagine synthetase B was monitored spectrophotometrically at 340 nm according to the following coupled reactions, developed by O'Brian (1976). Two moles of NADH are oxidized to NAD per mole of pyrophosphate produced.



The standard conditions for assay were 50 mM Tris-HCl (pH 8.0), 20 mM L-glutamine, 10 mM aspartic acid, 10 mM ATP, and 17 mM MgCl_2 . The soluble cell extract was stored at -70°C until needed.

Protein Concentration Determination

Protein concentration was measured using Bio-Rad Protein Assay (Bradford, 1976). Mouse immunoglobulin G was used to obtain a standard curve.

Isotope Partitioning Experiments with Radioactive L-Aspartate, Glutamine- and Ammonia-Dependent Reactions

A 105- μl solution of 50 mM Tris-HCl (pH 8.0), containing 0.50 mM L- $[^{14}\text{C}(\text{U})]$ aspartate (800 cpm/nmole), 2 mM MgCl_2 , and

1 nmole of ASB was incubated at 37°C for three minutes after which 62 μ l chase solution was added such that the final concentrations of substrates were: 50 mM Tris-HCl, pH 8.0, 5.0 mM ATP, 8.0 mM $MgCl_2$, 10 mM L-glutamine, and 30 mM unlabelled L-aspartate. The mixture was rapidly mixed, using vortex, for 3 sec. after which it was quenched by addition of 20 μ l of 4 M TCA. A control was done in a similar manner except that TCA was added prior to incubation to account for the background from labelled L-aspartate. A blank was also done in which labelled L-aspartate was added to the chase solution.

In experiments that included both ATP and labelled L-aspartate in the pulse solution, the concentration of ATP and $MgCl_2$ in the pulse were 2.0 mM and 3.0 mM, respectively.

In experiments that included both L-glutamine and labelled L-aspartate in the pulse solution, the concentration of L-glutamine in the pulse was 3.0 mM.

In experiments that included both NH_3 and labelled L-aspartate in the pulse solution, the concentration of NH_3 in the pulse was 100 mM. The final concentration of NH_3 following the addition of the chase solution was 165 mM.

After quenching, the reactions were neutralized by addition of 10 μ l of 3 M Tris buffer (pH not adjusted) and centrifuged for five minutes to remove precipitated proteins. It was determined that this brought pH to 6.5. Aliquots (5 μ l) of the reaction mixtures were spotted on DE-81 anion exchange chromatography paper (28 cm wide and 21 cm long). A

mixture of unlabelled L-aspartate and L-asparagine was also loaded on both edges of the paper to serve as standards. When the spots are air dried, the paper were placed vertically in a chromatography tank containing distilled water as eluant. The chromatography was stopped after 8 hours, and the paper air dried. The edges, where standards were spotted, were excised and sites of L-aspartate and L-asparagine were determined by spraying with a solution of 0.5% ninhydrin in absolute ethanol. The bands of radioactive L-aspartate and L-asparagine, located according to the unlabelled standards, were excised and put separately into vials with Scintivers™ II fluid. The radioactivity and quantity of L-aspartate and L-asparagine were determined by Beckman 60001C scintillation counter. The total radioactivity incorporated into L-asparagine were normalized to the same amount of enzyme used. The specific activity of the labelled L-aspartate (800 cpm/nmole) was determined after taking into account dilution factor and the percent of quenching associated with ^{14}C (25%), using paper chromatography.

All experiments were done in triplicate, and the data collected were evaluated by taking average of the samples from which the background (blank, labelled L-aspartate added to the chase) was subtracted.

Determination of K_d for L-Aspartate

In experiments to determine the K_d for L-aspartate, the following protocol was used. A 160 μ l solution of 50 mM Tris-HCl, (pH 8.0), containing 10.0 mM ATP, 12.0 mM MgCl₂, 2 nmole ASB, and labelled L-aspartate (0.15-0.53 mM) was incubated at 37°C for two minutes. A 65 μ l chase solution was added such that the final concentrations of substrates were: 50 mM Tris-HCl, pH 8.0, 12.0 mM ATP, 15.0 mM MgCl₂, 10 mM L-glutamine, and 30 mM unlabelled L-aspartate. The radioactivity and quantity of L-aspartate and L-asparagine were determined as before.

Isotope Partitioning Experiments with Radioactive ATP, Glutamine- and Ammonia-Dependent Reactions

A 120- μ l solution of 50 mM Tris-HCl (pH 8.0), containing 0.5 mM [2,8-³H]ATP (1300 cpm/nmole), 2 mM MgCl₂, and 1 nmole of ASB was incubated at 37°C for three minutes after which 65 μ l chase solution was added such that the final concentrations of substrates were: 50 mM Tris-HCl, pH 8.0, 30 mM ATP, 31 mM MgCl₂, 10 mM L-glutamine, and 10 mM unlabelled L-aspartate was added. The mixture was rapidly mixed by vortex for 3 sec. after which it was quenched by addition of 20 μ l of 4 M TCA. A control was done in which L-aspartate was omitted from the chase solution to account for other contaminating ATPase activities.

In experiments that included both L-aspartate and labelled ATP in the pulse solution, the concentration of L-aspartate in the pulse was 2.0 mM.

In experiments that included both L-glutamine and labelled ATP in the pulse solution, the concentration of L-glutamine in the pulse was 3.0 mM.

In experiments that included both NH_3 and labelled ATP in the pulse solution, the concentration of NH_3 in the pulse was 100 mM. The final concentration of NH_3 following the addition of the chase solution was 165 mM.

Following the quenching, the reactions were centrifuged for 5 min. Aliquots (5 μl) of the reaction mixtures were spotted on DE-81 anion-exchange chromatography paper. A mixture of unlabelled ATP, ADP and AMP was also loaded on both edges of the paper to serve as standards. After drying, the paper was developed using 1/50 saturated ammonium acetate (pH 2.8) as eluant. The chromatography was stopped after 3 hours, and the paper air dried, and unlabelled nucleotides were visualized on the paper by UV absorbance at 254 nm. The bands of radioactive ADP, ATP and AMP, located according to the unlabelled standards, were cut, put into vials with ScintiVers™ II fluid. The radioactivity and quantity of AMP, ADP and ATP were determined by Beckman 60001C scintillation counter. The total radioactivity associated with AMP were normalized to the same amount of enzyme used. The specific activity of the labelled ATP (1300 cpm/nmole) was determined after taking into account the dilution factor and the percent

of quenching associated with tritium (90%), using paper chromatography.

All studies were done in triplicate, and the data collected were evaluated by taking average of the samples from which the background was subtracted.

Aspartate-Dependent ATP Hydrolysis

The assay mixture (in all experiments, the reaction volume was 100 μ l) was consisted of the following: 50 mM Tris-HCl (pH 8.0), 2 mM L-aspartate, 2 mM $MgCl_2$, 0.5 mM [2,8- 3H]ATP (600 cpm/ nmole) and 0.5 nmole ASB. Assay mixtures were incubated at 37°C, and reactions were terminated by addition of 25 μ l of 4 M TCA at the indicated times. A control was done in a similar manner except the TCA was added prior to the incubation to account for the background from labelled ATP. A second control was done in which L-aspartate was omitted from the reaction mixture to account for other contaminating ATPase activity. The specific activity of labelled ATP was determined as described above.

Two other experiments were performed in the same manner except inorganic pyrophosphatase and/or pyrophosphate reagent was added to the reaction mixtures (the reaction volume was 100 μ l). Assay mixtures were treated as described before.

The ATP K_m for this reaction was obtained under the following conditions. The assay mixtures (100 μ l) contained 50 mM tris-HCl (pH 8.0), 1 mM L-aspartate, 2 mM $MgCl_2$ and

varying concentration of ATP (0.005-0.4 mM) (30,000 cpm/reaction). The assay mixtures were incubated 37°C for 3 min, and reactions were terminated by addition of 15 μ l of 4 M TCA at the indicated times. The control was done in which L-aspartate was removed from the reaction mixture to account for other contaminating ATPase activity.

Following the quenching, the reactions were treated as described before, and radioactivity and quantity of AMP, ADP and ATP were determined by Beckman 60001C scintillation counter. The total counts (30,000 cpm per reaction) was calculated by taking into account the dilution factor and the percent of quenching associated with tritium (90%), using paper chromatography.

Theory

Isotope trapping was used to obtain information about the order of addition of substrates for both the glutamine- and ammonia-dependent reactions of ASB. The following scheme illustrates the experimental procedure used. Enzyme and labelled substrate (*A) are incubated (pulse). This is followed by rapid dilution with a chase solution, containing a large excess of unlabelled substrate A and of the complementary reactants, B and C, which are allowed to react and stopped by a denaturant (acid or base) (Rose, 1980).



The labelled substrate has three fates; it can dissociate from the EA^* complex or it can dissociate from EA^*BC complex or it can incorporate into the product. The ability to trap A^* as P^* indicates that EA is formed in a catalytically competent manner and that A can bind first. If, however, product formation requires that B and/or C binds the enzyme before A , as in the case of an ordered mechanism, no labelled product will form. The trapping of the labelled substrate as product also requires that dissociation of A^* from any of the complexes, $(E.A^*)$, or $(E.A^*BC)$ be slow enough that a measurable quantity of the labelled substrate can proceed toward product formation. Therefore, the failure to trap A^* as P^* could be due to the following: the $E.A$ complex may not be catalytically competent (A must bind after B and C), A may dissociate from $E.A$ complex, or it may dissociate from $E.ABC$ complex (Rose, 1980).

Results

Isotope Partitioning Experiments with Radioactive L-Aspartate, Glutamine- and Ammonia-Dependent Reactions

Table 2.1 summarizes the results for both the glutamine- and ammonia-dependent AS reactions. A solution containing 1 nmole of AS, 0.50 mM ^{14}C -L-aspartate and 2 mM MgCl_2 was incubated for two minutes. Then a chase solution, containing a 60-fold excess of unlabelled L-aspartate and saturating concentrations of ATP, L-glutamine, and MgCl_2 , was added. This was followed by quenching and product analysis. When radioactive L-aspartate was the only substrate in the pulse, very little radioactive L-aspartate (0.10 ± 0.03 nmole), for every nmole of AS, was found trapped as L-asparagine. When the above experiment was modified to include ATP in the pulse, for every nmole of AS enzyme, about 0.90 ± 0.03 nmole of L-aspartate was trapped as labelled L-asparagine. When L-glutamine was included in the pulse with radioactive L-aspartate, about 0.12 ± 0.06 nmole of L-aspartate was trapped as labelled L-asparagine.

The isotope partitioning experiment with labelled L-aspartate was also performed for the ammonia-dependent reaction of AS. In the case where NH_3 (100 mM) was used in the pulse with radioactive L-aspartate, the chase solution was as described above except NH_3 was substituted for L-glutamine to a final concentration of 165 mM. L-aspartate

(0.15 ± 0.10 nmole) was trapped as radiolabelled L-asparagine, for every nmole of AS. When the above experiment was modified to include ATP in the pulse, about 0.70 ± 0.10 nmole of L-aspartate was trapped as labelled L-asparagine.

Using the isotope trapping methods, the K_d for L-aspartate was found to be 0.065 mM (± 0.02). The K_d was obtained from a double reciprocal plot of $1/[\text{nmole of trapped L-asparagine}]$ versus $1/\text{L-aspartate}$ (Fig. 2.1). The fact that reactivity is measured during a single catalytic turnover, therefore measuring the binding of L-aspartate (labelled), verifies that this is the K_d .

Isotope Partitioning Experiments with Radioactive ATP, Glutamine- and Ammonia-Dependent Reactions

Table 2.2 summarizes the results for both the glutamine- and ammonia-dependent AS reactions. A solution containing 1 nmole of AS, 0.50 mM labelled ATP and 2 mM MgCl_2 was incubated for three minutes. Then a chase solution was added to it, containing a 60-fold excess of unlabelled ATP and saturating concentrations of L-aspartate, L-glutamine, and MgCl_2 , followed by quenching and product analysis. When radioactive ATP was the only substrate in the pulse, 0.43 ± 0.10 nmole of ATP was found trapped as AMP, for every nmole of AS. When the above experiment was modified to include L-aspartate (2 mM) in the pulse, about 2.2 ± 0.25 nmole of ATP was trapped as AMP. When L-glutamine (3.0 mM) was included in

the pulse with radioactive ATP about 0.92 ± 0.06 nmole of ATP was trapped as AMP.

In the case where NH_3 (100 mM) was used in the pulse with radioactive ATP, the chase solution was as described above, except 65 mM NH_3 was substituted for L-glutamine, 0.2 ± 0.07 nmole of ATP was trapped as AMP, for every nmole of AS. The amount of ATP trapped in this experiment (0.2 nmole) is half of the amount trapped when labelled ATP was the only substrate in the pulse, for glutamine-dependent reaction (0.43 nmole).

Aspartate-Dependent ATP Hydrolysis

In the isotope partitioning experiment where both L-aspartate and labelled ATP were included in the pulse, for every nmole of AS enzyme, 2.2 ± 0.25 nmole of labelled ATP was trapped as labelled AMP but theoretically no more than 1 nmole of ATP should be trapped as AMP. This suggests that ATP hydrolysis may be occurring in the pulse, prior to the addition of chase solution that contains all the substrates. If this is the case, it should be possible to detect labelled ATP as labelled AMP in the absence of any nitrogen source. The following experiments were performed using labelled ATP, as described under Materials and Methods, and formation of labelled AMP was measured as a function of time in the absence of any nitrogen source. The rate of AMP formation was 0.3 nmole/min, which was linear with time for 15 min (Fig.

2.1). The rate of AMP formation was increased when pyrophosphate reagent or inorganic pyrophosphatase was present (3-4 times). No ATP hydrolysis (AMP formation) was observed in the control where L-aspartate was omitted from the reaction mixture (data not shown), suggesting that ATP hydrolysis is dependent on the presence of L-aspartate. It was possible that the ATP hydrolysis, in the presence of L-aspartate, was due to contaminating ammonia present in the reaction mixture, allowing the synthesis reaction (ammonia-dependent) to occur. To account for any possible contaminating NH_3 that could contribute to the ATP hydrolysis (AMP formation), the above experiment was carried out (for 40 minutes), using unlabelled ATP, and formation of L-asparagine was measured as a function of time using HPLC amino acid analysis. Amino acid analysis is performed on an applied Biosystems 130 A separation system (Schuster et al., 1993). No L-asparagine was detected even after 15 minutes. Very little L-asparagine (0.03 nmole/min) was detected after 20 minutes of incubation, suggesting that the contaminating NH_3 is responsible for the formation of only 1/10 of the AMP. If ATP hydrolysis was due to the presence of contaminating ammonia, stoichiometry would be observed between formation of L-asparagine and AMP.

Table 2.1 Trapping of L-aspartate from Complexes in the Steady State, Using (^{14}C) L-aspartate, Ammonia- and Glutamine-Dependent Reactions.

<u>Glutamine-Dependent</u>	<u>Pulse Condition</u>	<u>nmole of (^{14}C) Asn</u>
	L-Asp*	0.10 ± 0.03
	L-Asp* + ATP	0.90 ± 0.03
	L-Asp* + L-Gln	0.12 ± 0.06
<u>Ammonia-Dependent</u>	<u>Pulse Condition</u>	<u>nmole of (^{14}C) Asn</u>
	L-Asp* + NH_3	0.15 ± 0.07
	L-Asp* + ATP	0.70 ± 0.10

Isotope trapping experiments were performed under conditions described in Materials and Methods. All variations were done in triplicate and evaluated by taking the average from which the background was subtracted.

Table 2.2 Trapping of ATP from Complexes in the Steady State, Using (^3H) ATP, Ammonia- and Glutamine- Dependent Reactions.

<u>Glutamine-Dependent</u>	<u>Pulse Condition</u>	<u>nmole of (^3H) AMP</u>
	ATP*	0.43 ± 0.10
	ATP* + Asp	2.20 ± 0.25
	ATP* + L-Gln	0.92 ± 0.06
<u>Ammonia-Dependent</u>	<u>Pulse Condition</u>	<u>nmole of (^3H) AMP</u>
	ATP* + NH_3	0.19 ± 0.07

Isotope trapping experiments were performed under conditions described in Materials and Methods. All variations were done in triplicate and evaluated by taking the average from which the background was subtracted.

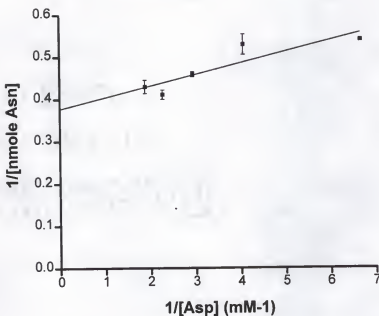


Fig. 2.1 Determination of K_d for Aspartate. A 160 μ l solution of 50 mM Tris-HCl, (pH 8.0), containing 10.0 mM ATP, 12.0 mM $MgCl_2$, 2 nmole ASB, and labelled L-aspartate (0.15-0.53 mM) was incubated at 37°C for two minutes. A 65 μ l chase solution was added such that the final concentrations of substrates were: 50 mM Tris-HCl, pH 8.0, 12.0 mM ATP, 15.0 mM $MgCl_2$, 10 mM L-glutamine, and 30 mM unlabelled L-aspartate. Following the quenching, the reactions were treated as described under Materials and Methods, and radioactivity and quantity of L-aspartate and L-asparagine were determined as described before.

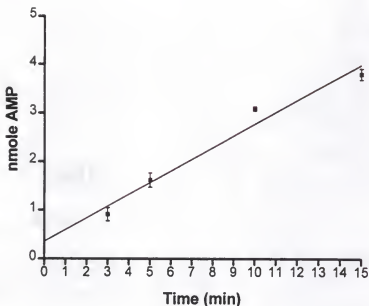


Fig. 2.2 Rate of AMP formation as a function of time. The assay mixtures (100 μ l) contained 50 mM Tris-HCl (pH 8.0), 0.5 mM ATP (600 cpm/ nmole), 2 mM L-aspartate, 2 mM $MgCl_2$ and 0.5 nmole of ASB. Assay mixtures were incubated at 37°C, and reactions were terminated by addition of TCA at the indicated times. Following the quenching, the reactions were treated as described under Materials and Methods, and radioactivity and quantity of AMP, ADP and ATP were determined as described before.

Discussion

To determine the order of substrate binding, isotope trapping experiments were done using either L- $[^{14}\text{C}(\text{U})]\text{Aspartate}$ or $[2,8\text{-}^3\text{H}]\text{ATP}$ in the presence or absence of other substrates. Our results, for the glutamine-dependent AS reaction, revealed little trapping (10%) of L-Asp* as L-Asn* when radioactive L-aspartate was used in the pulse in the presence or absence of L-glutamine. These data suggest that either L-aspartate can bind the free enzyme in a catalytically competent manner, or that it dissociates from binary (E-Asp*) or the ternary complex (E-Asp*-Gln) faster than it goes on to form the product. When isotope partitioning experiments were done with ATP in addition to the L-Asp* in the pulse solution, 90% of E-Asp*-ATP was trapped as L-Asn*. The ability to trap radioactive L-aspartate when ATP was included in the pulse solution suggests that the E-Asp*-ATP complex is formed in a catalytically competent manner. This strongly suggests that ATP binds free enzyme first followed by L-aspartate binding. An alternative suggestion is that in the presence of ATP, the rate of dissociation of L-Asp* decreased compared to the rate of overall product formation. What is very clear from these observations is that the binding and hydrolysis of L-glutamine is not required prior to the addition of ATP and L-aspartate, or no labelled L-asparagine would have been

trapped in the absence of L-glutamine. This is strikingly different from the mechanisms for AS suggested by Chou, 1970, Milman et al., 1980, Markin et al., 1981 and Hongo and Sato, 1985, who proposed that the binding of L-glutamine had to occur prior to ATP and L-aspartate binding, in order for the overall synthesis of L-asparagine to occur.

When isotope partitioning experiments were done with labelled ATP, in the absence of L-aspartate or L-glutamine, 50% of the E-ATP* complex was trapped as AMP*. This shows that the E-ATP* complex is formed in a catalytically competent manner, further suggesting that ATP binds free enzyme first. Under these conditions, only half of the enzyme bound ATP* was converted to AMP*. It is possible that ATP* was bound to the enzyme and partly equilibrated with the subsequently added unlabelled ATP, or that it dissociated from binary (E-ATP*) faster than it would go on to form the product. It is also possible that ATP* was bound to an additional site (an allosteric site, for which there is no evidence at this time), that was inhibitory to the ATP binding for the synthesis, therefore causing less trapping.

Using the isotope trapping techniques, we were unable to obtain the K_d for ATP. To determine the K_d for ATP, the concentration of the labelled ATP was varied (0.01-0.5 mM) in the pulse. Surprisingly, no trapping was detected below 0.5 mM ATP. It is possible that some ATP* equilibrated with the subsequently added unlabelled ATP, or that it dissociated

from binary (E-ATP*) faster than it would go on to form the product.

When isotope partitioning experiments were done with L-aspartate in addition to the ATP* in the pulse solution, E-ATP*-Asp was trapped as AMP*. These data suggested that the E-ATP*-Asp complex was formed in a catalytically competent manner, but the amount of product was puzzling. The fact that "trapped" AMP* was not stoichiometric with the amount of enzyme (220%) present suggested that either ATP hydrolysis was occurring prior to the addition of chase solution or product formation was occurring in the time scale of the pulse. We attempted to determine if the net ATP hydrolysis observed was an activity of the synthetase itself or that of some other contaminant. Our first results showed that the production of AMP was found to be L-aspartate dependent and was not stimulated by aspartate-tRNA. This suggests that the reaction was not a contaminant and not surely aspartyl tRNA synthetase. The fact that very little L-asparagine was detected during this reaction ruled out the possibility of *E. coli* ASA, with an apparent K_m for ammonia of less than $1 \mu M$ (unpublished data, Boehlein), being involved. The aspartate-dependent hydrolysis of ATP represented in Reaction 4,



which is linear with time, is only 1/100 of the overall reaction rate. As shown in the Figure 2.2, a value of about

3.8 nmole was reached indicating that the L-aspartate-dependent hydrolysis, in the 15 minutes period, was about 8-fold turnover of the enzyme. The effect of the presence of the contaminating NH_3 , determined by L-asparagine formation, seems to be responsible for the formation of only 1/10 of AMP*. This would eliminate the possibility of synthesis reaction by ASB being responsible for the most of the AMP* formation. Extrapolation of the line (Fig. 2.2) predicts an intersection point of approximately 0.5 nmole AMP/0.5 nmole AS, stoichiometric with the amount of enzyme, further supporting that the reaction is not a contaminant, and that the chemistry is very fast compared to the release of the products. However, whether L-aspartate attacks ATP, forming aspartyl-AMP, or L-aspartate stimulates ATP hydrolysis is not clear at this moment. The addition of pyrophosphate reagent or pyrophosphatase to the reaction mixture produced some increase in the rate of this reaction (3-4 fold). The slowness of the partial reaction to the overall synthetase reaction is not a limit to its acceptance as bona fide partial reaction of AS, because enzyme theory recognizes the phenomenon of "substrate synergism" (Bridger et al., 1968). That is the accelerating effect on a partial reaction of the presence of the complementary substrate, in this case L-glutamine, of the enzyme. The hydrolysis seems to be irreversible as shown in reaction 4, since it has not been possible to detect $^{32}\text{PP}_i$ -ATP exchange for ASB (unpublished

data), presumably because PP_i and AMP dissociate from the enzyme during this catalytic process.

Given the above data it was somewhat surprising that when L-glutamine was included in the pulse, about 90% of E-ATP*-Gln was trapped as AMP*. This suggests that an E-ATP*-Gln complex is formed in a catalytically competent manner. The E-ATP* complex seems to be tightly bound in the presence of L-glutamine since the amount of the AMP* trapped is stoichiometric with the amount of enzyme present. No stimulation of ATP hydrolysis was observed by L-glutamine (data not shown). But rather, it seems that in the presence of L-glutamine, ATP binding to the active site is stabilized.

The lines of evidence presented here indicate that for the glutamine-dependent reaction of AS the mechanism is ordered, with ATP binding first to free enzyme. However, we can not rule out some alternative ordered mechanism with L-aspartate binding free enzyme, because a small amount of L-Asp* was trapped as L-Asn* when no ATP was included in the pulse.

In the case of the ammonia-dependent AS reaction, very little L-Asp* (15%) was trapped as L-Asn* when NH_3 was included in the pulse solution with radioactive L-aspartate, suggesting that the presence of NH_3 most likely increased the rate of product formation relative to the dissociation rate of L-Asp* from free enzyme. The ability to trap radioactive L-aspartate (70%) when ATP was included in the pulse solution, shows that an E-Asp*-ATP complex is formed in a

catalytically competent manner, implying that ATP has to bind first. When isotope partitioning experiments were done with labelled ATP and NH_3 in the pulse, 20% of the $\text{E-ATP}^*\text{-NH}_3$ was trapped as AMP^* . This suggests that the NH_3 binding is not required prior to the binding of ATP^* and/or L-Asp^* or the level of AMP^* and/or L-Asn^* trapped should be close to the amount of enzyme present. The data also suggest that the mechanism is ordered such that ATP binds first followed by L-aspartate binding.

The amount of *ATP trapped as *AMP when NH_3 was included in the pulse with labelled ATP (0.2 nmole), for every nmole AS, is less than the amount trapped when *ATP alone was in the pulse for the glutamine-dependent reaction (0.43 nmole). It is possible that NH_3 (100 mM) interfered with the ATP binding. It is also possible that presence of L-glutamine in the chase, by stabilizing the ATP binding, prevented the dissociation of the bound *ATP from the binary (E-ATP^*) complex, so that it would go on to product.

Major conclusions derived from the isotope partitioning experiments regarding the kinetic mechanism of ASB are as follows:

1. The enzyme catalyzes aspartate-dependent ATP hydrolysis. This partial reaction, although very slow (1/100 of the overall rate), provides a direct evidence for the mechanism of *E. coli* ASB, in which the hydrolysis requires no nitrogen source. Argininosuccinate synthetase is another example where such partial reaction has been observed

(Rochovansky and Ratner, 1967). The enzyme catalyzed conversion of citrulline to arginine involves an ATP-dependent condensation between citrulline and L-aspartate. Both L-aspartate and citrulline could induce cleavage of ATP. The time course of the aspartate-dependent hydrolysis differed from that of citrulline-dependent. The aspartate-dependent hydrolysis was linear over the course of experiment (30 min), while the citrulline-dependent hydrolysis reached a maximum in 2 minutes. The aspartate-dependent hydrolysis reached a value that was about 3-fold turnover of the enzyme. The cleavage was suggested to be irreversible, since it had not been possible to detect an aspartate-dependent PP_i -ATP exchange reaction. However, the citrulline-dependent hydrolysis reached a value that was stoichiometric with the amount of enzyme present. Basically, the reaction had come to a halt, probably because the products remained enzyme bound.

2. The mechanism is probably ordered, with ATP binding first and L-aspartate second, the preferred, but not mandatory order.

3. The binding and hydrolysis of L-glutamine or the binding of ammonia is not required prior to ATP and L-aspartate binding for the synthesis reaction.

These are significantly different from what were reported in the past for the AS mechanism. The differences seem to be due to the fact that the previous investigators relied solely on steady state kinetic methods, and isotope trapping was not used. In addition, they failed to consider

other models to explain their data, as discussed in the next chapter.

CHAPTER 3
SUBSTRATE BINDING AND PRODUCT RELEASE OF ASPARAGINE
SYNTHETASE B STUDIED BY STEADY STATE KINETICS

Introduction

The proposed kinetic mechanisms for the glutamine-dependent reaction of AS has been reported for the enzymes from beef (Schuster et al., 1981) and mouse (Milman et al., 1980) pancreases, and rat liver (Hongo and Sato, 1985), as discussed in chapter 1. In all three cases, steady state kinetic methods were used to elucidate the kinetic mechanism. There are dramatic differences between the data presented, but all three reports agree that L-glutamine is the first substrate to bind. Milman et al. (1980), Markin et al. (1981) and Hongo and Sato, (1985) all present mechanisms that start with a glutaminase reaction mainly because AS exhibits a glutaminase activity.

There are major differences between the data presented in the past and that for *E. coli* ASB. Using isotope partitioning techniques, evidence was presented regarding the kinetic mechanism of ASB. The results suggested that, (a) the kinetic mechanism for glutamine- and ammonia-dependent reactions is preferentially ordered, with ATP binding first followed by addition of L-aspartate, (b) the enzyme catalyzes an aspartate-dependent ATP hydrolysis that requires no

nitrogen source, and (c) glutamine binding and hydrolysis is not required prior to the binding of the other substrates. To determine whether the difference in the conclusions was associated with using a different enzyme or with the techniques employed, the following initial velocity experiments, including studies with inhibition by products and substrate analogs, were performed. The experimental approach used here was that of Frieden (1959), which also allowed us to distinguish the sequential mechanism from ping-pong mechanisms.

Materials and Methods

Chemicals and Reagents

Trichloroacetic acid (TCA) was purchased from Fisher Scientific (Orlando, FL). The pyrophosphate reagent for following PP_i production, MgCl₂, ATP, L-aspartate, L-asparagine, L-glutamine, L-glutamate, AMP, PP_i, ammonium acetate, L-glutamic acid γ -monohydroxamate, ninhydrin, Tris(hydroxymethyl) aminomethane (Tris-HCl), and Bis(2-hydroxyethyl)iminotris (hydroxymethyl)methane (Bis Tris), were all purchased from Sigma. Dithiothreitol (DTT) was obtained from Promega Corporation (Madison, Wisconsin).

Expression of the Protein and Purification

Protein expression, cell culture and enzyme purification was carried out as described before (chapter 2).

Protein Concentration Determination

Protein concentration was measured using Bio-Rad Protein Assay (Bradford, 1976). Mouse immunoglobulin G was used to obtain a standard curve.

Enzyme Assays

The velocities were measured spectrophotometrically by assaying for PP_i production (O'Brian, 1976), as described in chapter 2. The assay mixture contained the following components: 50 mM Tris-HCl (pH 8.0), and varying amounts of ATP (0.2-0.5 mM), L-aspartate (0.2-0.7 mM), L-glutamine (0.2-0.7 mM), AMP (3-15 mM), L-glutamate (5-50 mM), L-asparagine (0.05-0.25 mM), and ammonium acetate (3-50 mM). MgCl₂ concentration was kept constant (3 mM), unless stated otherwise. The volume of the total reaction mixture was kept at 160 µl. All reactions were carried out at 37°C, using 7.4 µg of enzyme per reaction. In all experiments, L-glutamine solutions were freshly prepared using recrystallized L-glutamine (Sheng et al., 1993). Under all experimental conditions initial velocity was verified.

All studies were done in duplicate, and the data collected were evaluated by taking average of the samples

from which the background (representing the ATPase activity) was subtracted. Velocities were reported as nmole of PPi produced per minute per milligram of protein. The data were then plotted in the form of double reciprocal plot or a Dixon plot (Dixon, 1953) depending upon the type of experiments and weighted using the computer program, Ultrafit, purchased from Biosoft.

When PPi was used in product-inhibition studies, the velocities were measured by monitoring the conversion of L-aspartate to L-asparagine by HPLC amino acid analysis (Sheng et al., 1993). The assay mixture (in all experiments, the reaction volume was 200 μ l) was consisted of the following: 50 mM Tris-HCl (pH 7.0), and varying amounts of ATP, L-aspartate, L-glutamine, and PPi. Value of pH 7.0 was chosen to overcome precipitation of $MgCl_2$ by PPi. Concentration of $MgCl_2$ was kept so that it would be 1 mM above ATP and PPi. Assay mixtures were incubated for 15 minutes at 37°C after addition of enzyme (1 μ g/reaction mixture) and terminated by addition of 50 μ l of 20% (1.22 M) trichloroacetic acid (TCA) containing 0.2 mM L-histidine as an internal control. The controls were performed in a similar pattern except that TCA was added prior to the incubation. An aliquot of the reaction mixture (10 μ l) was then injected into the amino acid analyzer. Amino acid analysis is performed on an applied Biosystems 130 A separation system (Sheng et al., 1993). Under all experimental conditions enzyme stability and

initial velocity were verified, doing time course experiments.

All studies were done in triplicate, and the data collected were evaluated by taking average of the samples. Velocities were reported as nmole of L-asparagine produced per minute per milligram of protein.

Stoichiometry of PP_i and L-Glutamate

In this experiment the assay mixtures (100 μ l) contained 50 mM Tris-HCl (pH 8.0), 1 mM ATP, 1 mM L-aspartate, 5 mM MgCl₂ and varying concentration of L-glutamine (0.1-20 mM). The assay mixtures and the enzyme were preincubated at 37°C for 3 min. The reactions were initiated by the addition of the enzyme (3 μ g/reaction) and were incubated 37°C for 4 min before being terminated by addition of 20% TCA (15 μ l). Modified glutaminase assay (Bernt and Bergmeyer, 1974) was used to measure L-glutamate concentrations. PP_i production was measured by modifying the continuous spectrophotometric assay (O'Brian, 1976) to an end point assay. In this case, 385 μ l of the coupling buffer (50 mM imidazole, pH not adjusted, and 20 μ l of pyrophosphate reagent, which was originally reconstituted in 1 ml of ddH₂O), was added to the reaction mixtures, following TCA kill, and incubated at room temperature for 30 min. The absorbance of the resulting solution was measured at 340 nm, and the amount of PP_i produced in the reaction determined from a standard curve.

The ratio of L-glutamate/PPi *versus* concentration of L-glutamine was used in plotting.

Results

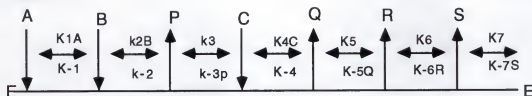
Initial Rate Studies

For determination of the order of the addition of the substrates in the *E. coli* ASB, initial velocity studies were performed and substrates varied in a systematic way. In particular, to determine the order of addition of substrates in the glutamine-dependent reaction, the concentrations of two of the three substrates, L-aspartate, L-glutamine and ATP were varied while maintaining the third substrate fixed and subsaturating in the absence of any products (Frieden, 1959). Keeping the concentration of L-glutamine fixed and subsaturating, the plot of $1/v$ *versus* $1/[L\text{-aspartate}]$ at different ATP concentrations (or *vice versa* (data not shown)) was found to be intersecting (Fig. 3.1A) which was confirmed by slope and intercept plots (Fig. 3.1B). Parallel lines were obtained when $1/v$ *versus* $1/[L\text{-Glutamine}]$ (constant and subsaturating L-aspartate) was plotted at varied ATP concentrations, and $1/v$ *versus* $1/[L\text{-aspartate}]$ (constant and subsaturating ATP) was plotted at varied L-glutamine concentrations (Fig. 3.2A and Fig. 3.3A, respectively). These were confirmed by slope and intercept plots (Fig. 3.2B and Fig. 3.3B). Interestingly, this suggests that a product is

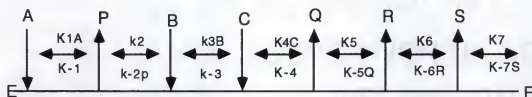
released between the addition of each pair of substrates. Kinetic parameters determined from these data were K_{ASP} of 0.05 mM, K_{ATP} of 0.05 mM, and K_{Gln} of 0.20 mM.

Of all the possible mechanisms available, two mechanisms that have been shown from the literature, to be associated with AS are as follows: Scheme A, the bi-uni-uni addition of substrates, and Scheme B, the uni-uni-bi addition of substrates.

(Scheme A)



(Scheme B)



Using the method of Fromm (1975), the steady-state initial velocity equations were derived for the two mechanisms shown above, assuming no product present. Equations 1 and 2 were derived from Schemes A and B, respectively.

$$\text{equation 1)} \quad 1/v = 1/V (\phi/[A] + \phi/[B] + \phi/[AB] + \phi/[C] + 1)$$

$$\text{equation 2)} \quad 1/v = 1/V (\phi/[A] + \phi/[B] + \phi/[C] + \phi/[BC] + 1)$$

Equation 1 predicts that substrate C (L-glutamine) affects only the intercept of the $1/v$ versus $1/[A]$ or versus $1/[B]$ (ATP and L-aspartate or vice versa) which would result in parallel lines, characteristic of a ping-pong mechanism, which indicates that the addition of each pair of substrates are separated by the release of a product. However, equation 1 indicates that substrates A and B (ATP and L-aspartate or vice versa) affect both the slope and intercept of $1/v$ versus $1/[B]$ and versus $1/[A]$ plots, respectively, resulting in intersecting lines, which suggests that the addition of A and B is sequential. Similarly we see from equation 2 that substrate A (L-glutamine) affects only the intercept of the $1/v$ versus $1/[B]$ or $1/[C]$ plots, predicting parallel lines. Equation 2 also predicts that substrates B and C (ATP and L-aspartate or vice versa) affect both the slope and intercept of the plots of $1/v$ versus $1/[C]$ and versus $1/[B]$, respectively, resulting in intersecting lines. In other words, our initial rate studies agree with the theoretical results obtained for both equations 1 and 2!

The ammonia-dependent AS reaction was examined kinetically. It was found that the plot of $1/v$ versus $1/[ATP]$ at different L-aspartate concentrations, keeping the concentration of ammonium acetate fixed (50 mM), shows intersecting lines (Fig. 3.4A). This was verified by plotting the slope and intercept (Fig. 3.4B). A similar pattern was

observed when $1/v$ versus $1/[ATP]$ at different L-aspartate concentrations was plotted (data not shown). These data suggest that for the ammonia-dependent reaction, the addition of ATP and L-aspartate is sequential. The plots of $1/v$ versus $1/[ATP]$ at varied ammonium acetate concentrations, keeping L-aspartate constant and subsaturating (1 mM), (Fig. 3.5A) and of $1/v$ versus $1/[L-aspartate]$ at varied ammonium acetate concentrations, keeping ATP constant and subsaturating (1 mM), (Fig. 3.6A) show parallel lines. This was confirmed by slope and intercept plots (Fig. 3.5B and Fig. 3.6B, respectively). These data suggest that the addition of each pair of substrates are separated by the release of a product. The results for the ammonia-dependent AS reaction are in agreement with the theoretical predictions of equation 1. Equation 1 predicts that NH_3 (C) affects only the intercept of the $1/v$ versus $1/[ATP]$ or versus $1/[L-aspartate]$ plot (A and B or vice versa) which would result in parallel lines. Equation 1 also predicts that substrates ATP and L-aspartate (A and B or vice versa) affect both the slope and intercept of $1/v$ versus $1/[L-aspartate]$ and versus $1/[ATP]$ plots, respectively, resulting in intersecting lines. The data indicate that the addition of ATP and L-aspartate is sequential, therefore suggesting that ATP and L-aspartate will bind first, presumably forming aspartyl-AMP. This is followed by release of PP_i (P) and addition of the NH_3 . However, the result for the ammonia-dependent reaction would not be comparable with those predicted for equation 2 (see

discussion). Kinetic parameters determined from these data were K_{Asp} of 0.05 mM, K_{ATP} of 0.05 mM, and K_{NH_3} of 10.0 mM.

The initial rate study of beef pancreas AS (Markin et al., 1981) showed intersecting lines for the plot of $1/v$ versus $1/\text{ATP}$ at varied L-glutamine concentration, suggesting ATP and L-glutamine bind sequentially. This was completely different from the observations made by Milman et al., 1980, Sato, 1985 and by us. The double reciprocal plot of the velocity dependence on ATP at various constant concentrations of the L-glutamine was shown to be parallel (Fig. 3.2A), which indicates that the addition of each pair of substrates is separated by the release of a product. To resolve this difference, the following initial rate experiment was performed using L-glutamine and an alternative substrate, L-glutamic acid γ -monohydroxamate (LGH). Control experiments showed that LGH was a competitive inhibitor of L-glutamine ($K_i = 0.2 \text{ mM}$) (Fig. 3.7). For the initial rate experiment, the concentration of ATP was varied (0.1-0.7 mM), while keeping L-aspartate constant and subsaturating (1 mM), at fixed concentration of L-glutamine and LGH (0.2 mM). The velocities were measured spectrophotometrically as described before. The plot of $1/v$ versus $1/\text{ATP}$ at fixed concentration of L-glutamine and LGH (Fig. 3.8) shows that the substitution of LGH for L-glutamine did not have any effect on the slope of the line, characteristic of a ping-pong mechanism. This indicates that the addition of ATP and L-glutamine are separated by the release of a product (see discussion).

In order to determine the effect of substrate saturation on the kinetic behavior, the initial rate studies were also performed under saturating conditions of the substrates. When the concentration of L-glutamine was kept constant and saturating (20 mM), the plot of $1/v$ versus $1/[L\text{-aspartate}]$ at different ATP concentrations (Fig. 3.9) showed parallel lines, suggesting that the addition of each pair of substrates was separated by the release of a product (see discussion). In the case where L-aspartate was kept constant and saturating (> 2 mM), the plot of $1/v$ versus $1/[L\text{-glutamine}]$ at varied ATP concentration showed what appears to be substrate inhibition (Fig. 3.10). The pattern changed from parallel to intersecting. In other words, the slope of the double reciprocal plot began to increase (but not intercepts), which represents competitive substrate inhibition. The same type of observation became evident for the plot of $1/v$ versus $1/[L\text{-glutamine}]$ at varied L-aspartate concentrations when ATP was kept constant and saturating (>5 mM). Very high ATP concentration made L-aspartate become an inhibitor of synthetase reaction.

Inhibition by Substrate Analogs

Substrate analogs were tested as inhibitors of ASB to obtain more information about the substrate binding order (data provided with Dr. S. Boehlein). This alternative approach requires that a competitive inhibitor be available

for each substrate. Experimentally, the concentration of the substrate to be studied is varied at fixed varied concentration of the analog. The remaining substrates are held at fixed and subsaturating concentrations. Experimental details are described in the table legend. The substrate analogs used in this set of experiments were, AMP-PNP, β -methyl aspartate and L-glutamic acid γ -methyl ester. Table 3.1 shows the inhibition patterns for all the substrate analogs tested for the glutamine-dependent reaction of ASB. Initial velocity studies in the presence of AMP-PNP demonstrated competitive inhibition with respect to ATP, suggesting it competes with the ATP for the same site on the enzyme. AMP-PNP was found to be noncompetitive with respect to L-aspartate and uncompetitive with respect to L-glutamine. β -methyl aspartate was found to be competitive with L-aspartate and noncompetitive with respect to ATP and L-glutamine. L-glutamic acid γ -methyl ester was competitive with L-glutamine, uncompetitive with ATP and noncompetitive with L-aspartate. The rate equations for the effect of analogs (competitive inhibitors) of each substrate were derived for the two mechanisms (A and B). Although there were some disagreements, initial rate results (Table 3.1) in most cases agreed with predicted patterns obtained from rate equations for both mechanisms (see discussion).

Stoichiometry of Glutamine-dependent Reaction

E. coli ASB can function as a glutaminase (reaction 3) when L-aspartate and ATP are not present, showing that L-glutamine can be bound by the free enzyme. In order to determine the relevance of the glutaminase reaction to the glutamine-dependent synthetase mechanism, a stoichiometry experiment was performed. In this experiment, the concentration of L-glutamine was varied while keeping ATP and L-aspartate constant and subsaturating (1 mM). The concentrations of L-glutamate and PP_i produced were measured simultaneously. The synthesis of L-asparagine has been shown to be stoichiometric with PP_i formation (data not shown) under all circumstances. Stoichiometry should also be observed between formation of L-glutamate and PP_i if no glutaminase was occurring during the synthesis of L-asparagine. However, as shown in Figure 11, plotting the ratio of L-glutamate/ PP_i versus L-glutamine concentration resulted in a hyperbolic curve, approaching a plateau with increasing concentrations of L-glutamine. This shows that the L-glutamate and PP_i production is non-stoichiometric, indicating that glutaminase reaction is occurring at the same time as the synthetase reaction and at a much faster rate than the synthetase reaction as concentration of L-glutamine increases, approaching approximately 2:1.

Product Inhibition Studies

Our initial velocity studies proved somewhat inconclusive information regarding the order of addition of the substrates. To obtain additional information about the order of product release, product inhibition of the initial velocity was studied for both the L-glutamine-dependent and ammonia-dependent L-asparagine synthetase reactions. The velocities were measured spectrophotometrically by assaying for PP_i production (O'Brian, 1976). Figures 12 through 17 and Table 3.2 show the product inhibition patterns and constants for the ammonia-dependent AS reaction. When the concentration of one substrate is varied, the remaining substrates are held at fixed concentrations: ATP, 1 mM, L-aspartate, 1 mM, and ammonium acetate, 50 mM. L-asparagine was found to be competitive with respect to ammonia ($K_i = 0.08 \pm 0.025$ mM), and noncompetitive with respect to ATP and L-aspartate ($K_i = 0.190 \pm 0.002$ and 0.26 ± 0.002 mM, respectively). AMP was noncompetitive with respect to all the three substrates. The K_i for ATP, L-aspartate and ammonia were 3 ± 0.001 , 8 ± 0.001 and 15 ± 0.002 mM. The fact that L-asparagine was competitive with ammonia, suggesting they bind to the same enzyme form, allows us to place L-asparagine after ammonia (Q) followed by AMP (R).

Figures 18 through 28 and Table 3.3 show the product inhibition patterns and constants for the glutamine-dependent

AS reaction. When the concentration of one substrate was varied, the remaining substrates were held at fixed and subsaturating concentrations (1 mM). The MgCl_2 concentration was kept constant (3 mM), unless stated otherwise. L-asparagine was found to be competitive with respect to L-glutamine ($K_i = 0.015 \pm 0.003$ mM), suggesting it binds to the same enzyme form as L-glutamine. L-asparagine was noncompetitive with respect to ATP ($K_i = 0.09 \pm 0.001$ mM) and L-aspartate ($K_i = 0.27 \pm 0.001$ mM), suggesting it binds the free enzyme and enzyme-substrate complex. PP_i was competitive with respect to ATP and L-aspartate ($K_i = 0.05 \pm 0.002$ and 0.39 ± 0.01 mM, respectively). L-glutamate was a poor inhibitor and was shown to be noncompetitive with respect ATP ($K_i = 47 \pm 0.001$ mM). L-glutamate was found to be competitive with respect to L-aspartate ($K_i = 23 \pm 0.001$ mM) and noncompetitive with respect to L-glutamine ($K_i = 52 \pm 0.001$ mM). AMP was also a poor inhibitor. AMP was noncompetitive with respect to all the three substrates. The K_i for L-glutamine, L-aspartate and ATP were 14 ± 0.001 , 9 ± 0.001 , and 5 ± 0.001 mM.

For further clarification of the order of product release, more specifically the first product, the following initial velocity experiments were performed. L-aspartate and L-glutamine concentrations were varied against each other in the presence of L-glutamate (50 mM), keeping the ATP concentration constant and subsaturating (1 mM). In another experiment, concentrations of L-aspartate and L-glutamine

were varied in the presence of PPi (0.4 mM), while keeping the ATP concentration constant and subsaturating (1 mM). If L-glutamate is the first product released between L-aspartate and L-glutamine, then a double reciprocal plot of $1/v$ versus $1/[\text{L-aspartate}]$ at various L-glutamine concentrations will produce intersecting lines in the presence of L-glutamate. If however, L-glutamate is not the product released between the addition of L-glutamine and L-aspartate, then the double reciprocal plot will result in parallel lines. On the other hand, if PPi is the first product released between L-aspartate and L-glutamine, intersecting lines will be observed for the plot of $1/v$ versus $1/[\text{L-aspartate}]$, varying the L-glutamine concentration. Figures 29 and 30 show the results of $1/v$ versus $1/[\text{L-aspartate}]$ at various the L-glutamine concentrations in the presence of L-glutamate or PPi . The parallel lines in the presence of L-glutamate (Fig. 3.29) suggests that L-glutamate can not be the first product (P) released between L-aspartate and L-glutamine. Parallel lines were also observed in the presence of PPi (Fig 3.30) which suggest that PPi cannot be the first product off (see discussion).

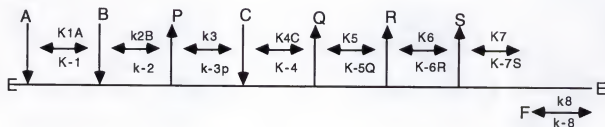
To obtain more information about the order of product release (Q, R, S), double-inhibition studies were performed for the glutamine-dependent AS reaction. This set of experiments examines the relation between the products, determining whether the two products interact with each other on the enzyme's surface. For this set of experiments, the

concentration of all the substrates was held constant (1 mM), and concentrations of two of the products were varied against each other. If L-asparagine and AMP interact with each other (are next to each other in the release order), then a Dixon plot (1953) of $1/v$ versus [L-asparagine] at various AMP concentrations will give intersecting lines (Segel, 1975). If, however, their binding is separated by another product, then the Dixon plot will show parallel lines. Figures 3.31, 3.32, and 3.33 show the dual-inhibition studies of the $1/v$ versus. [L-asparagine] and [L-glutamate] at different concentrations of L-asparagine, and AMP, accordingly. The plot of $1/v$ versus. [L-asparagine] at varied AMP concentrations (Fig. 3.31) shows intersecting lines. This shows that the presence of L-asparagine enhances AMP inhibition or vice versa, therefore, indicating that they can combine sequentially with the enzyme. The plots of $1/v$ versus. [L-glutamate] at different AMP and L-asparagine concentrations (Fig. 3.32 and Fig. 3.33) revealed parallel lines. The presence of L-glutamate would not enhance L-asparagine or AMP inhibition or vice versa, which suggests that the products are mutually exclusive. Based on these observations we are now able to place the AMP and L-glutamate release steps (R and S, respectively) after the release of L-asparagine (Q).

The rate equation for the proposed mechanism (Scheme A) was derived assuming the products P, Q, R and S were present, and the product inhibition patterns predicted were compared

with experimental results. There are some disagreements between the predicted patterns and the experimental results. Other considerations are necessary to explain the experimental data (see discussion). One of the most obvious possibilities is the existence of an isomerization step following the release of the last product shown below.

(Scheme C)



The iso-mechanism predicts a non-competitive inhibition pattern between the last product and first substrate which would otherwise be competitive. In other words, after the release of S, L-glutamate, the enzyme is in a conformation that is not accessible to A, as is indicated by the symbol F (Segel, 1975). The F form has to convert back to E by a reaction indicated by rate constants k_8/k_{-8} . The rate equation for the proposed mechanism with the iso step (Scheme C) was also derived assuming all products were present and was compared with the rate equation for the same mechanism with no iso step (Scheme A). The equation for the Scheme C was very different and much more complex than that of the

equation for Scheme A (see discussion). The differences that were useful for the comparison of the two mechanisms were as such:

$$\text{equation 3)} \quad 1/v = 1/V (\phi[RS]/[AB])$$

$$\text{equation 4)} \quad 1/v = 1/V (\phi[RS]/[AB] + \phi[RS])$$

The equation for the mechanism with no iso step (equation 3) predicts that the RS term affects only the slope of $1/v$ *versus*. $1/A$ (or $1/B$) which would result in a competitive pattern (lines intersecting on $1/v$ axis). Similarly the equation for the mechanism with iso step (equation 4) predicts that RS term affects both the slope and the intercept of the plot of $1/v$ *versus*. $1/A$ (or $1/B$) which results in a noncompetitive pattern (lines intersecting to the left of the $1/v$ axis). According to our proposed mechanism (Scheme A), A and B are ATP and L-aspartate or *vice versa*, and R and S are AMP and L-glutamate, respectively.

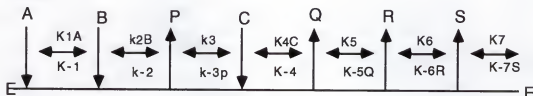
To verify if there is an isomerization step in our proposed mechanism leading to unusual product inhibition patterns, the following initial velocity experiment was performed: The concentration of L-aspartate was varied, at fixed varied concentrations of L-glutamate and AMP in a constant ratio ($[L\text{-glutamate}] = 5[AMP]$), while keeping ATP and L-glutamine constant and subsaturating (1 mM). The plot of $1/v$ *versus*. $1/L\text{-aspartate}$ (Fig. 3.34) shows intersecting lines whose intersection is to the left of $1/v$ axis (noncompetitive). This result agrees with the theoretical

prediction of equation 4, supporting a proposed mechanism with an iso step (Scheme C).

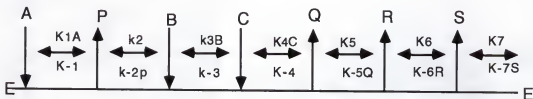
Discussion

The initial velocity patterns of the relationship between pairs of substrate obtained for both the ammonia- and glutamine- dependent reactions were similar. From these data we proposed the two mechanisms (A and B). Scheme A, the bi-uni-uni addition of substrates, and Scheme B, the uni-uni-bi addition of substrates.

(Scheme A)



(Scheme B)



The data presented for the ammonia-dependent reaction are only consistent with mechanism A (bi-uni-uni-bi ping-pong).

According to mechanism A, ATP and L-aspartate bind first, forming aspartyl-AMP. This is followed by release of PPi (P) and addition of NH₃. The results for the ammonia-dependent reaction do not support mechanism B (uni-uni-bi-bi ping-pong). According to equation 2 (derived to fit mechanism B), substrate A affects only the intercept of the 1/v versus 1/[B] or 1/[C] plots, which predicts parallel lines. This indicates that the addition of each pair of substrates is separated by the release of a product. Therefore, if mechanism B is the correct mechanism, following the addition of NH₃, a product must be released prior to the addition of the second substrate, which is not possible.

When the ammonia-dependent reaction was studied for the beef pancreatic AS (Markin et al., 1981), the kinetic mechanism was proposed to be significantly different from that of ASB. According to their previous proposed mechanism, NH₃ bound first followed by a random addition of ATP and L-aspartate. When evaluating the ammonia-dependent AS reaction, these workers found that the plots of 1/v versus 1/NH₃ at varied L-aspartate concentrations (at saturating ATP) and 1/v versus 1/NH₃ at varied ATP concentrations (with saturating L-aspartate) resulted in parallel lines. This was proposed to indicate either a random addition of ATP and L-aspartate or the release of a product between their additions. No information was provided regarding the pattern between ATP and L-aspartate (with saturating NH₃), and no experimental

evidence was provided to support the notion that the addition of ATP and L-aspartate was random.

Although our data from initial velocity studies supported a bi-uni-uni-bi ping-pong mechanism (mechanism A), for the ammonia-dependent reaction of ASB, we were still unable to determine whether the addition of ATP and L-aspartate is ordered or random. The data from isotope trapping experiments clearly indicated that the mechanism is ordered such that ATP binds first followed by L-aspartate binding (see Chapter 2). These data together support mechanism A (ordered bi-uni-uni-bi ping-pong) for the ammonia-dependent AS reaction. The rate equation and kinetic parameters have been worked out (Fromm, 1975). For this reaction the rate equation is as follows:

$$\text{equation 5)} \quad 1/v = 1/V \left(\frac{1}{[ABC] - [PQRS]} (\phi_1[C] + \phi_2[AB] + \phi_3[AC] + \phi_4[BC] + \phi_5[ABC] + \phi_6[P] + \phi_7[PQ] + \phi_8[AP] + \phi_9[CR] + \phi_{10}[PR] + \phi_{11}[QR] + \phi_{12}[ABP] + \phi_{13}[ABQ] + \phi_{14}[APQ] + \phi_{15}[BQR] + \phi_{16}[PQR] + \phi_{17}[BCR] + \phi_{18}[CQR] + \phi_{19}[ABCQ] + \phi_{20}[ABPQ] + \phi_{21}[BCQR] + \phi_{22}[BPQR]) \right)$$

The data for the glutamine-dependent AS reaction, however, are consistent with both mechanisms (A and B). According to mechanism A, a bi-uni-uni-ter ping-pong mechanism, ATP and L-aspartate sequentially bind followed by Ppi release. This is followed by L-glutamine which is the last substrate to bind. According to mechanism B, a uni-uni-bi-ter ping-pong mechanism, L-glutamine binds first followed by the release of the L-glutamate. ATP is then the second

substrate to add, followed by the addition of L-aspartate or *vice versa*.

Kinetic studies done under saturating condition provided evidence of substrate inhibition (Fig. 3.10). Under these conditions substrate inhibition was observed with ATP and L-aspartate. This is an artifact that is common in ping-pong mechanisms and has been reported for other enzymes including fatty acid synthetase (Katiyar et al., 1975), 5-enolpyruvylshikimate-3-phosphate synthase (EPSPS) (Gruys et al., 1992), UDP-N-Acetylenolpyruvylglucosamine reductase (Dhalla et al., 1995) and nucleoside diphosphate kinase (Garces and Cleland, 1969). Substrate inhibition usually is caused by the substrates binding to the improper forms of the enzyme which would result in dead-end complexes. The inhibition effect is competitive because the substrates interact with the same enzyme form (A and B with E), which is characterized by an increase in the slopes and not the intercepts of reciprocal plot. Interestingly, when the concentration of L-glutamine was kept constant and high (20.0 mM) ($100 \times K_m$), a parallel pattern was seen for the plot of L-aspartate *versus* ATP (Fig. 3.9), suggesting that the addition of this pair of substrates are separated by the release of a product. If we were to accept the parallel pattern for the plot of L-aspartate *versus* ATP, and not the intersecting pattern obtained under nonsaturating concentration of L-glutamine (1 mM), we could argue that the mechanism of glutamine-dependent reaction of ASB is totally

random with respect to all the three substrates. Therefore, this would rule out both proposed mechanisms A and B. However, according to Fromm (1975), the nonvaried substrate, L-glutamine in this case, must be kept above its respective K_m , but nonsaturating. This is because if it is raised to a saturating concentration ($100 \times K_m$), artifactual parallel lines may be observed in the double-reciprocal plot. In other words, the magnitude of either ϕ/AB (mechanism A) or ϕ/BC (mechanism B) would change such that the slope term disappears. This in fact can explain some of the discrepancies between our data and the data presented by Markin et al., (1981). In their study, the plot of L-aspartate versus ATP showed parallel lines when they kept L-glutamine constant and saturating (16.67 mM).

The double-reciprocal plot of ATP versus L-glutamine, at constant concentrations of L-aspartate, was parallel for *E.coli* ASB (Fig. 3.3A), rat liver AS (Hongo and Sato, 1985) and mouse pancreatic AS (Milman et al., 1980). Yet, the beef pancreatic AS displayed an intersecting pattern (Markin et al., 1981). This discrepancy was the motivation for using an alternative substrate. LGH was substituted for L-glutamine in the initial rate studies. We showed that the plot of $1/v$ versus $1/ATP$ at varied fixed concentration of L-glutamine or LGH (0.2 mM), resulted in parallel lines. It appeared that the substitution of the LGH for L-glutamine did not alter the magnitude of either the ϕ/AB or the ϕ/BC , therefore, no slope effect become evident. In other words, according to equation

1 (derived to fit mechanism A), the slope term ϕ/AB ($A = \text{ATP}$ and $B = \text{L-aspartate}$ or *vice versa*) is independent of C . Therefore, regardless of what C is (L-glutamine or LGH), the plot of $1/v$ versus $1/\text{ATP}$ would result in parallel lines. On the other hand, according to equation 2 (derived to fit mechanism B), the slope term ϕ/BC ($B = \text{ATP}$ and $C = \text{L-aspartate}$ or *vice versa*) is independent of A . Therefore, no matter what A is (L-glutamine or LGH), parallel pattern will be observed for the plot of $1/v$ versus $1/\text{ATP}$, indicating that the addition of ATP and L-glutamine are separated by the release of a product.

Substrate analogs were used to obtain more information about the reaction mechanism, mainly the substrate binding order. Rate equations for the effect of analogs (competitive inhibitors) of the substrates for mechanism A were derived. The rate equation for the effect of AMP-PNP with respect to A (ATP) is described as follows:

$$\text{equation 6) } 1/v = 1/V_{\max} + K_a/V_{\max}(A) (1 + I/K_i) + K_b/V_{\max}(B) + K_{ia}K_b/V_{\max}(A)(B) (1 + I/K_i) + K_c/V_{\max}C$$

The equation shows that for the double reciprocal plot of $1/v$ versus $1/\text{ATP}$ at different concentrations of AMP-PNP, only the the slope term is altered; i.e.,

$$\text{equation 7) } \text{Slope} = K_a/V_{\max}(A) (1 + I/K_i) + K_{ia}K_b/V_{\max}(A)(B) (1 + I/K_i)$$

therefore, equation 6 predicts that AMP-PNP is a competitive inhibitor of ATP.

On the other hand , when B (L-aspartate) is the varied substrate, the double reciprocal plot at different fixed concentrations of AMP-PNP will show an increase in both the slope and intercept terms,

equation 8) $\text{Intercept} = 1/V_{\max} \{1 + K_a/(A) (1 + I/K_i)\}$

equation 9) $\text{Slope} = 1/V_{\max} \{K_b + K_{ia}K_b/(A) (1 + I/K_i)\}$

and when C (L-glutamine) is the varied substrate, only the intercept term increases.

equation 10) $\text{Intercept} = 1/V_{\max} \{1 + K_a/(A) (1 + K_i) + K_{ia}K_b/(A) (B) (1 + I/K_i)\}$

Therefore, equation 6 predicts that AMP-PNP is a noncompetitive inhibitor of B (L-aspartate) and an uncompetitive inhibitor of C (L-glutamine). These predicted patterns obtained from equation 6 are therefore comparable with the experimental results obtained with AMP-PNP with respect to ATP, L-aspartate and L-glutamine, respectively (see Table 3.1).

The rate equation for the effect of β -methyl aspartate of L-aspartate is described by eq. (11).

equation 11) $1/v = 1/V_{\max} + K_a/V_{\max}(A) + K_b/V_{\max}(B) (1 + I/K_i) + K_{ia}K_b/V_{\max}(A) (B) + K_c/V_{\max}C$

As can be seen from equation 11, a competitive inhibitor with respect to L-aspartate will show uncompetitive inhibition with respect to ATP and L-glutamine. However, there is some disagreement with the experimental result, in that β -methyl aspartate was found to be noncompetitive with respect to ATP and L-glutamine.

When the rate equation for the effect of L-glutamic acid γ -methyl ester of L-glutamine is derived, the following relationship is obtained.

$$\text{equation 12)} \quad 1/v = 1/V_{\max} + K_a/V_{\max}(A) + K_b/V_{\max}(B) + K_{ia}K_b/V_{\max}(A)(B) + K_c/V_{\max}C (1 + I/K_i)$$

The equation predicts that a competitive inhibitor with respect to C (L-glutamine) should be uncompetitive with respect ATP and L-aspartate. However, L-glutamic acid γ -methyl ester was found to be noncompetitive with respect to L-aspartate.

The rate equations were also obtained for the effect of analogs of the substrates for mechanism B. The rate equation for the effect of L-glutamic acid γ -methyl ester on L-glutamine is described as follows:

$$\text{equation 13)} \quad 1/v = 1/V_{\max} + K_a/V_{\max}(A) (1 + I/K_i) + K_b/V_{\max}(B) + K_c/V_{\max}(C) + K_{ib}K_c/V_{\max}(B)(C)$$

According to the equation, the inhibitor that is competitive with respect to A (L-glutamine), will be uncompetitive with respect to (B) ATP and (C) L-aspartate. However, the experimental result is somewhat different in that L-glutamic acid γ -methyl ester was found to be noncompetitive with respect to L-aspartate.

The rate equation was derived for the effect of AMP-PNP with respect with B (ATP) as shown below:

$$\text{equation 14)} \quad 1/v = 1/V_{\max} + K_a/V_{\max}(A) + K_b/V_{\max} (B) (1 + I/K_i) + K_c/V_{\max}(C) + K_{ib}K_c/V_{\max}(B)(C) (1 + I/K_i)$$

Equation 14 predicts that a competitive inhibitor with respect to ATP (namely AMP-PNP) should be noncompetitive with respect to L-aspartate and uncompetitive with respect to L-glutamine. These predictions are comparable with the experimental results (see Table 3.1).

The rate equation for the effect of β -methyl aspartate of L-aspartate is described as follows:

$$\text{equation 15)} \quad 1/v = 1/V_{\max} + K_a/V_{\max}(A) + K_b/V_{\max}(B) + K_c/V_{\max}(C) (1 + I/K_i) + K_{ib}K_c/V_{\max}(B)(C) 1/V_{\max}$$

The equation predicts that a competitive inhibitor with respect to L-aspartate should be noncompetitive with respect to ATP and uncompetitive with respect to L-glutamine. This disagrees with the experimental results (see Table 3.1) in that it was found to be noncompetitive with respect to ATP and L-glutamine. For most cases the experimental data agreed with the theoretical results, however it was not possible to differentiate between bi-uni-uni ter ping-pong (Scheme A) and uni-uni-bi ter ping-pong (Scheme B) mechanisms using this approach.

AS can function as a glutaminase in the presence or absence of the ATP and L-aspartate. Other glutamine amidotransferases such as carbamyl phosphate synthetase (Nagano et al., 1970), cytidine triphosphate synthetase (Levitzki and Koshland, 1971) and glutamine phosphoribosylpyrophosphate amidotransferase (Mei and Zalkin, 1989) have also been shown to have this activity. In most cases, however, the relative amount of glutaminase activity

appeared to be far less than the overall reaction rate, except for the AS from leukemia cells that was shown to have higher glutaminase activity compared to synthetase (2:1) activity. Our data showed that the formation of L-glutamate was higher than that of PP_i for ASB. It also showed that ratio of L-glutamate to PP_i increased with increasing concentration of L-glutamine. This suggests that glutaminase activity is happening at the same time as synthetase activity, and by increasing the concentration of L-glutamine, the glutaminase activity increases significantly over the synthetase activity.

The rate equation for the proposed mechanism A (ordered bi-uni-uni-ter ping-pong) was derived assuming the products P, Q, R and S were present, as shown below.

$$\text{equation 16)} \quad 1/v = 1/V \{ 1/[ABC] - [PQRS] (\phi_1[C] + \phi_2[AB] + \phi_3[BC] + \phi_4[AC] + \phi_5[ABC] + \phi_6[P] + \phi_7[PQ] + \phi_8[PS] + \phi_9[PQR] + \phi_{10}[PQS] + \phi_{11}[SPR] + \phi_{12}[SPQR] + \phi_{13}[SQR] + \phi_{14}[AP] + \phi_{15}[CS] + \phi_{16}[APQ] + \phi_{17}[APB] + \phi_{18}[ABQ] + \phi_{19}[CRS] + \phi_{20}[BCS] + \phi_{21}[APQR] + \phi_{22}[ABPQ] + \phi_{23}[ABQR] + \phi_{24}[BQRS] + \phi_{25}[ABCQ] + \phi_{26}[CQRS] + \phi_{27}[ABCR] + \phi_{28}[BCRS] + \phi_{29}[ABPQR] + \phi_{30}[BPQRS] + \phi_{31}[ABCQR] + \phi_{32}[BCQRS]) \}$$

Assuming Q, R, and S = 0, equation 16 becomes

$$\text{equation 17)} \quad 1/v = 1/V (\phi_1/[AB] + \phi_2/[C] + \phi_3/[A] + \phi_4/[B] + \phi_5 + \phi_6[P]/[ABC] + \phi_{14}[P]/[BC] + \phi_{17}[P]/[C])$$

Equation 17 predicts that P (PP_i) is noncompetitive with respect to ATP and L-aspartate and competitive with respect to L-glutamine which are contrary to the experimental

results. PP_i was found to be competitive with respect to ATP (Fig. 3.21) and L-aspartate (Fig. 3.22). No definite inhibition pattern was obtained *versus* L-glutamine, however. Therefore, the AS mechanism is different from mechanism (A) in which competitive inhibition of PP_i versus L-glutamine is the expected pattern.

Assuming P, R, and S = 0,
equation 18) $1/v = 1/V (\phi_1/[AB] + \phi_2/[C] + \phi_3/[A] + \phi_4/[B] + \phi_5 + \phi_{18}[Q]/[C])$

Equation 18 predicts that Q (L-asparagine) is competitive with respect to L-glutamine and uncompetitive with respect to ATP and L-aspartate. L-asparagine was found to be competitive with respect to L-glutamine (Fig. 3.18), however. It was found to be noncompetitive with respect to ATP and L-aspartate (Fig. 3.19 & Fig. 3.20).

Assuming P, Q, and S = 0,
equation 19) $1/v = 1/V (\phi_1/[AB] + \phi_2/[C] + \phi_3/[A] + \phi_4/[B] + \phi_5 + \phi_{27}[R])$

Equation 19 predicts that R (AMP) is uncompetitive with respect to all the three substrates. These are different from experimental results in that noncompetitive inhibition patterns were observed (Fig. 3.26, Fig. 3.27. & Fig. 3.28)

Assuming P, R, and S = 0,
equation 20) $1/v = 1/V (\phi_1/[AB] + \phi_2/[C] + \phi_3/[A] + \phi_4/[B] + \phi_5 + \phi_{15}[S]/[AB] + \phi_{20}[S]/[A])$

According to equation 20, L-glutamate would be competitive with respect to ATP, noncompetitive with respect to L-

aspartate and uncompetitive with respect to L-glutamine. However, L-glutamate was found to be uncompetitive, competitive and noncompetitive with respect to ATP, L-aspartate and L-glutamine, respectively (Fig. 3.23, Fig. 24, & Fig. 3.25).

The rate equation for the mechanism B (ordered uni-uni-bi-ter ping-pong) was also derived assuming the products P, Q, R and S were present.

$$\text{equation 21)} \quad 1/v = 1/V \{1/[ABC] - [PQRS] (\phi_1[PQR] + \phi_2[PQ] + \phi_3[P] + \phi_4[BC] + \phi_5[PC] + \phi_6[APQR] + \phi_7[PQRS] + \phi_8[APQ] + \phi_9[AP] + \phi_{10}[ABC] + \phi_{11}[ACP] + \phi_{12}[AQR] + \phi_{13}[QRS] + \phi_{14}[AQ] + \phi_{15}[A] + \phi_{16}[AC] + \phi_{17}[ABCQR] + \phi_{18}[BCQRS] + \phi_{19}[CPQRS] + \phi_{20}[ABQR] + \phi_{21}[ABCQ] + \phi_{22}[BQRS] + \phi_{23}[PRS] + \phi_{24}[ABCR] + \phi_{25}[BCRS] + \phi_{26}[CPRS] + \phi_{27}[ABQ] + \phi_{28}[PQS] + \phi_{29}[PS] + \phi_{30}[AB] + \phi_{31}[BCS] + \phi_{32}[CPS])\}$$

The product inhibition equation (equation 21), from which the terms containing two or three products have been omitted, has the expression:

$$\text{equation 22)} \quad 1/v = 1/V \{1/[ABC] (\phi_3[P] + \phi_4[BC] + \phi_5[PC] + \phi_9[AP] + \phi_{10}[ABC] + \phi_{11}[ACP] + \phi_{14}[AQ] + \phi_{15}[A] + \phi_{16}[AC] + \phi_{21}[ABCQ] + \phi_{24}[ABCR] + \phi_{27}[ABQ] + \phi_{30}[AB] \phi_{31}[BCS])\}$$

assuming A = L-glutamine, B = ATP, C = L-aspartate, P = L-glutamate, Q = PP_i, R = AMP and S = L-asparagine.

The rate equation was also derived for the uni-uni-bi-ter Theorell-Chance mechanism assuming the products P, Q, R and S were present. The product inhibition equation from

which the terms containing two or three products have been omitted, has the expression:

$$\text{equation 23)} \quad 1/v = 1/V (1/[ABC] (\phi_3[P] + \phi_4[BC] + \phi_5[PC] + \phi_9[AP] + \phi_{10}[ABC] + \phi_{11}[ACP] + \phi_{14}[AQ] + \phi_{15}[A] + \phi_{16}[AC] + \phi_{24}[ABCR] + \phi_{27}[ABQ] + \phi_{30}[AB] + \phi_{31}[BCS]))$$

There is basically one difference between the predicted patterns obtained from equation 22 (ordered uni-uni-bi-ter ping-pong) and those from equation 23 (uni-uni-bi-ter Theorell-Chance). According to the ordered mechanism (equation 22), PP_i should be noncompetitive with respect to ATP, whereas according to the Theorell-Chance mechanism (equation 23), it should be competitive with respect to ATP. Although PP_i was shown to be competitive with respect to ATP (Fig. 3.21), other disagreements with Theorell-Chance mechanism were found to exist.

The product inhibition studies did not allow us unequivocally to rule out any of the proposed mechanisms. Yet, they provided information as to where some of the products can be placed in the scheme. L-asparagine was found to be competitive with respect to L-glutamine (competing for the same enzyme form), therefore they have to be next to each other. PP_i was competitive versus ATP and L-aspartate, which can be placed following the addition of these two substrates. To determine the product released between the addition of L-aspartate and L-glutamine, initial velocity experiments were performed where L-aspartate and L-glutamine were varied in the presence of L-glutamate or PP_i . The parallel lines in the

presence of L-glutamate (Fig. 3.29) suggests that L-glutamate cannot be the first product (P) released between L-aspartate and L-glutamine. However, given the fact that L-glutamate is a poor inhibitor ($K_i \gg 20 \text{ mM}$), this can also suggest that L-glutamate cannot bind tightly enough for the reverse reaction to occur. Parallel lines were also observed in the presence of PP_i (Fig 3.30) which suggest that PP_i cannot be the first product off either. However, this can also suggest that PP_i binds the enzyme such that the reverse reaction can not take place. In other words, it can not form the complex that is catalytically competent for the reverse reaction. The double inhibition studies were performed to determine the relationship between the products, therefore trying to define their release order. The results in Figure. 3.31 show that the presence of L-asparagine enhances AMP inhibition. This suggests that they combine sequentially with the enzyme, therefore they must be next to each other (Segel, 1975) in order. However, the presence of L-glutamate shows no enhancement to either L-asparagine or AMP inhibition (Fig. 3.32 and 3.33), suggesting that their binding is separated by another product or some other step.

Our data from initial velocity studies supported a bi-uni-uni-bi ping-pong mechanism (mechanism A), for ammonia-dependent reaction of ASB. Initial velocity, product inhibition (single or double) studies were performed in an attempt to come up with a mechanism, for glutamine-dependent AS reaction. Initial velocity experiments were also performed

in the presence of either L-glutamate or PP_i to obtain information about the first product released in the mechanism (Fig. 3.28 and 3.29), from which similar results (parallel pattern) were obtained. Studies using saturating concentrations of the substrates, and the use of alternative substrate helped to explain some of the discrepancies that existed between the data presented in the past and this work. These studies, in general, showed us that the mechanism is ping-pong and not sequential. However, it became quite evident that relying solely on steady state kinetics, neither one of the mechanisms (A or B) could be ruled out. This is where the importance of isotope trapping experiments become obvious. The lines of evidence presented in chapter 2 indicated that for the glutamine-dependent reaction the mechanism is ordered, ATP being first and L-aspartate second. This is followed by release of PP_i and subsequent addition of L-glutamine. Initial velocity studies, on the other hand, showed us that the mechanism is ping-pong and not sequential. These results together clearly support an ordered bi-uni-uni-ter ping-pong mechanism for the glutamine-dependent reaction of *E. coli* ASB. The steady-state initial velocity rate equation, containing all rate constants, for the proposed mechanism (A) in the absence of products is as follows:

equation 24) $1/v = K_{ia} K_{mb} / (V_{max} [AB]) + K_{mc} / (V_{max} [C]) + K_{ma} / (V_{max} [A]) + K_{mb} / (V_{max} [B]) + 1 / (V_{max})$

Where,

$$K_{ma} = k_3 k_5 k_6 k_7 / (k_1 (k_5 k_6 k_7 + k_3 k_6 k_7 + k_3 k_5 k_7 + k_3 k_5 k_6))$$

$$K_{mb} = k_5 k_6 k_7 (k_3 + k_{-2}) / (k_2 (k_5 k_6 k_7 + k_3 k_6 k_7 + k_3 k_5 k_7 + k_3 k_5 k_6))$$

$$K_{mc} = k_3 k_6 k_7 (k_5 + k_{-4}) / (k_4 (k_5 k_6 k_7 + k_3 k_6 k_7 + k_3 k_5 k_7 + k_3 k_5 k_6))$$

$$K_{mbKia} = k_5 k_6 k_7 k_{-1} (k_3 + k_{-2}) / k_1 k_2 (k_5 k_6 k_7 + k_3 k_6 k_7 + k_3 k_5 k_7 + k_3 k_5 k_6)$$

$$V_{max} = k_3 k_5 k_6 k_7 / (k_5 k_6 k_7 + k_3 k_6 k_7 + k_3 k_5 k_7 + k_3 k_5 k_6) [E_{total}]$$

A = ATP, B = L-aspartate, and C = L-glutamine

We can now place L-asparagine release after the addition of L-glutamine, which is in turn followed by the release of AMP. Yet, as discussed earlier, there are disagreements between the predicted patterns and the experimental results. The predicted noncompetitive inhibition of PP_i *versus* ATP and L-aspartate are contrary to the observed competitive inhibition (Fig 3.21 and 3.22). There were other disagreements between the predicted patterns and experimental results for AMP and L-glutamate which can be due to their poor ability to inhibit. Another possibility is the existence of an isomerization step (Scheme C). The rate equation for the proposed mechanism with the iso step was also derived, assuming the products P, Q, R and S were present.

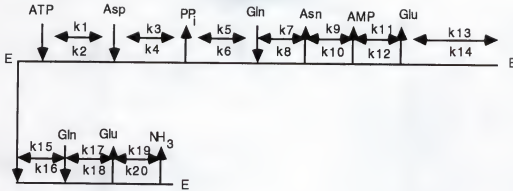
$$\text{equation 25) } 1/v = 1/V (1/[ABC] - [PQRS]) (\phi_1[PQRS] + \phi_2[PQR] + \phi_3[PQ] + \phi_4[BC] + \phi_5[P] + \phi_6[C] + \phi_7[APQRS] + \phi_8[APQR] + \phi_9[APQ] + \phi_{10}[AP] + \phi_{11}[AC] + \phi_{12}[ABPQRS] + \phi_{13}[BPQRS] +$$

$$\begin{aligned} &\phi_{14}[\text{ABPQR}] + \phi_{15}[\text{ABPQ}] + \phi_{16}[\text{ABP}] + \phi_{17}[\text{ABC}] + \phi_{18}[\text{QRS}] + \\ &\phi_{19}[\text{ABQRS}] + \phi_{20}[\text{BQRS}] + \phi_{21}[\text{ABQR}] + \phi_{22}[\text{ABQ}] + \phi_{23}[\text{AB}] + \\ &\phi_{24}[\text{ABCQRS}] + \phi_{25}[\text{BCQRS}] + \phi_{26}[\text{CQRS}] + \phi_{27}[\text{ABCQ}] + \phi_{28}[\text{PRS}] + \\ &\phi_{29}[\text{CRS}] + \phi_{30}[\text{ABCRS}] + \phi_{31}[\text{BCRS}] + \phi_{32}[\text{ABCR}] + \phi_{33}[\text{PQS}] + \\ &\phi_{34}[\text{CS}] + \phi_{35}[\text{ABCS}] + \phi_{36}[\text{BCS}] + \phi_{37}[\text{PS}]] \end{aligned}$$

We focused on the terms that were not only different in the two equations, but also could be used to differentiate the two mechanisms, with and without the iso step (Scheme A and C). The iso-mechanism predicts a non-competitive inhibition pattern between the last product and first substrate which would otherwise be competitive. The results from figure 3.34, which is the plot of $1/v$ versus $1/L$ -aspartate at fixed varied concentrations of L -glutamate and AMP in a constant ratio ($[L\text{-glutamate}] = 5[\text{AMP}]$), are compatible with the predicted pattern from equation 4 (simplified version of the equation 13), therefore suggesting that there is an iso step following the release of the last product (Scheme C).

One other important kinetic property of the *E. coli* ASB that was examined in this chapter was the glutaminase reaction. The reaction was shown to be occurring at the same time as the synthetase reaction and seemed to be increased with an increasing concentration of L -glutamine.

Based on these results we propose the following mechanism for the glutamine-dependent AS reaction (Scheme D):



According to this mechanism, the simple ordered bi-uni-uni-ter ping-pong mechanism is not applicable to *E. coli* ASB enzyme. We have two different reactions happening at the same time, glutaminase and synthetase. It has also been shown that ATP stimulates the glutaminase (Boehlein et al., 1994). Therefore, it is very likely that by increasing the concentration of the substrates, the enzyme preferentially goes through L-glutamine hydrolysis and not the asparagine synthesis reaction, causing what will appear kinetically as substrate inhibition (Cleland, 1983). The steady-state initial velocity rate equation, containing all rate constants, for the proposed mechanism in the absence of products is as follows:

$$\text{equation 26)} \quad v = \frac{((k_1 k_3 k_5 k_7 k_9 k_{11} k_{13}) (k_{16} + k_{17}) k_{19} [ABC] + k_2 (k_4 + k_5) k_7 k_9 k_{11} k_{13} k_{15} k_{17} k_{19} [C^2] + k_3 k_5 k_7 k_9 k_{11} k_{13} k_{15} k_{17} k_{19} [BC^2]))}{k_2 k_7 k_9 k_{11} k_{13} k_{19} (k_4 + k_5) (k_{16} + k_{17}) [C] + k_2 k_4 k_8 k_{11} k_{13} k_{15} k_{17} k_{19} [C] + k_2 k_5 (k_8 + k_9) k_{11} k_{13} k_{15} k_{17} k_{19} [C] + k_3 k_5 k_7 k_9 k_{11} k_{13} k_{19}}$$

$$\begin{aligned}
& (k_{16} + k_{17}) [BC] + k_3 k_5 (k_8 + k_9) k_{11} k_{13} k_{15} k_{17} k_{19} [BC] + \\
& k_1 k_7 k_9 k_{11} k_{13} k_{19} (k_4 + k_5) (k_{16} + k_{17}) [AC] + k_1 k_3 k_5 \\
& (k_8 + k_9) k_{11} k_{13} (k_{16} + k_{17}) [AB] + k_1 k_3 k_7 k_9 k_{11} k_{13} (k_{16} \\
& + k_{17}) [ABC] + k_1 k_3 k_5 k_7 k_{11} k_{13} (k_{16} + k_{17}) k_{19} [ABC] + k_1 \\
& k_3 k_5 k_7 k_9 k_{13} (k_{16} + k_{17}) k_{19} [ABC] + k_1 k_3 k_5 k_7 k_9 k_{11} \\
& (k_{16} + k_{17}) k_{19} [ABC] + k_1 k_3 k_5 k_7 k_9 k_{11} k_{13} k_{17} [ABC] + k_4 \\
& k_7 k_9 k_{11} k_{13} k_{15} k_{17} k_{19} [C^2] + k_2 k_4 k_7 k_{11} k_{13} k_{15} k_{17} k_{19} \\
& [C^2] + k_2 (k_4 + k_5) (k_7 k_9 k_{13} k_{15} k_{17} k_{19} [C^2] + k_2 (k_4 + k_5) \\
& k_7 k_9 k_{11} k_{15} k_{17} k_{19} [C^2] + k_2 (k_4 + k_5) k_7 k_9 k_{11} k_{13} k_{15} \\
& k_{19} [C^2] + k_2 (k_4 + k_5) k_7 k_9 k_{11} k_{13} k_{15} k_{17} [C^2] + k_3 k_7 k_9 \\
& k_{11} k_{13} k_{15} k_{17} k_{19} [BC^2] + k_2 k_5 k_7 k_{11} k_{13} k_{15} k_{17} k_{19} [BC^2] \\
& + k_3 k_5 k_7 k_9 k_{13} k_{15} k_{17} k_{19} [BC^2] + k_3 k_5 k_7 k_9 k_{11} k_{15} k_{17} \\
& k_{19} [BC^2] + k_3 k_5 k_7 k_9 k_{11} k_{13} k_{15} k_{19} [BC^2] + k_3 k_5 k_7 k_9 \\
& k_{11} k_{13} k_{15} k_{17} [BC^2]
\end{aligned}$$

A = ATP, B = L-aspartate and C = L-glutamine.

Due to the complexity of the mechanism, we were unable to predict any pattern or to design an experiment to test it. However, computer modeling with the program Quatro, was used to examine the proposed mechanism through simulation. Arbitrary numbers were assigned for the substrates (A, B and C) and the rate constants, and the data were plotted in the form of double reciprocal plot.

Assuming all the rate constants (k_1 to k_{19}) = 1, the plot of $1/v$ versus $1/[ATP]$ at different L-aspartate concentrations (constant L-glutamine) will result in what appears to be substrate inhibition. In other words, the lines, instead of being intersecting as was shown before

(Fig. 3.1), show slopes increasing with L-aspartate (Fig. 3.35), and this is true whether L-glutamine is equal to 1 or equal to 20.

Assuming $k_{15} = 0$ (k_{on} for L-glutamine for the side reaction), therefore eliminating any term that has this rate constant, equation 23 becomes equation 1 (derived to fit a simple mechanism, which is ordered bi-uni-uni-ter ping-pong). Therefore, the plot of $1/v$ versus $1/[ATP]$ at different L-aspartate concentrations (constant L-glutamine) will result in intersecting lines (Fig. 3.36). This is true whether L-glutamine is equal to 1 or equal to 20.

As we increase k_{15} (0.001 to 0.005), Keeping L-glutamine constant and high (20), the plot of $1/v$ versus $1/[ATP]$ at different L-aspartate concentrations will gradually change from intersecting lines to parallel lines (Fig. 3.37). However, by increasing k_{15} (> 0.005) we start seeing what appears to be substrate inhibition. On the other hand, if we keep k_{15} constant (0.002), but increase L-glutamine (from 1 to 20), the plot of $1/v$ versus $1/[ATP]$ at different L-aspartate concentrations will gradually change from intersecting lines to parallel lines (Fig. 3.38 through 3.40). This parallel pattern was observed experimentally (Fig. 3.9), when ATP was varied at fixed varied concentration of L-aspartate, keeping L-glutamine constant and saturating (20 mM). According to Fromm (1975), the nonvaried substrate, L-glutamine in this case, must be kept above its respective K_m , but nonsaturating. This predicts that if L-glutamine is

raised to a saturating level ($100 \times K_m$), artifactual parallel lines may be observed in the double-reciprocal plot, however, the literature offers no explanation as to why this will happen. Our modeling strongly suggests one reason for the proposed results. By increasing L-glutamine concentration or in turn by increasing k_{15} (k_{on} for L-glutamine for the side reaction), the enzyme preferentially goes through L-glutamine hydrolysis and not the asparagine synthesis reaction, causing apparent substrate inhibition.

In further modeling, keeping L-glutamine constant and subsaturating (1 mM), the plot of $1/v$ versus. $1/[ATP]$ at different L-aspartate concentrations will change from intersecting lines to parallel lines only when k_{15} is 0.05 and higher (not shown). On the other hand, assuming $k_{15} = 0$, the plot of $1/v$ versus. $1/[ATP]$ at different L-glutamine concentrations (constant L-aspartate) will result in intersecting lines (plot not shown). As we increased k_{15} , keeping L-aspartate constant and high (5), the plot of $1/v$ versus. $1/[ATP]$ at different L-glutamine concentrations will still show parallel lines (as observed experimentally (Fig 3.2A & 3.3A)).

The computer modeling was also used to examine the simple mechanism, ordered bi-uni-uni-ter ping-pong (Scheme A). Keeping L-glutamine constant and subsaturating (1 mM), the plot of $1/v$ versus. $1/[ATP]$ at different L-aspartate concentrations will change from intersecting lines to parallel lines (as observed experimentally (Fig 3.2A & 3.3A)).

only when either k_5 or k_6 or k_7 is a negative number (Fig. 3.41), a situation which is not possible experimentally.

Using the computer modeling, we were able to examine the proposed mechanism (Scheme D). We were able to show the change of pattern from intersecting lines to parallel lines, further supporting that the proposed mechanism (Scheme D) is correct. According to the mechanism, the simple ordered bi-uni-uni-ter ping-pong mechanism would not be applicable to *E. coli* ASB enzyme. This enzyme catalyzes two different reactions at the same time, a glutaminase and an asparagine synthetase. It is now clear that by increasing the L-glutamine concentration, therefore pushing the enzyme through an alternative path, glutaminase, one observes substrate inhibition, in which infinite substrate gives a finite, but reduced rate. The mechanism of asparagine synthetase, therefore is an ordered bi-uni-uni-ter ping-pong mechanism with a side reaction, glutaminase.

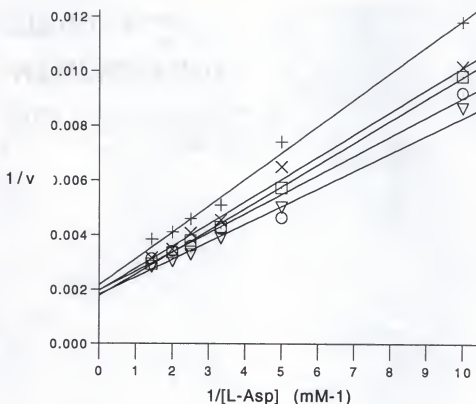


Fig. 3.1A Double-reciprocal plot of initial velocity versus L-aspartate concentration at various fixed concentrations of ATP. Each initial velocity is the average of two experiments. The L-aspartate concentrations were 0.1, 0.2, 0.3, 0.4, 0.5 and 0.7 mM at various fixed concentrations of ATP: (plus) 0.2 mM, (cross) 0.3 mM, (square) 0.4 mM, (lower triangle) 0.5 mM, (open circle) 0.7 mM. The concentrations of L-glutamine and $MgCl_2$ were maintained at 1 and 3 mM, respectively. 7.4 μ g of enzyme per assay was used.

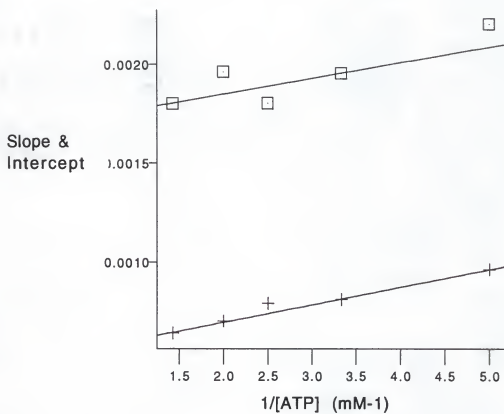


Fig. 3.1B plot of the reciprocal-fixed variable substrate ATP versus slope (plus) and intercept (square) from Fig.3.1A.

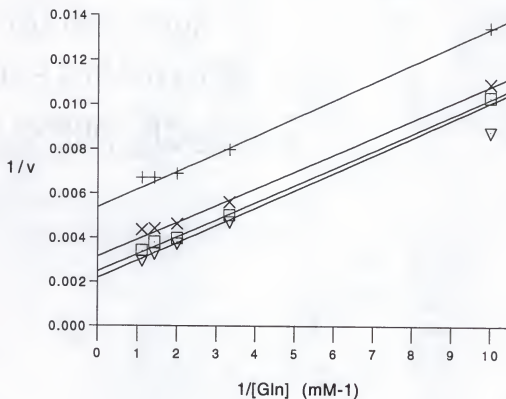


Fig. 3.2A Double-reciprocal plot of initial velocity versus L-glutamine concentration at various concentrations of ATP. Each initial velocity is the average of two experiments. The L-glutamine concentrations were 0.1, 0.3, 0.5, 0.7 and 0.9 mM at various fixed concentrations of ATP: (plus) 0.1 mM, (cross) 0.2 mM, (square) 0.3 mM, (lower triangle) 0.5 mM. The concentrations of L-aspartate and MgCl_2 were 1 and 3 mM, respectively. 7.4 μg of enzyme per assay was used.

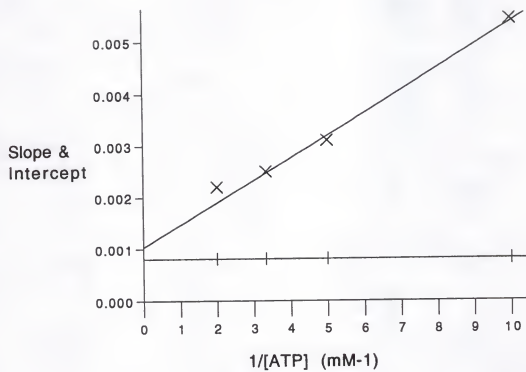


Fig. 3.2B plot of the reciprocal-fixed variable substrate ATP versus slope (plus) and intercept (cross) from Fig. 3.2A.

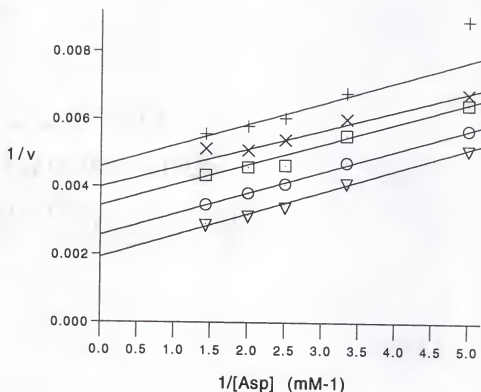


Fig. 3.3A Double-reciprocal plot of initial velocity versus L-aspartate concentration at various fixed concentrations of L-glutamine. Each initial velocity is the average of two experiments. The L-aspartate concentrations were 0.2, 0.3, 0.4, 0.5 and 0.7 mM at various fixed concentrations of L-glutamine: (plus) 0.2 mM, (cross) 0.3 mM, (square) 0.4 mM, (open circle) 0.5 mM, (lower triangle) 0.7 mM. The concentrations of ATP and $MgCl_2$ were 1 and 3 mM, respectively. 7.4 μg of enzyme per assay was used.

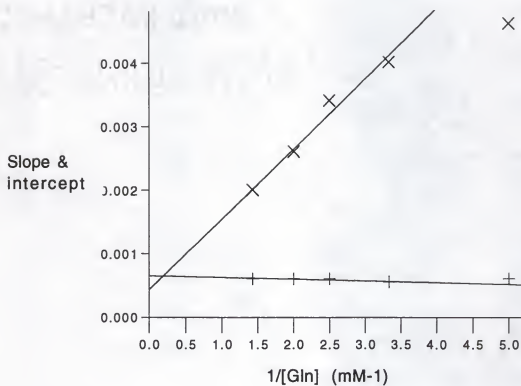


Fig. 3.3B plot of the reciprocal-fixed variable substrate L-glutamine versus slope (plus) and intercept (cross) from Fig. 3.3A.

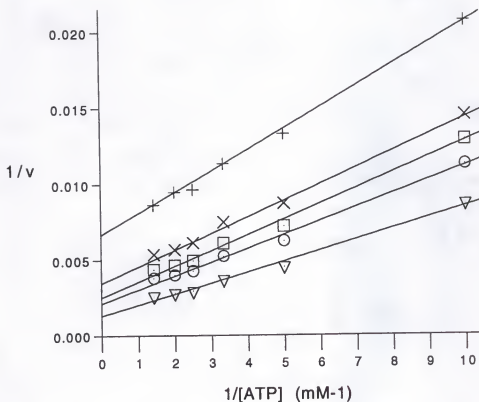


Fig. 3.4A Double-reciprocal plot of initial velocity versus ATP concentration at various fixed concentrations of L-aspartate. Each initial velocity is the average of two experiments. The ATP concentrations were 0.1, 0.2, 0.3, 0.4, 0.5 and 0.7 mM at various fixed concentrations of L-aspartate: (plus) 0.1 mM, (cross) 0.2 mM, (square) 0.3 mM, (open circle) 0.4 mM, (lower triangle) 0.5 mM. The concentrations of NH_3 and MgCl_2 were 50 and 3 mM, respectively. 7.4 μg of enzyme per assay was used.

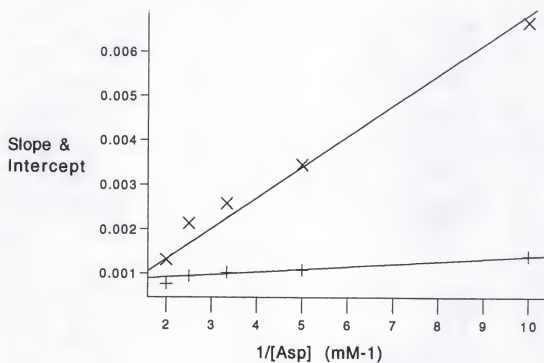


Fig. 3.4B plot of the reciprocal-fixed variable substrate L-aspartate versus slope (plus) and intercept (cross) from Fig. 3.4A.

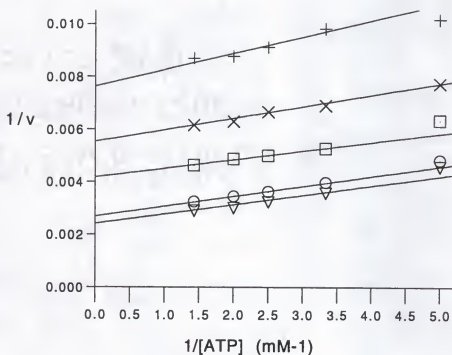


Fig. 3.5A Double-reciprocal plot of initial velocity versus ATP concentration at various fixed concentrations of NH_3 . Each initial velocity is the average of two experiments. The ATP concentrations were 0.2, 0.3, 0.4, 0.5 and 0.7 mM at various fixed concentrations of NH_3 : (plus) 3.0 mM, (cross) 6.0 mM, (square) 12.0 mM, (open circle) 24.0 mM, (lower triangle) 36.0 mM. The concentrations of L-aspartate and MgCl_2 were 1 and 3 mM, respectively. 7.4 μg of enzyme per assay was used.

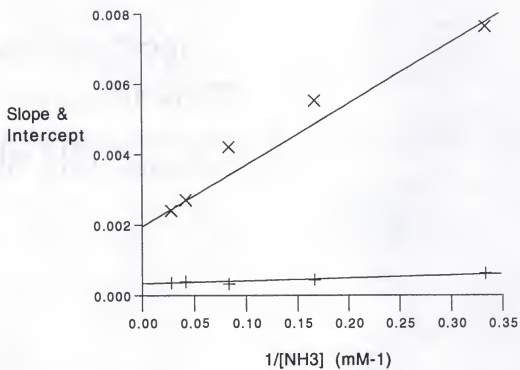


Fig. 3.5B plot of the reciprocal-fixed variable substrate NH_3 versus slope (plus) and intercept (cross) from Fig .3.5A.

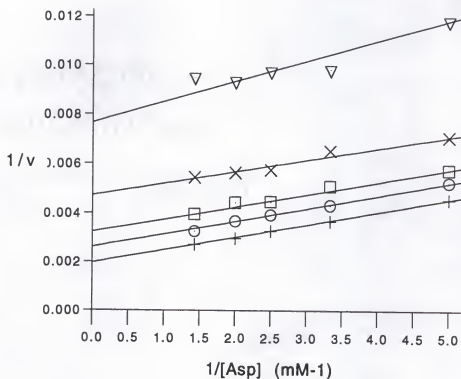


Fig. 3.6A Double-reciprocal plot of initial velocity versus L-aspartate concentration at various fixed concentrations of NH_3 . Each initial velocity is the average of two experiments. The L-aspartate concentrations were 0.2, 0.3, 0.4, 0.5 and 0.7 mM at various fixed concentrations of NH_3 : (lower triangle) 3.0 mM, (cross) 6.0 mM, (square) 12.0 mM, (open circle) 24.0 mM, (plus) 36.0 mM. The concentrations of ATP and $MgCl_2$ were 1 and 3 mM, respectively. 7.4 μg of enzyme per assay was used.

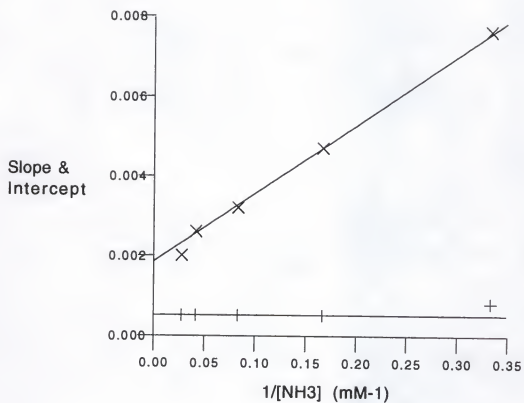


Fig. 3.6B plot of the reciprocal-fixed variable substrate NH_3 versus slope (plus) and intercept (cross) from Fig. 3.6A.

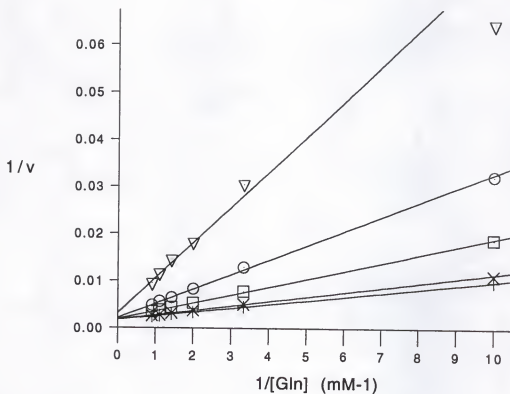


Fig. 3.7 Double-reciprocal plot of initial velocity versus L-glutamine concentration at fixed concentration of LGH. Each initial velocity is the average of two experiments. The L-glutamine concentrations were 0.21, 0.3, 0.5, 0.7, 0.9 and 1.1 mM at various fixed concentrations of LGH: (plus) 0.0, mM, (cross) 0.08 mM, (square) 0.5 mM, (open circle) 1.0 mM, (lower triangle) 3.0 mM. The concentrations of ATP, L-aspartate and $MgCl_2$ were 1, 1 and 3 mM, respectively. 7.4 μ g of enzyme per assay was used.

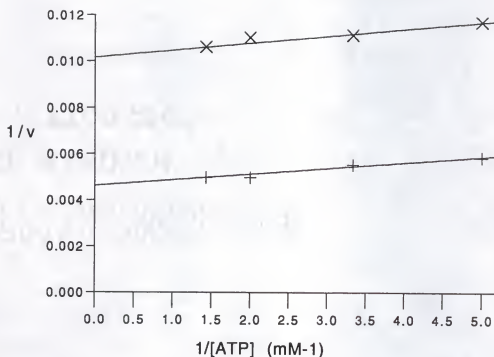


Fig. 3.8 Double-reciprocal plot of initial velocity versus ATP concentration at fixed concentration of L-glutamine (plus) and LGH (cross) (0.2 mM). Each initial velocity is the average of two experiments. The ATP concentrations were 0.2, 0.3, 0.5 and 0.7 mM. The concentrations of L-aspartate and MgCl_2 were 1 and 3 mM, respectively. 7.4 μg of enzyme per assay was used.

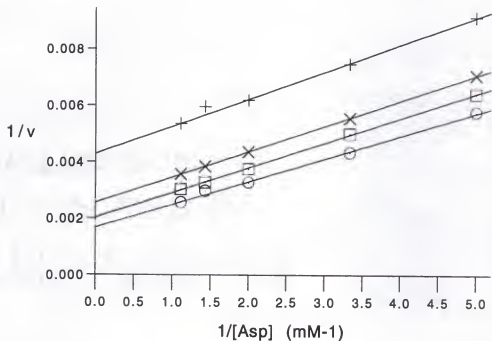


Fig. 3.9 Double-reciprocal plot of initial velocity versus L-aspartate concentration at various fixed concentrations of ATP. Each initial velocity is the average of two experiments. The L-aspartate concentrations were 0.2, 0.3, 0.5, 0.7, and 0.9 mM at various fixed concentrations of ATP: (plus) 0.1 mM, (cross) 0.2 mM, (square) 0.3 mM, (open circle) 0.7 mM. The concentrations of L-glutamine and $MgCl_2$ were maintained at 20 and 3 mM, respectively. 7.4 μg of enzyme per assay was used.

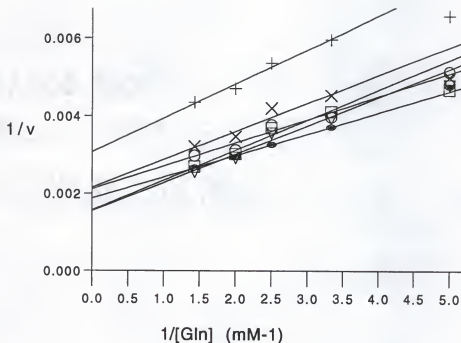


Fig. 3.10 Double-reciprocal plot of initial velocity versus L-glutamine concentration at various concentrations of ATP. Each initial velocity is the average of two experiments. The L-glutamine concentrations were 0.1, 0.2, 0.4, 0.5 and 0.7 mM at various fixed concentrations of ATP: (plus) 0.1 mM, (cross) 0.2 mM, (open circle) 0.3 mM, (square) 0.5 mM, (lower triangle) 0.5 mM, (eye) 0.7 mM. The concentrations of L-aspartate and $MgCl_2$ were 2 and 3 mM, respectively. 7.4 μ g of enzyme per assay was used.

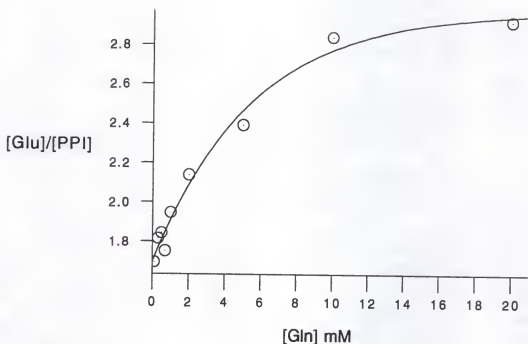


Fig. 3.11 The ratio of L-glutamate produced/PPI produced versus concentration of L-glutamine. The assay mixtures (100 μ l) contained 50 mM Tris-HCl (pH 8.0), 1 mM ATP, 1 mM L-aspartate, 3 mM $MgCl_2$ and varying concentration of L-glutamine (0.1-20.0 mM). The concentrations of L-glutamate and PPI were measured, as described under Materials and Methods. Each initial velocity is the average of two experiments.

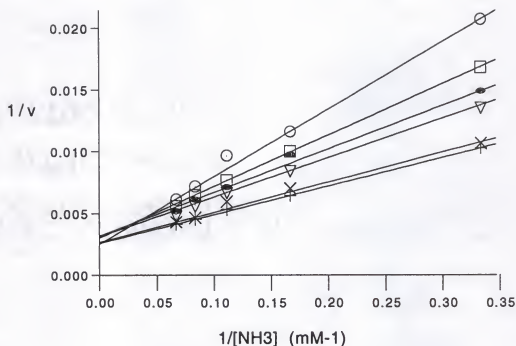


Fig. 3.12 Double-reciprocal plot of initial velocity versus NH_3 concentration at various fixed concentrations of L-asparagine. Each initial velocity is the average of two experiments. The NH_3 concentrations were 3.0, 6.0, 9.0, 12.0, and 15.0 mM at various fixed concentrations of L-asparagine: (plus) 0.0 mM, (cross) 0.025 mM, (lower triangle) 0.05 mM, (eye) 0.075 mM, (square) 0.10, (open circle) 0.15. The concentrations of L-aspartate, ATP and $MgCl_2$ were 1, 1, and 3 mM, respectively. 7.4 μg of enzyme per assay was used.

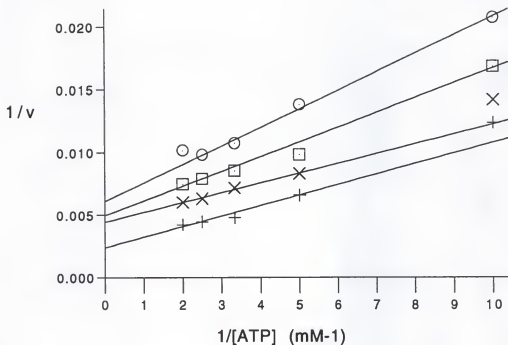


Fig. 3.13 Double-reciprocal plot of initial velocity versus ATP concentration at various fixed concentrations of L-asparagine. Each initial velocity is the average of two experiments. The ATP concentrations were 0.1, 0.3, 0.3, 0.4, and 0.5 mM at various fixed concentrations of L-asparagine: (plus) 0.0 mM, (cross) 0.05 mM, (square) 0.10 mM, (open circle) 0.15 mM. The concentrations of L-aspartate, NH_3 and MgCl_2 were 1, 50, and 3 mM, respectively. 7.4 μg of enzyme per assay was used.

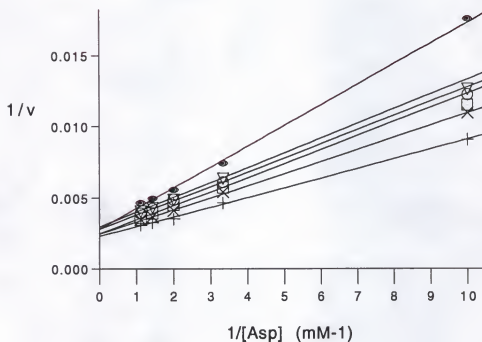


Fig. 3.14 Double-reciprocal plot of initial velocity versus L-aspartate concentration at various fixed concentrations of L-asparagine. Each initial velocity is the average of two experiments. The L-aspartate concentrations were 0.1, 0.3, 0.5, 0.7, and 0.9 mM at various fixed concentrations of L-asparagine: (plus) 0.0 mM, (cross) 0.025 mM, (square) 0.05 mM, (open circle) 0.075 mM, (lower triangle) 0.10 mM, (eye) 0.15 mM. The concentrations of ATP, NH_3 and $MgCl_2$ were 1, 50, and 3 mM, respectively. 7.4 μg of enzyme per assay was used.

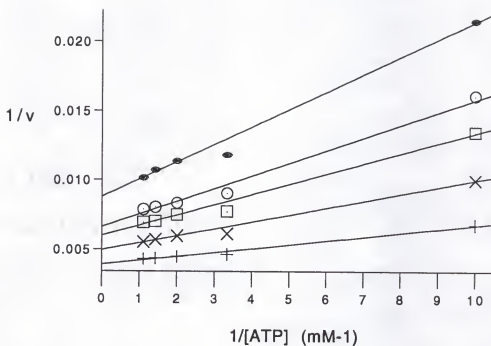


Fig. 3.15 Double-reciprocal plot of initial velocity versus ATP concentration at various fixed concentrations of AMP. Each initial velocity is the average of two experiments. The ATP concentrations were 0.1, 0.3, 0.5, 0.7, and 0.9 mM at various fixed concentrations of AMP: (plus) 0.0 mM, (cross) 3.0 mM, (square) 6.0 mM, (open circle) 9.0 mM, (eye) 12.0 mM. The concentrations of L-aspartate and NH_3 were 1 and 50 mM, respectively. MgCl_2 concentration was as to provide 1 mM excess above ATP and AMP. 7.4 μg of enzyme per assay was used.

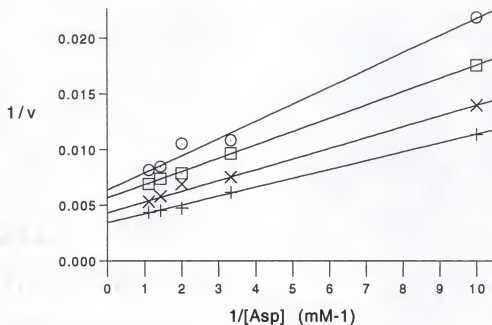


Fig. 3.16 Double-reciprocal plot of initial velocity versus L-aspartate concentration at various fixed concentrations of AMP. Each initial velocity is the average of two experiments. The ATP concentrations were 0.1, 0.3, 0.5, 0.7, and 0.9 mM at various fixed concentrations of AMP: (plus) 0.0 mM, (cross) 3.0 mM, (square) 6.0 mM, (open circle) 9.0 mM. The concentrations of ATP and NH_3 were 1 and 50 mM, respectively. MgCl_2 concentration was as to provide 1 mM excess above ATP and AMP. 7.4 μg of enzyme per assay was used.

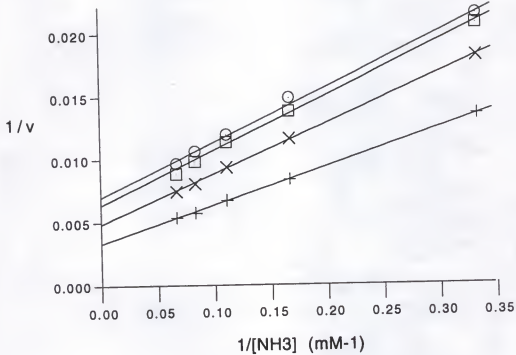


Fig. 3.17 Double-reciprocal plot of initial velocity versus NH_3 concentration at various fixed concentrations of AMP. Each initial velocity is the average of two experiments. The NH_3 concentrations were 3.0, 6.0, 9.0, 12.0, and 15 mM at various fixed concentrations of AMP: (plus) 0.0 mM, (cross) 3.0 mM, (square) 6.0 mM, (open circle) 9.0 mM. The concentrations of ATP and L-aspartate were 1 and 1 mM, respectively. $MgCl_2$ concentration was as to provide 1 mM excess above ATP and AMP. 7.4 μg of enzyme per assay was used.

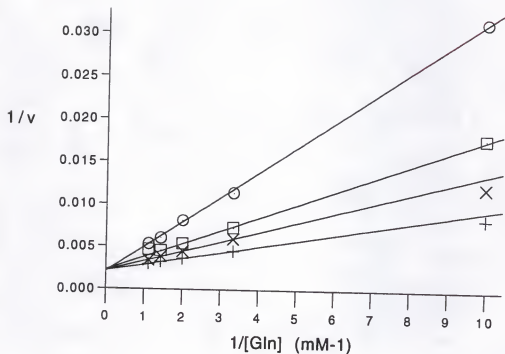


Fig. 3.18 Double-reciprocal plot of initial velocity versus L-glutamine concentration at various fixed concentrations of L-asparagine. Each initial velocity is the average of two experiments. The L-glutamine concentrations were 0.1, 0.3, .05, 0.7 and 0.9 mM at various fixed concentrations of L-asparagine: (plus) 0.0 mM, (cross) 0.05 mM, (square) 0.10 mM, (open circle) 0.15 mM. The concentrations of L-aspartate, ATP and $MgCl_2$ were 1, 1, and 3 mM. 7.4 μg of enzyme per assay was used.

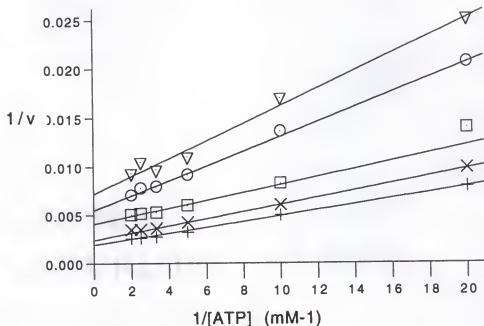


Fig. 3.19 Double-reciprocal plot of initial velocity versus ATP at various fixed concentrations of L-asparagine. Each initial velocity is the average of two experiments. The ATP concentrations were 0.05, 0.1, 0.2, 0.3, 0.4, and 0.5 mM at various fixed concentrations of L-asparagine: (plus) 0.0 mM, (cross) 0.05 mM, (square) 0.10 mM, (open circle) 0.15 mM, (lower triangle) 0.20 mM. The concentrations of L-aspartate, L-glutamine and $MgCl_2$ were 1, 1, and 3 mM. 7.4 μg of enzyme per assay was used.

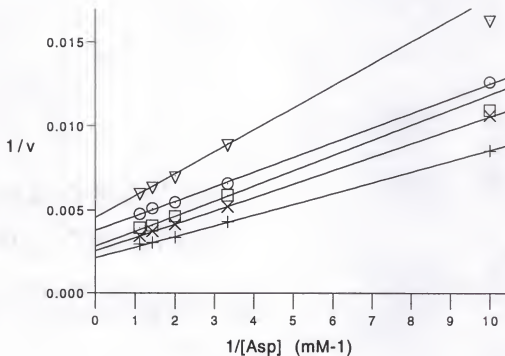


Fig. 3.20 Double-reciprocal plot of initial velocity versus L-aspartate concentration at various fixed concentrations of L-asparagine. Each initial velocity is the average of two experiments. The L-aspartate concentrations were 0.1, 0.3, 0.5, 0.7 and 0.9 mM at various fixed concentrations of L-asparagine: (plus) 0.0 mM, (cross) 0.05 mM, (square) 0.10 mM, (open circle) 0.15 mM, (lower triangle) 0.20 mM. The concentrations of L-glutamine, ATP and $MgCl_2$ were 1, 1, and 3 mM. 7.4 μ g of enzyme per assay was used.

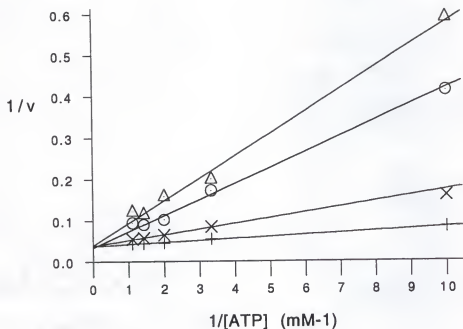


Fig. 3.21 Double-reciprocal plot of initial velocity versus ATP concentration at various fixed concentrations of PPi . Each initial velocity is the average of three experiments. The ATP concentrations were 0.1, 0.3, 0.5, 0.7 and 0.9 mM at various fixed concentrations of PPi : (plus) 0.0 mM, (cross) 0.20 mM, (open circle) 0.60 mM, (upper triangle) 0.80 mM. The concentrations of L-glutamine and L-aspartate were 1 and 1 mM. MgCl_2 concentration was as to provide 1 mM excess above ATP and PPi . 7.4 μg of enzyme per assay was used.

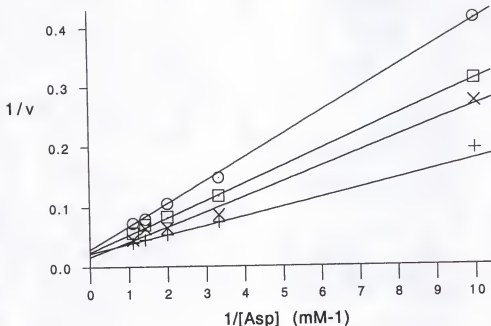


Fig. 3.22 Double-reciprocal plot of initial velocity versus L-aspartate concentration at various fixed concentrations of PPi . Each initial velocity is the average of three experiments. The L-aspartate concentrations were 0.1, 0.3, 0.5, 0.7 and 0.9 mM at various fixed concentrations of PPi : (plus) 0.0 mM, (cross) 0.20 mM, (square) 0.4 mM, (open circle) 0.60 mM. The concentrations of L-glutamine and ATP were 1 and 1 mM. MgCl_2 concentration was as to provide 1 mM excess above ATP and PPi . 7.4 μg of enzyme per assay was used.

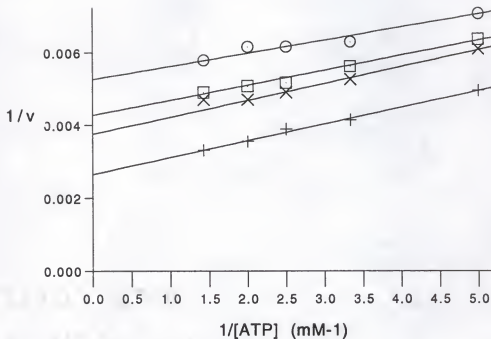


Fig. 3.23 Double-reciprocal plot of initial velocity versus ATP concentration at various fixed concentrations of L-glutamate. Each initial velocity is the average of two experiments. The ATP concentrations were 0.1, 0.2, 0.3, 0.4, 0.5, and 0.7 at various fixed concentrations of L-glutamate: (plus) 0.0 mM, (cross) 15.0 mM, (square) 20.0 mM, (open circle) 40.0 mM. The concentrations of L-glutamine and L-aspartate were 1 and 1 mM, respectively. MgCl_2 concentration was kept constant (3 mM). 7.4 μg of enzyme per assay was used.

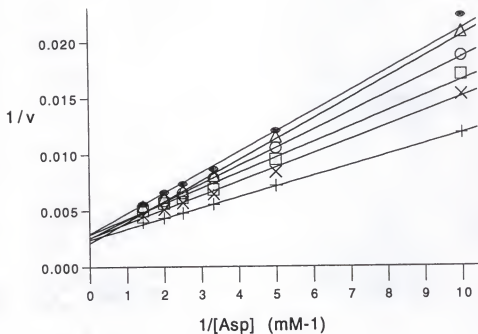


Fig. 3.24 Double-reciprocal plot of initial velocity versus L-aspartate concentration at various fixed concentrations of L-glutamate. Each initial velocity is the average of two experiments. The L-aspartate concentrations were 0.1, 0.2, 0.3, 0.4, 0.5, and 0.7 mM at various fixed concentrations of L-glutamate: (plus) 0.0 mM, (cross) 5.0, (square) 10.0, (open circle) 15.0 mM, (upper triangle) 20.0 mM, (eye) 30.0 mM. The concentrations of L-glutamine and ATP were 1 and 1 mM, respectively. $MgCl_2$ concentration was kept constant (3 mM). 7.4 μg of enzyme per assay was used.

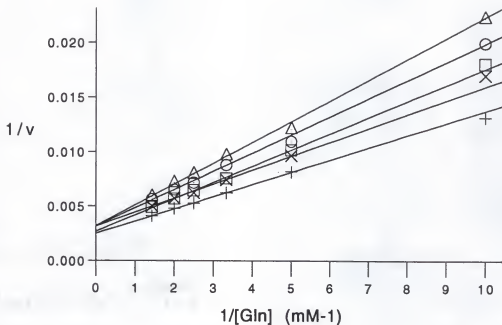


Fig. 3.25 Double-reciprocal plot of initial velocity versus L-glutamine concentration at various fixed concentrations of L-glutamate. Each initial velocity is the average of two experiments. The L-glutamine concentrations were 0.1, 0.2, 0.3, 0.4, 0.5, and 0.7 at various fixed concentrations of L-glutamate: (plus) 0.0 mM, (cross) 10.0, (square) 20.0, (open circle) 30.0 mM, (Δ) 40.0 mM. The concentrations of L-aspartate and ATP were 1 and 1 mM, respectively. $MgCl_2$ concentration was kept constant (3 mM). 7.4 μg of enzyme per assay was used.

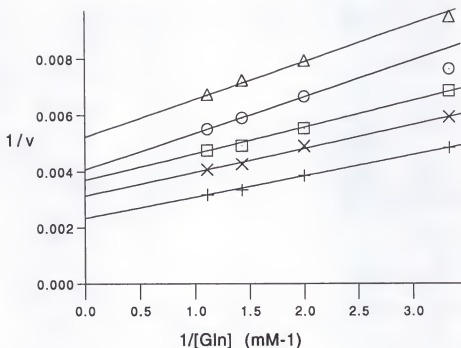


Fig. 3.26 Double-reciprocal plot of initial velocity versus L-glutamine concentration at various fixed concentrations of AMP. Each initial velocity is the average of two experiments. The L-glutamine concentrations were 0.1, 0.3, 0.5, 0.7 and 0.9 mM at various fixed concentrations of AMP: (plus) 0.0 mM, (cross) 3.0, (square) 6.0, (open circle) 9.0 mM, (upper triangle) 12.0 mM. The concentrations of L-aspartate and ATP were 1 and 1 mM, respectively. MgCl_2 concentration was as to provide 1 mM excess above ATP and AMP. 7.4 μg of enzyme per assay was used.

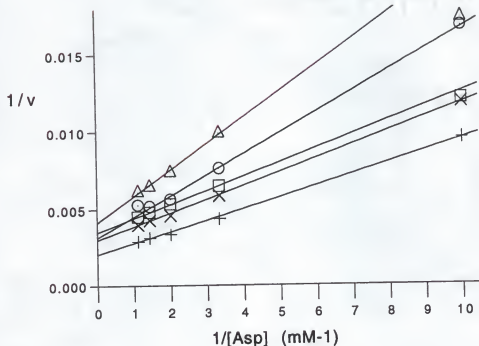


Fig. 3.27 Double-reciprocal plot of initial velocity versus L-aspartate concentration at various fixed concentrations of AMP. Each initial velocity is the average of two experiments. The L-aspartate concentrations were 0.1, 0.3, 0.5, 0.7 and 0.9 mM at various fixed concentrations of AMP: (plus) 0.0 mM, (cross) 3.0, (square) 6.0, (open circle) 9.0 mM, (upper triangle) 12.0 mM. The concentrations of L-glutamine and ATP were 1 and 1 mM. $MgCl_2$ concentration was as to provide 1 mM excess above ATP and AMP. 7.4 μg of enzyme per assay was used.

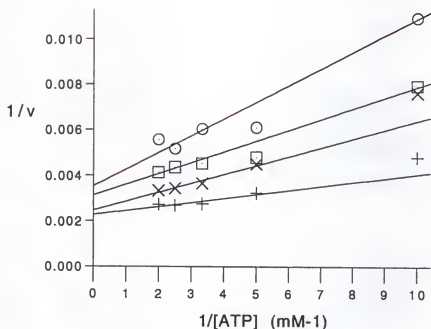


Fig. 3.28 Double-reciprocal plot of initial velocity versus ATP concentration at various fixed concentrations of AMP. Each initial velocity is the average of two experiments. The ATP concentrations were 0.1, 0.2, 0.3, 0.4, 0.5, mM at various fixed concentrations of AMP: (plus) 0.0 mM, (cross) 3.0, (square) 6.0, (open circle) 12.0 mM. The concentrations of L-aspartate and L-glutamine were 1 and 1 mM, respectively. MgCl_2 concentration was as to provide 1 mM excess above ATP and AMP. 7.4 μg of enzyme per assay was used.

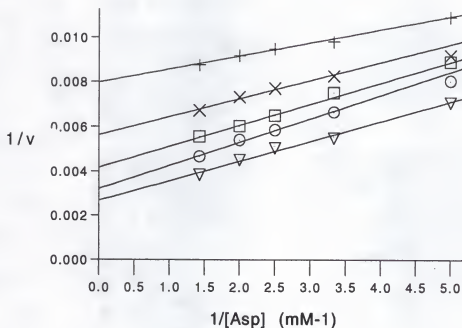


Fig. 3.29 Double-reciprocal plot of initial velocity versus L-aspartate concentration at various fixed concentrations of L-glutamine in the presence of L-glutamate (50 mM). Each initial velocity is the average of two experiments. The L-aspartate concentrations were 0.1, 0.2, 0.3, 0.5, and 0.7 mM at various fixed concentrations of L-glutamine: (plus) 0.1 mM, (cross) 0.2 mM, (square) 0.3 mM, (open circle) 0.4 mM, (lower triangle) 0.7 mM. The concentrations of ATP and $MgCl_2$ were 1 and 3 mM, respectively. 7.4 μg of enzyme per assay was used.

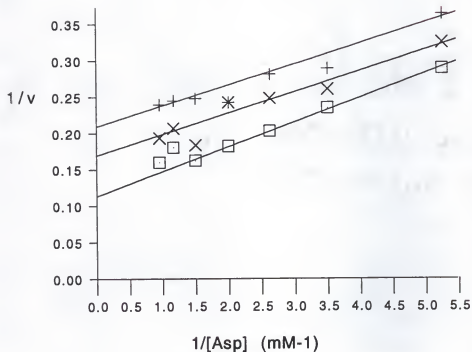


Fig. 3.30 Double-reciprocal plot of initial velocity versus L-aspartate concentration at various fixed concentrations of L-glutamine in the presence of PP_i (0.4 mM). Each initial velocity is the average of two experiments. The L-aspartate concentrations were 0.2, 0.3, 0.4, 0.5, 0.7 mM, 0.9 and 1.1 mM at various fixed concentrations of L-glutamine: (plus) 0.2 mM, (cross) 0.3 mM, (square) 0.4 mM. The concentrations of ATP and $MgCl_2$ were 1 and 3 mM, respectively. 7.4 μ g of enzyme per assay was

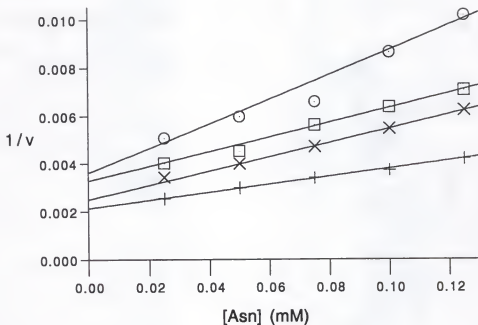


Fig. 3.31 Double inhibition studies plot of L-asparagine concentration versus reciprocal initial velocity at various fixed concentrations of AMP. Each initial velocity is the average of two experiments. The L-asparagine concentrations were 0, 0.025, 0.05, 0.075, 0.1, and 0.125 mM at various fixed concentrations of AMP: (plus) 0.0, (cross) 3.0 mM, (square) 9.0 mM, (open circle) 18.0 mM. The ATP, L-aspartate, and L-glutamine were all kept constant and subsaturating (1 mM). $MgCl_2$ concentration was as to provide 1 mM in excess of total nucleotide concentrations. 7.4 μ g of enzyme per assay was used.

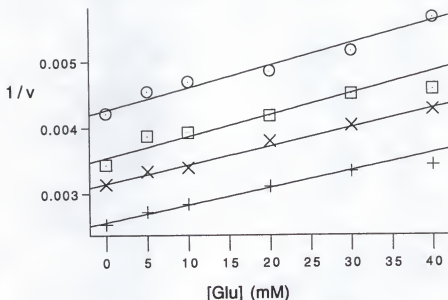


Fig. 3.32 Double inhibition studies plot of L-glutamate concentration versus reciprocal initial velocity at various fixed concentrations of AMP. Each initial velocity is the average of two experiments. The L-glutamate concentrations were 0, 5.0, 10.0, 20.0, 30.0, and 40.0 mM at various fixed concentrations of AMP: (plus) 0.0, (cross) 3.0 mM; (square) 9.0 mM, (open circle) 18.0 mM. The ATP, L-aspartate, and L-glutamine were all kept constant and subsaturating. MgCl_2 concentration was as to provide 1 mM in excess of total nucleotide concentrations. 7.4 μg of enzyme per assay was used.

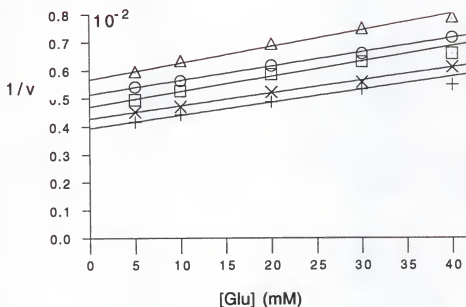


Fig. 3.33 Double inhibition studies plot of L-glutamate concentration versus reciprocal initial velocity at various fixed concentrations of L-asparagine. Each initial velocity is the average of two experiments. The L-glutamate concentrations were 0, 5.0, 10.0, 20.0, 30.0, and 40.0 mM at various fixed concentrations of L-asparagine: (plus) 0, (cross) 0.025 mM, (square) 0.05 mM, (open circle) 0.075 mM, and (upper triangle) 0.1 mM. The ATP, L-aspartate, and L-glutamine were all kept constant and subsaturating. MgCl_2 concentration was maintained at 3 mM. 7.4 μg of enzyme per assay was used.

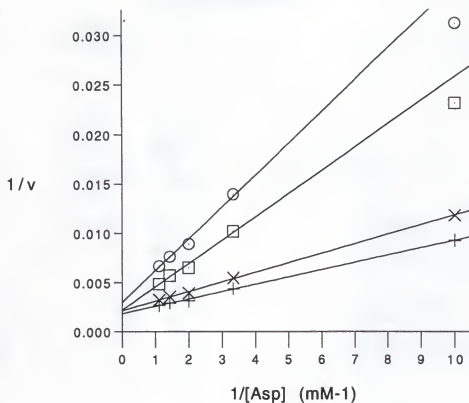


Fig. 3.34 Double-reciprocal plot of initial velocity versus L-aspartate concentration at fixed varied concentrations of L-glutamate and AMP in a constant ratio ($[L\text{-glutamate}] = 5 [AMP]$). Each initial velocity is the average of two experiments. The L-aspartate concentrations were 0.1, 0.3, 0.5, 0.7 and 0.9 mM at fixed varied concentrations of L-glutamate: (plus) 0.0 mM, (cross) 10.0 mM, (square) 50.0 mM, (open circle) 70.0 mM, and of AMP: (plus) 0.0 mM, (cross) 2.0 mM, (square) 10.0 mM, (open circle) 14.0 mM at a fixed ration (5). The concentrations of ATP and L-glutamine were 1 and 1 mM, respectively. $MgCl_2$ concentration was as to provide 1 mM in excess of total nucleotide concentrations. 7.4 μg of enzyme per assay was used.

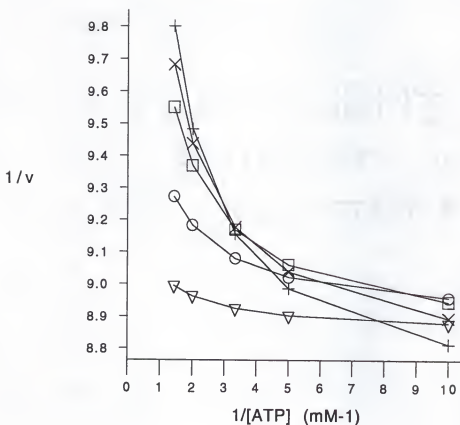


Fig. 3.35. Double-reciprocal plot of initial velocity versus ATP concentration at various fixed concentrations of L-aspartate. This plot was generated by the Quatro program using equation 25, derived to fit the complex mechanism (Scheme D). The ATP concentrations were assumed to be 0.1, 0.2, 0.3, 0.5, and 0.7 mM at various fixed concentrations of L-aspartate: (plus) 0.1 mM, (cross) 0.2 mM, (square) 0.3 mM, (open circle) 0.5 mM, (lower triangle) 0.7 mM. The concentration of L-glutamine was maintained at 1 mM. All k_s' were assumed to be equal to 1.

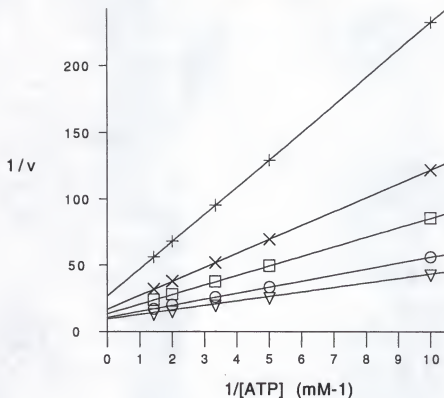


Fig. 3.36. Double-reciprocal plot of initial velocity versus ATP concentration at various fixed concentrations of L-aspartate. This plot was generated by the Quatro program using equation 25, derived to fit the complex mechanism (Scheme D). The ATP concentrations were assumed to be 0.1, 0.2, 0.3, 0.5, and 0.7 mM at various fixed concentrations of L-aspartate: (plus) 0.1 mM, (cross) 0.2 mM, (square) 0.3 mM, (open circle) 0.5 mM, (lower triangle) 0.7 mM. The concentration of L-glutamine was maintained at 1 mM. All k_s' with exception of k_{15} were assumed to be equal to 1. k_{15} (k_{on} for L-glutamine for the side reaction) was assumed to be equal to 0.

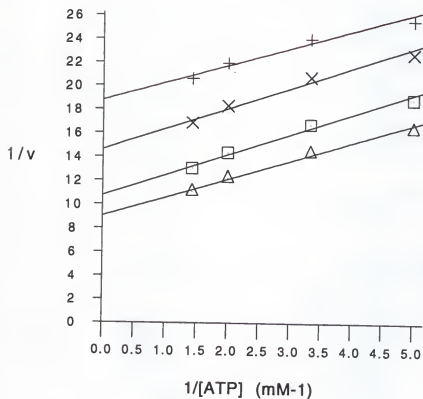


Fig. 3.37. Double-reciprocal plot of initial velocity versus ATP concentration at various fixed concentrations of L-aspartate. This plot was generated by the Quatro program using equation 25, derived to fit the complex mechanism (Scheme D). The ATP concentrations were assumed to be 0.2, 0.3, 0.5, and 0.7 mM at various fixed concentrations of L-aspartate: (plus) 0.2 mM, (cross) 0.3 mM, (square) 0.5 mM, (upper triangle) 0.7 mM. The concentration of L-glutamine was maintained at 20 mM. All k_s' with exception of k_{15} were assumed to be equal to 1. k_{15} (k_{on} for L-glutamine for the side reaction) was assumed to be equal to 0.004.

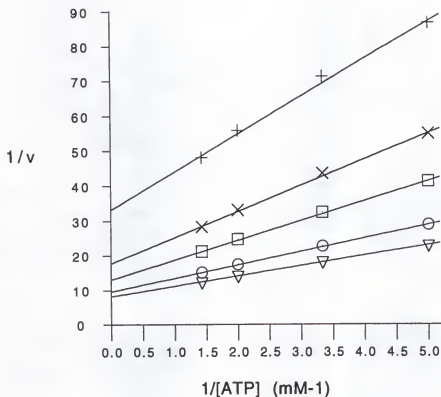


Fig. 3.38 Double-reciprocal plot of initial velocity versus ATP concentration at various fixed concentrations of L-aspartate. This plot was generated by the Quatro program using equation 25, derived to fit the complex mechanism (Scheme D). The ATP concentrations were assumed to be 0.2, 0.3, 0.5, and 0.7 mM at various fixed concentrations of L-aspartate: (plus) 0.1 mM, (cross) 0.2 mM, (square) 0.3 mM, (open circle) 0.5 mM, (lower triangle) 0.7 mM. The concentration of L-glutamine was maintained at 5 mM. All k_s' with exception of k_{15} were assumed to be equal to 1. k_{15} (k_{on} for L-glutamine for the side reaction) was assumed to be equal to 0.002.

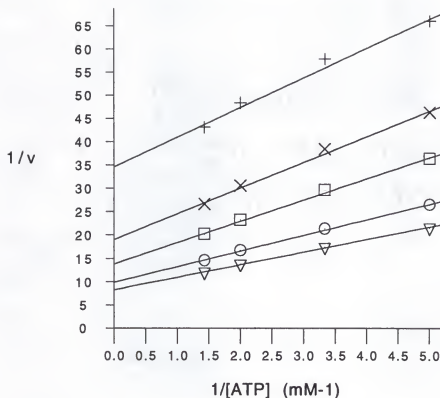


Fig. 3.39 Double-reciprocal plot of initial velocity versus ATP concentration at various fixed concentrations of L-aspartate. This plot was generated by the Quatro program using equation 25, derived to fit the complex mechanism (Scheme D). The ATP concentrations were assumed to be 0.2, 0.3, 0.5, and 0.7 mM at various fixed concentrations of L-aspartate: (plus) 0.1 mM, (cross) 0.2 mM, (square) 0.3 mM, (open circle) 0.5 mM, (lower triangle) 0.7 mM. The concentration of L-glutamine was maintained at 10 mM. All k_s' with exception of k_{15} were assumed to be equal to 1. k_{15} (k_{on} for L-glutamine for the side reaction) was assumed to be equal to 0.002.

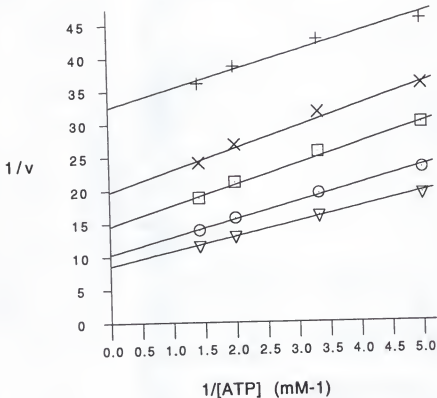


Fig. 3.40 Double-reciprocal plot of initial velocity versus ATP concentration at various fixed concentrations of L-aspartate. This plot was generated by the Quatro program using equation 25, derived to fit the complex mechanism (Scheme D). The ATP concentrations were assumed to be 0.2, 0.3, 0.5, and 0.7 mM at various fixed concentrations of L-aspartate: (plus) 0.1 mM, (cross) 0.2 mM, (square) 0.3 mM, (open circle) 0.5 mM, (lower triangle) 0.7 mM. The concentration of L-glutamine was maintained at 20 mM. All k_s' with exception of k_{15} were assumed to be equal to 1. k_{15} (k_{on} for L-glutamine for the side reaction) was assumed to be equal to 0.002.

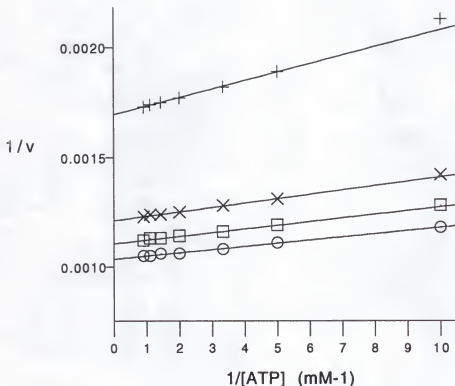


Fig. 3.41 Double-reciprocal plot of initial velocity versus ATP concentration at various fixed concentrations of L-aspartate. This plot was generated by the Quatro program using equation 24, derived to fit the simple mechanism (Scheme A). The ATP concentrations were assumed to be 0.1, 0.2, 0.3, 0.5, 0.7, 0.9 and 1.1 mM at various fixed concentrations of L-aspartate: (plus) 0.1 mM, (cross) 0.2 mM, (square) 0.3 mM, (open circle) 0.5 mM. The concentration of L-glutamine was maintained at 1 mM. All k_s' with exception of k_7 were assumed to be equal to 1. k_{off} for L-glutamate was assumed to be equal to -0.02.

Table 3.1 Inhibition patterns for ASB obtained with β -methyl aspartate, AMP-PNP and L-glutamic acid γ -methyl ester with respect to L-aspartate, ATP and L-glutamine.

Substrates	Analogs	pattern	Kis (mM)	Kii (mM)
ATP	AMP-PNP	C	0.91	-
L-aspartate		NC	5.2	4.5
L-glutamine		UC	-	3.2
ATP	β -methyl aspartate	NC	8.15	15
L-aspartate		C	18	>50
L-glutamine		NC	93	16.5
ATP	L-glutamic acid γ -methyl ester	U	-	10.4
L-aspartate		UC/NC	-	9
L-glutamine		C	6.6	3.2

The velocities were measured spectrophotometrically as described before. Each initial velocity is the average result of two parallel experiments. The assay mixture contained the following components: 100 mM Tris-HCl (pH 8.0), 5.0 mM MgCl₂, and varying amounts of ATP (0.05-0.6 mM), L-aspartate (0.1-1.1 mM), L-glutamine (0.1-0.9 mM). Analogs were varied from 0 to 3.0 mM (β -methyl aspartate), 0 to 4.0 mM (AMP-PNP) and 0 to 5.0 mM (L-glutamic acid γ -methyl ester). The volume of the total reaction mixture was kept at 160 μ l. All reactions were carried out at 37°C, using 5.0 μ g of enzyme per reaction. ^a C = competitive, NC = noncompetitive, and UC = uncompetitive

Table 3.2 Product inhibition data for ammonia-dependent reaction of ASB.

Varied ^a Substrate	Inhibitor	Inhibition Pattern*	K _i (mM)	
			Slope	Intercept
NH ₃	AMP	NC	15 ± 0.002	7 ± 0.001
L-Asp	AMP	NC	8 ± 0.001	11 ± 0.001
ATP	AMP	NC	3 ± 0.001	12 ± 0.001
NH ₃	L-Asn	C	0.08 ± 0.025	-----
L-Asp	L-Asn	NC	0.26 ± 0.002	0.7 ± 0.001
ATP	L-Asn	NC	0.19 ± 0.002	0.15 ± 0.001

The velocities were measured spectrophotometrically as described under Materials and Methods.

^a Other substrates are at saturating constant levels.

* C, competitive; NC, noncompetitive

Table 3.3 Product inhibition data for glutamine-dependent reaction of ASB.

Varied ^a Substrate	Inhibitor	Inhibition Pattern*	K _i (mM)	
			Slope	Intercept
L-Gln	L-Asn	C	0.015 ± 0.003	-----
L-Asp	L-Asn	NC	0.09 ± 0.001	0.25 ± 0.001
ATP	L-Asn	NC	0.27 ± 0.001	0.17 ± 0.002
L-Asp	PP _i	C	0.39 ± 0.01	-----
ATP	PP _i	C	0.05 ± 0.002	-----
L-Gln	AMP	NC	14 ± 0.001	10 ± 0.001
L-Asp	AMP	NC	9 ± 0.001	47 ± 0.001
ATP	AMP	NC	5 ± 0.001	22 ± 0.001
L-Gln	L-Glu	NC	52 ± 0.001	133 ± 0.001
L-Asp	L-Glu	C	23 ± 0.001	-----
ATP	L-Glu	NC	47 ± 0.002	47 ± 0.001

The velocities were measured spectrophotometrically as described under Materials and Methods.

^a Other substrates are at saturating constant levels.

* C, competitive; NC, noncompetitive

CHAPTER 4
EFFECT OF TEMPERATURE ON THE ASPARAGINE SYNTHETASE B

Introduction

The glutamine and ammonia-dependent reactions catalyzed by *E. coli* asparagine synthetase B were studied extensively in the steady-state (Chapters 2 and 3). The reactions were found to occur by an ordered ternary ping-pong mechanism. In this chapter, we present the steady state kinetics of *E. coli* ASB over a range of temperatures. Arrhenius plots were used to detect any changes in the rate limiting steps for the enzyme catalyzed reactions. We wished to determine whether a change in slope of the plot can be detected in either reaction, and whether such a change can be different with glutamine- and ammonia-dependent reactions. In other words, is the rate limiting step different for the ammonia- and glutamine-dependent reactions?

Materials and Methods

Chemicals and Reagents

Trichloroacetic acid (TCA) was purchased from Fisher Scientific (Orlando, FL). The pyrophosphate reagent for following PP_i production, MgCl₂, ATP, L-aspartate, L-

glutamine, ammonium acetate, Tris(hydroxymethyl) aminomethane (Tris-HCl), were all purchased from Sigma. Dithiothreitol (DTT) was obtained from Promega Corporation (Madison, Wisconsin).

Expression of the Protein and Purification

Protein expression, cell culture and enzyme purification was carried out as described before (Chapter 2).

Protein Concentration Determination

Protein concentration was measured using Bio-Rad Protein Assay (Bradford, 1976). Mouse immunoglobulin G was used to obtain a standard curve.

Enzyme Assays

The effect of temperature on the kinetic parameters was investigated with experiments conducted at 0.6, 5, 10, 15, 20, 25, 30, 35, and 40°C. The initial rate assays were carried out at pH 8.0 in 50 mM Tris-HCl. The pH was adjusted at each temperature. The concentration of substrates when varied were 0.1-1.1 mM for ATP, L-aspartate and L-glutamine and 5-40 mM for ammonium acetate. The concentration of the substrates when held constant and saturating were 5 mM, 10 mM, 10 mM and 50 mM for ATP, L-aspartate, L-glutamine and ammonia, respectively. $MgCl_2$ concentration was kept constant (8 mM). A typical assay was performed as follows. To a 80 μ l

reaction mixture containing all the substrates minus the enzyme, preincubated for 3.5 min at desired temperature, 20 μ l of ASB (7.4 μ g) was added to start the reaction. Reactions were terminated by addition of 20% TCA (15 μ l). PP_i production was measured by modifying the continuous spectrophotometric assay (O'Brian, 1976) to an end point assay. In this case, 385 μ l of the coupling buffer (50 mM imidazole, pH not adjusted, and 20 μ l of pyrophosphate reagent, which was originally reconstituted in 1 ml of ddH_2O), was added to the reaction mixtures, following TCA termination, and incubated at room temperature for 30 min. The absorbance of the resulting solution was measured at 340 nm, and the amount of pyrophosphate produced in the reaction determined from a standard curve.

The exact temperature in the reaction mixture was monitored by a thermometer during the experiment. At the highest temperature (40°C) the enzyme was stable during the assay period. All studies were done in duplicates, and V_{max} and K_m were obtained from least-square analyses of the double reciprocal plots of $1/V$ vs $1/[substrate]$ at each temperature.

Thermodynamics of Activation

Activation energies, entropic and enthalpic components at a given temperature were calculated from slopes of plots of log velocity versus $1/T$, using the following equations:

$$\Delta G^* = RT \ln(k_B T/h) - RT \ln(k)$$

$$k = A \exp[-E_a/RT]$$

$$E_a = \Delta H^* + RT$$

$$\Delta G^* = \Delta H^* - T\Delta S^*$$

where K_B is Boltzmann's constant, h is Planck's constant, k is the forward rate constant, E_a^* is the Arrhenius activation energy, A is a constant. The free energy of activation, ΔG^* , is directly related to the reaction rate. The enthalpy of activation, ΔH^* is a measure of the energy barrier that the reacting molecules must overcome. ΔS^* is the entropy of activation.

Results and Discussion

To investigate the effect of temperature upon *E. coli* ASB, initial rates were measured at different temperatures (0-40°C). The Log of maximum steady state velocity was plotted against $1/T$. Our results are shown in Figures 4.1-4.3 for the ammonia-dependent reaction (varying NH_3 , ATP and L-aspartate, respectively) and Figure 4.4 for the glutamine-dependent reactions (varying L-glutamine). In all cases, regardless of what the varied substrate was, straight lines were obtained which suggested that the velocity is controlled by one rate constant over the temperature range. This can also suggest an overall structural change in the protein that is common to both reactions. From the plot of Log V_{max} versus temperature ($1/T$), varying NH_3 , the Arrhenius activation energy was calculated to be 63.3 kJ/mol. The energetic

parameters for the ammonia-dependent reaction, varying NH_3 , were calculated to be (at 37°C) 132 kJ/mol, 61 kJ/mol, and -72 kJ/mol for ΔG^* , ΔH^* , $T\Delta S^*$, respectively. When L-aspartate and ATP were the varied substrates, the energetic parameters calculated from the plots were about the same (not shown). The Arrhenius activation energy for the glutamine-dependent reaction, varying L-glutamine, (at 37°C) was found to be 44.2 kJ/mol, and ΔG^* , ΔH^* and $T\Delta S^*$ were found to be 114 kJ/mol, 42 kJ/mol and -72 kJ/mol, respectively. Similar values were obtained when ATP and L-aspartate were the varied substrates (not shown). As the data show, the entropies of activation are essentially the same for both reactions. On the other hand, the ΔG^* is lower for the glutamine-dependent reaction than for the ammonia-dependent reaction which is essentially enthalpic in nature. This strongly suggests that at the transition state, the electrostatic interaction is more favored in the presence of L-glutamine than in the presence of NH_3 . It is possible that the ASB rigidly holds the L-glutamine in place so that it can attack the aspartyl-AMP intermediate as soon as it is formed. It also possible that ASB by polarizing the glutamine bonds, makes it a better nucleophilic group, lowering the activation energy (Hammes, 1964).

The K_m values for ATP, L-aspartate and L-glutamine did not change with temperature for ammonia- and glutamine-dependent reactions. This suggests that the energy in ΔG° is from $T\Delta S^\circ$ (100%). However, the K_m is the sum of rate

constants (Chapter 2), and no information regarding the effect of temperature on these rate constants is available at this time.

Based on the data presented in Chapter 1 and 2, the glutamine- and ammonia-dependent reactions were found to occur by an ordered ternary ping-pong mechanism. According to the mechanism, ATP and L-aspartate bind first, forming aspartyl-AMP. This is followed by release of P_i (P) and addition of NH_3 or L-glutamine for ammonia- and glutamine-dependent reaction, respectively. Basically, the kinetic mechanism up to the formation of aspartyl-AMP is the same for the two reactions. This suggests that activation energy should be the same for the two reactions up to the formation of aspartyl-AMP. However, our data showed that activation energy was different for ammonia- and glutamine-dependent reactions. This suggests the activation energy that we have measured corresponds to a step following the aspartyl-AMP formation; that is the addition of NH_3 or L-glutamine. The fact that activation energy was lower for glutamine-dependent reaction suggests that L-glutamine binds the enzyme which would in turn polarize the glutamine bonds, making it a better nucleophilic group. This would then attack aspartyl-AMP. NH_3 , however, which is a better nucleophile, cannot bind the enzyme as well, therefore having a higher activation energy.

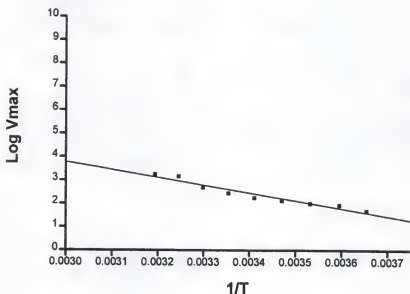


Fig. 4.1. Arrhenius plot of the V_{\max} values for the ammonia-dependent reaction, varying NH_3 concentration. The initial rate assays were carried out at pH 8.0 in 50 mM Tris-HCl. The NH_3 concentration was varied (5-40 mM), while the concentrations of L-aspartate, ATP and MgCl_2 were maintained at 10, 5 and 8 mM, respectively. 7.4 μg of enzyme per assay was used. All studies were done in duplicate, and the data were analyzed by the double reciprocal of $1/V$ vs $1/[\text{NH}_3]$. Velocities, used in the Arrhenius plot, were reported as nmole of L-asparagine produced per minute per milligram of protein.

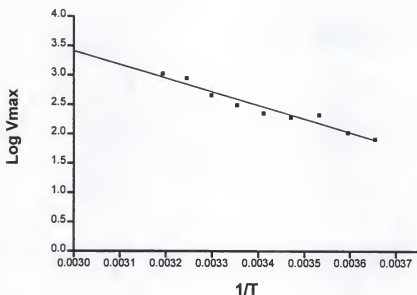


Fig. 4.2. Arrhenius plot of the V_{max} values for the ammonia-dependent reaction, varying ATP concentration. The initial rate assays were carried out at pH 8.0 in 50 mM Tris-HCl. The ATP concentration was varied (0.1.1 mM), while the concentrations of L-aspartate, L-glutamine and MgCl_2 were maintained at 10, 10 and 8 mM, respectively. 7.4 μg of enzyme per assay was used. All studies were done in duplicate, and the data were analyzed by the double reciprocal of $1/V$ vs $1/[\text{ATP}]$. Velocities, used in the Arrhenius plot, were reported as nmole of L-asparagine produced per minute per milligram of protein.

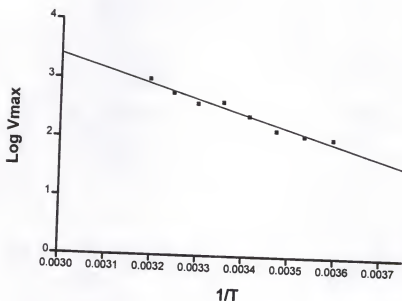


Fig. 4.3. Arrhenius plot of the V_{\max} values for the ammonia-dependent reaction, varying L-aspartate concentration. The initial rate assays were carried out at pH 8.0 in 50 mM Tris-HCl. The L-aspartate concentration was varied (0.1-1.1 mM), while the concentrations of L-aspartate, ATP and $MgCl_2$ were maintained at 10, 5 and 8 mM, respectively. 7.4 μ g of enzyme per assay was used. All studies were done in duplicate, and the data were analyzed by the double reciprocal of $1/V$ vs $1/[L\text{-aspartate}]$. Velocities, used in the Arrhenius plot, were reported as nmole of L-asparagine produced per minute per milligram of protein.

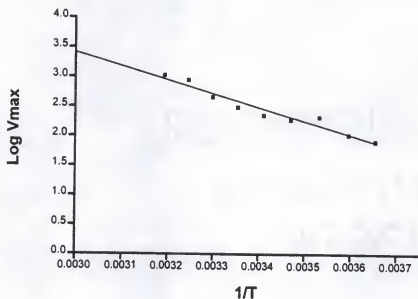


Fig. 4.4. Arrhenius plot of the V_{\max} values for the glutamine-dependent reaction, varying L-glutamine concentration. The initial rate assays were carried out at pH 8.0 in 50 mM Tris-HCl. The L-glutamine concentration was varied (0.1-1.1 mM), while the concentrations of L-aspartate, ATP and $MgCl_2$ were maintained at 10, 5 and 8 mM, respectively. 7.4 μ g of enzyme per assay was used. All studies were done in duplicate, and the data were analyzed by the double reciprocal of $1/V$ vs $1/[L\text{-glutamine}]$. Velocities, used in Arrhenius plot, were reported as nmole of L-asparagine produced per minute per milligram of protein.

Table 4.1 Thermodynamic properties for ammonia- and glutamine-dependent reactions of ASB.

ASB reactions	ΔG^* kJ mol ⁻¹ , (37°C)	ΔH^* kJmol ⁻¹ , (0.5-37°C)	ΔS^* Jmol ⁻¹ K ⁻¹ , (0.5-37°C)	$T\Delta S^*$ kJ mol ⁻¹ , (37°C)
1) NH ₃ + L-Asp + ATP---- L-Asn + AMP + PP _i	132 ± 13	61 ± 6.1	-231 ± 23	-72 ± 7
2) L-gln + L-Asp + ATP---- L-Asn + AMP + PP _i + L-Glu	114 ± 11	42 ± 4	-233 ± 23	-72 ± 7

The initial rates were determined at pH 8.0 in 50 mM Tris-HCl at different assay temperatures (0.6-40°C), under conditions described in materials and methods.

CHAPTER 5

SUMMARY AND CONCLUSIONS

The successful remission of certain types of cancers upon treatment with *E. coli* asparaginase as the chemotherapeutic agent has been correlated to a decreasing concentration of the amino acid L-asparagine. Such observations led to the suggestion that a highly specific and potent inhibitor of asparagine synthetase (AS), the enzyme responsible for synthesis of L-asparagine, might be effective in treating tumors. Therefore, understanding the biosynthesis of L-asparagine is important for the development of AS inhibitors that would otherwise decrease the availability of endogenous L-asparagine. To increase our knowledge of L-asparagine metabolism, the enzyme AS has been investigated from several different sources. Very little information is available regarding the chemical mechanism of AS. Previous studies have clearly indicated that the enzyme utilizes an aspartyl-AMP intermediate. Attempts to define the pathway by which the amide nitrogen is transferred from the L-glutamine to this activated complex in AS have been reported. To date, the most widely accepted mechanistic hypothesis involves the nucleophilic attack upon aspartyl-AMP by ammonia, implying that L-glutamine undergoes hydrolysis (Zalkin et al., 1989). Evidence for this hypothesis was provided by the alignment of the primary sequences of several glutamine-dependent

amidotransferases, including human AS, which revealed the presence of a conserved triad consisting of histidine (His-101), cysteine (Cys-1) and aspartic acid (Asp-29) residues (see Chapter 1). Mutagenesis of these residues resulted in the loss of glutamine- but not ammonia-dependent activity, suggesting that Cys-1 participates in an amide hydrolysis reaction to release ammonia, and His and Asp act as general bases in the reaction. This hypothesis was later challenged by Richards and Schuster (1992). Upon finding that *E. coli* ASB lacks the conserved His residue in the proposed catalytic triad but still exhibits similar specificity to human AS, they suggested a new proposal for the nitrogen transfer mechanism in which glutamine reacts directly with aspartyl-AMP to form an imide intermediate. The reason why this is so important is that if an imide intermediate is formed, it opens numerous possibilities for design of new, potent mechanism-based inhibitors. It was for this reason that the mechanism is important.

The kinetic mechanism of *E. coli* ASB was studied to obtain information about the order of the binding of the substrates and release of products. This was done therefore, to eliminate possible intermediates in the mechanism. For example, if L-glutamate was released prior to the binding of either ATP or L-aspartate, the current mechanistic hypothesis involving the imide intermediate (Richards and Schuster, 1992) would effectively be ruled out.

In chapter 2 of this work the kinetic mechanism of *E. coli* ASB was examined using isotope partitioning. When radioactive L-aspartate was used in the pulse in the presence or absence of L-glutamine (Table 2.1), very little L-Asp* (10%) was trapped as L-Asn*. However, when isotope partitioning experiments were done with ATP in addition to the L-Asp* in the pulse solution, 90% of E-Asp*-ATP was trapped as L-Asn*. The ability to trap radioactive L-aspartate when ATP was included in the pulse solution suggests that the E-Asp*-ATP complex is formed in a catalytically competent manner. When isotope partitioning experiments were done with labeled ATP, in the absence of L-aspartate or L-glutamine (Table 2.2), 50% of the E-ATP* complex was trapped as AMP*. This shows that the E-ATP* complex is formed in a catalytically competent manner, further suggesting that ATP binds free enzyme first. When isotope partitioning experiments were done with L-aspartate in addition to the ATP* in the pulse solution, E-ATP*-Asp was trapped as AMP*. These data suggested that E-ATP*-Asp complex was formed in a catalytically competent manner. The produced AMP* was not stoichiometric with the amount of enzyme present suggesting that ATP hydrolysis was occurring prior to the addition of chase solution. The hydrolysis of ATP was found to be L-aspartate dependent. This partial reaction, although very slow (1/100 of the overall rate), provides a direct evidence for the mechanism of *E. coli* ASB, in which the hydrolysis requires no nitrogen source.

The data presented indicated that for the glutamine-dependent AS reaction, the mechanism is ordered, with ATP binding first to free enzyme. It was also quite clear from the data that the binding and hydrolysis of L-glutamine is not required prior to the addition of ATP and L-aspartate, or no labeled L-asparagine would have been trapped in the absence of L-glutamine. Having said this, it was surprising that when L-glutamine was included in the pulse, about 90% of E-ATP*-Gln was trapped as AMP*, which suggested that an E-ATP*-Gln complex is formed in a catalytically competent manner. No ATP hydrolysis was stimulated by addition of L-glutamine, therefore suggesting that the presence of L-glutamine stabilized ATP binding to the active site because the amount of the AMP* trapped was stoichiometric with the amount of enzyme present.

In the case of ammonia-dependent AS reaction, very little L-Asp* was trapped as L-Asn* when NH₃ was included in the pulse solution with radioactive L-aspartate. The ability of ASB to trap radioactive L-aspartate (70%) when ATP was included in the pulse solution, shows that an E-Asp*-ATP complex is formed in a catalytically competent manner, implying that ATP binds first. On the other hand, when isotope partitioning experiments were done with labeled ATP and NH₃ in the pulse, 20% of the E-ATP*-NH₃ was trapped as AMP*. These data suggested that the NH₃ binding is not required prior to the binding of ATP and L-aspartate or that the level of AMP* or L-Asn* trapped should be close to the

amount of enzyme present. The data also suggest that the mechanism is ordered such that ATP binds first followed by L-aspartate binding.

It is quite obvious from this set of data that the mechanism for both the glutamine- and ammonia-dependent reactions is the same with ATP binding first to the free enzyme and L-aspartate second. This is followed by the release of PP_i . This was further supported by aspartate-dependent ATP hydrolysis that requires no nitrogen source. Our proposed mechanism for ASB is completely different from other proposed mechanisms for AS (Milman et al., 1980, Markin et al., 1981 and Hongo and Sato, 1985) in that the former ones rationalized the ability of AS to behave as a glutaminase. They all agreed that L-glutamine is the first substrate to bind, and L-glutamate is the first product released.

It was important, therefore, to study the kinetic mechanism of ASB using steady state kinetic methods in order to obtain more information about the overall mechanism and to determine whether the difference in the data was associated with using a different enzyme or with the technique employed (Chapter 3). Initial velocity experiments including product inhibition studies were performed. The data were in agreement with a bi-uni-uni-bi ping-pong mechanism (mechanism A), for the ammonia-dependent reaction of ASB (see Chapter 3). This was further supported with the data from isotope trapping experiments showing that the mechanism is ordered and not

random, such that ATP binds first followed by L-aspartate binding (see Chapter 3). However, it was interesting and frustrating at the same time to note that for the glutamine-dependent AS reaction neither one of the mechanisms (A or B) could be ruled out. Alternative substrate studies helped to explain some of the discrepancies that existed between the data presented in the past and this work. The product inhibition studies, single and/or double, provided information as to where some of the products can be placed. We went further and examined other mechanisms, including Milman's, uni-uni-bi-ter ping-pong Theroll-Chance mechanism, none of which fit our data. It became quite clear that steady state kinetics alone could not distinguish between mechanism A (bi-uni-uni-bi ping-pong) from mechanism B (uni-uni-bi-ter ping-pong) for the glutamine-dependent reaction. The results from the isotope trapping experiments, however, indicated that the glutamine-dependent reaction the mechanism was ordered, ATP being first and L-aspartate second. These results together clearly support an ordered bi-uni-uni-ter ping-pong mechanism for the glutamine-dependent reaction of *E. coli* ASB.

The product inhibition studies did not allow us to rule out any of the proposed mechanisms. Yet, they provided information as to where some of the products can be placed in the scheme. The rate equation for the proposed mechanism (Scheme A) was derived assuming the products P, Q, R and S were present, and the predicted product inhibition patterns

were compared with experimental results. There are some disagreements between the predicted patterns and the experimental results. One explanation was the poor ability of AMP and L-glutamate to inhibit the reaction. Another possibility was the existence of an isomerization step following the release of the last product (Scheme C). The results obtained from studies appeared to be compatible with an iso ping-pong mechanism.

Another very important observation made in this work was that the glutaminase reaction was shown to be occurring at the same time as the synthetase reaction, and in fact increasing with increasing concentration of L-glutamine. Such uncoupling of reactions was also reported for AS from leukemia cells (Horowitz and Meister, 1972). They suggested that such uncoupling could be associated with the modification of the enzyme during isolation, for which they offered no evidence. It is also possible that such uncoupling observed with ASB may have something to do with cellular regulatory mechanism of this enzyme.

Based on all these observations we came up with a model for the glutamine-dependent AS reaction. According to our model the reaction mechanism is more complex, and a simple ordered bi-uni-uni-ter ping-pong mechanism would not be applicable to *E. coli* ASB enzyme. We have two different reactions occurring at the same time, asparagine synthetase and glutaminase. The non-stoichiometry observed between formation of L-glutamate and PP_i supports this proposed

model. The results from substrate inhibition studies are also in agreement with the presence of another pathway, that is selected over synthetase when substrate concentration is high. The steady-state initial velocity rate equation for the proposed mechanism (Scheme D) in the absence of products was derived, and computer modeling was used to examine the proposed mechanism through the simulation. We were able to show the change of pattern from intersecting lines to parallel lines using this complex mechanism, further supporting that the proposed mechanism (Scheme D) is right.

Studying the kinetic mechanism allowed us to draw certain conclusions about the order of the binding of the substrates and release of products. It is quite clear that L-glutamate release can occur prior to the formation of aspartyl-AMP. However, the critical question is whether this early release of L-glutamate is required for the synthetase reaction to occur. Our studies showed that (1) the kinetic mechanism for glutamine-dependent reactions is preferentially ordered, with ATP binding first followed by addition of L-aspartate, and that (2) the binding and hydrolysis of L-glutamine is not required prior to the formation of aspartyl-AMP. The kinetic mechanism of ASB is a complex mechanism with two reactions occurring at the same time. Therefore, this makes it difficult to rule out any of the proposed chemical mechanisms.

Furthermore, our examination of K_i 's suggests that the potent inhibitors of AS should be analogs of L-asparagine

which was found to be competitive with L-glutamine ($K_i = 0.015 \text{ mM}$). These inhibitors should not inhibit nor be hydrolyzed by any other enzyme such as asparaginase or asparagine transaminase. In addition, examination of K_m 's suggests that the analogs of L-glutamine would be better inhibitors of AS than that of ATP or L-aspartate. It would be easier to compete off L-glutamine with a K_m of 0.2 mM as compared to that of ATP or L-aspartate ($K_m = 0.05 \text{ mM}$)

The combined studies using steady state and isotope partitioning analysis of ASB demonstrated the importance of relying on both techniques to understand enzymatic reaction mechanisms. It can be seen that an incomplete picture can be obtained from the steady state kinetics alone leading to an incomplete picture for the reactions occurring at the active site. Both approaches, therefore, together provide a more complete view of the kinetic pathway.

LIST OF REFERENCES

- Andrulis, I. L., Chen, J., and Ray, P. N. 1987. Mol. Cell. Biol. 7, 2435-2443
- Arfin, S. M. 1967. Biochem. Biophys. Acta. 136, 233-244
- Barlett, P. A., and Marlowe, C. K. 1983. Biochemistry. 22, 4618-4624
- Boehlein, S. K., Richards, N. G. J., and Schuster, S. M. 1994. J. Biol. Chem. 269, 7450-7457
- Bradford, M. M. 1976. Anal. Biochem. 72, 246-256
- Brent, E., and Bergmeyer, H. U. 1974. In Methods of Enzymatic Analysis. Bergmeyer, H. U., Ed. Academic Press, New York. pp 1704-1708
- Bridger, W. A., Millen, W. A., and Boyer, P. D. 1968. Biochemistry. 7, 3608-3615
- Broome, J. D. 1963. J. Exp. Med. 118, 99-148
- Broome, J. D. 1968. J. Exp. Med. 127, 1055-1072
- Burchall, J. J., Reichelt, E. C., and Wolin, M. J. 1964. J. Biol. Chem. 239, 1794-1798
- Ceder, H., and Schwartz, J. H. 1969a. J. Biol. Chem. 244, 4112-4121
- Ceder, H., and Schwartz, J. H. 1969b. J. Biol. Chem. 244, 4122-4127

- Chou, T. C. 1970. Ph.D. Dissertation, University of Michigan, Ann Arbor, Michigan
- Cleland, W. W. 1983. Contemporary Enzyme Kinetics and Mechanism. Academic Press, New York. Purich, D. ed. Substrate inhibition. pp.253-265
- Coony, D. A., and Handsschumacher, R. E. 1970. Ann. Rev. Pharmacol. 10, 421-440
- Dhalla, A. M., Yanchunas, J. Jr., Ho. Hsu-Tso., Falk. P. J., Villafranca, J. J., and Robertson, J. G. 1995. Biochemistry. 34, 5390-5402
- Dixon, M. 1953. Biochem.J. 55, 170
- Ertel, I. J., Nesbit, M. G., Hammond, D., Weiner, J., and Sather, Harland. 1979. Cancer Research. 39, 3893-3896
- Felton, J., Michaelis. S., and Wright, A. 1980. J. Bactrol. 142, 212-220
- Frieden, C. 1959. J. Biol. Chem. 234, 2891-2896
- Fromm, H. J. 1975. Initial Rate Enzyme Kinetics, Springer-Verlag, New York
- Garces, E., and Cleland, W. W. 1969. Biochemistry. 8, 633-640
- Gruys, K. J., Walker, M. C., and Sikorski, J. A. 1992. Biochemistry. 31, 5534-5544
- Hammes, G. G. 1964. Nature. 204, 342-343
- Hinchman, S. K., Henikoff, Steven., and Schuster, S. M. . 1992. J. Biol. Chem. 267, 144-149

- Hongo, S., Matsumoto, T., and Sato, T. 1978. Biochem. Biophys. Acta. 522, 258-266.
- Hongo, S., and Sato, T. 1985. Arch. Biochem. Biophys. 238, 410-417
- Horowitz, B., and Meister, A. 1972. J. Biol. Chem. 247, 6708-6719
- Humbert, R., and Simoni, R. D. 1980. J. Bacteriol. 142, 212-220
- Katiyar, S. S., Cleland, W. W., and Porter, J. W. 1975. J. Biol. Chem. 250, 2709-2717
- Kidd, J. G. 1953. J. Exp. Med. 98, 565-582
- Krishnaswamy, P. R., and Pamiljans, V., and Meister, A. 1962. J. Biol. Chem. 237, 2932-2940
- Land, V. J., Sutow, W. W., Fernback, D. S., Lane, D. M., and Williams, T. E. 1972. Advanced Leukemia Cancer. 30, 339-347
- Levitzki, A., and Koshland, J. M. 1971. J. Biol. Chem. 246, 4713-4719
- Lewis, D. A., and Villafranca, J. J. 1989. Biochemistry. 28, 8454-8459
- Luehr, C. A., and Schuster, S. M. 1985. Arch. Biochem. Biophys. 237, 335-346
- Markin, R. S., Luehr, C. A., Schuster, S. M. 1981. Biochem. J. 20, 7226-7232
- Mei, B., and Zalkin, H. 1989. J. Biol. Chem. 264, 16613-16619

- Meister, A., Soben, H. A., Tice, S. V., and Frasen, P. E. 1952. J. Biol. Chem. 197, 319-330
- Milman, H. A., Conney, D. A., and Huang, C. L. 1980. J. Biol. Chem. 255, 1862-1866
- Moraga-A, D. A., Kathleen, M., MacPhee-Quigley, K. G., Keefer, J. F., and Schuster, S. M. 1989. Arch. Biochem. Biophys. 268, 314-326
- Nagano, H., Zalkin, H., and Henderson, E. J. 1971. J. Biol. Chem. 245, 3810-3820
- Nakamura, M. A., Yamada, M., Hirota, Y., Sugimoto, K., Oka, A., and Takanami, M. 1981. Nucleic Acid Res. 9, 4669-4676
- O'Brien, W. 1976. Anal. Biochem. 76, 423-425
- Oettgen, H. F., Old, L. J., Boyse, E. A., Campbell, H. A., Philips, F. S., Clarkson, B. D., Tallal, L., Leeper, R. D., Schwartz, M. K., and Kim, J. 1967. Cancer Res. 27, 2619-2631
- Piette, J., Nyunoya, H., Lusty, C. J., Cunin, R., Weyens, G., Crabeel, M., Charlier, D., Glansdroff, N., and Pierard, A. 1984. Proc. Natl. Acad. Sci. U.S.A. 81, 4143-4138
- Ramos, F., and Wiame, J. M. 1979. Eur. J. Biochem. 94, 409-417
- Ramos, F., and Wiame, J. M. 1980. Eur. J. Biochem. 108, 373-377
- Ravel, J. M., Norton, S. J., Humphreys, J. S., and Shive, W. 1962. J. Biol. Chem. 237, 2845-2849
- Reitzer, L. J., Magasanik, B. 1982. J. Bacteriol. 151, 1299-1313

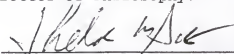
- Richards N. G. J., and Schuster, S. M. 1992. FEBS. 313, 98-102
- Rochovansky, O., and Ratner, S. 1967. J. Biol. Chem. 242, 3839-3840
- Rose, I. A. 1980. Methods enzymol. 64, 47-59.
- Rose, I. A., O'Connell, E., and Litwin, S. 1974. J. Biol. Chem. 249, 5163-5168
- Scofield, M. A., Lewis, W. S, Schuster, S. M. 1990. J. Biol. Chem. 265, 12895-12902
- Segel, I. H. 1987. in Enzyme Kinetics. John Wiley and sons, New York, 2nd ed.
- Sheng, S., Moraga-A, D. A., Van Heeke, G., Allison, R. D., Richards, N. G., and Schuster, S. M. 1993. J. Biol. Chem. 268, 16771-16780
- Spiro, R. G. 1969. New England. J. Med. 281, 991-1000
- Terebello, H. R., Anderson, K., and Wiernik, P. H. 1986. Am. J. Clin. Oncol. 9, 411
- Uren, J. R., Chang, P. K., and Handschumacher, R. E. 1977. Biochem. Pharmacol. 26, 1405-1410
- Uyeda, K. 1970. J. Biol. Chem. 245, 2268-2275
- VanHeeke, G., and Schuster, S. M. 1989. J. Biol. Chem. 264, 19475-19477
- Vauquelin, L. N., and Robiquet, P. I. 1806. Ann. Chem., paris. 57, 88-93
- Walker, J. E., Gay, N. J., Sarate, M., and Eberle, A. N. 1984. Biochem. J. 224, 799-815

- Weng, M., Makaroff, C. A., and Zalkin, H. 1986. J. Biol. Chem. 261, 5568-5574
- Weng, M., and Zalkin, H. 1987. J. Bacteriol. 169, 3023-3028
- Wilkinson, K. D., and Rose, I. A. 1979. J. Biol. Chem. 254, 12567-12572
- Wilkinson, K. D., and Rose, I. A. 1981. J. Biol. Chem. 256, 9890-9894
- Zalkin, H., and Truit, C. D. 1977. J. Biol. Chem. 252, 5431-5436

BIOGRAPHICAL SKETCH

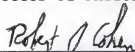
I, Pouran H-Tari, was born June of 1960 in Tehran, Iran. I got married the summer of 1978 and came to the United States. I lived in Sacramento for 3.5 years. Then I moved to Fresno and graduated in 1983 with a BA degree in biology from California State University. I then moved to Utah where I completed my master's degree in biological science with an emphasis in plant pathology from Utah State University, in Logan. I then went to work for a company called Gull Laboratory in Salt Lake City. In August of 1988, I moved to Gainesville, Florida. For one year I worked in protein core, after which I joined the Department of Biochemistry and Molecular Biology. I joined Dr. Schuster's laboratory the summer of 1990. I gave birth to my daughter Maryam on May 9, 1992. I will receive my Ph.D. summer of 1996, after which I will go back home, to Tehran. I would stay there several months to relax and spend time with my daughter and my family.

I certify that I have read this study and that in my opinion it conforms to acceptable standards of scholarly presentation and is fully adequate, in scope and quality, as a dissertation for the degree of Doctor of Philosophy.



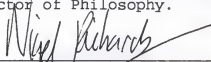
Sheldon M. Schuster, Chair
Professor of Biochemistry
and Molecular Biology

I certify that I have read this study and that in my opinion it conforms to acceptable standards of scholarly presentation and is fully adequate, in scope and quality, as a dissertation for the degree of Doctor of Philosophy.



Robert J. Cohen
Associate Professor of
Biochemistry and Molecular
Biology

I certify that I have read this study and that in my opinion it conforms to acceptable standards of scholarly presentation and is fully adequate, in scope and quality, as a dissertation for the degree of Doctor of Philosophy.



Nigel G. Richards
Assistant Professor of
Chemistry

I certify that I have read this study and that in my opinion it conforms to acceptable standards of scholarly presentation and is fully adequate, in scope and quality, as a dissertation for the degree of Doctor of Philosophy.



Brian D. Cain
Associate Professor of
Biochemistry and Molecular
Biology

I certify that I have read this study and that in my opinion it conforms to acceptable standards of scholarly presentation and is fully adequate, in scope and quality, as a dissertation for the degree of Doctor of Philosophy.

Ben M. Dunn

Ben M. Dunn
Professor of Biochemistry
and Molecular Biology

This dissertation was submitted to the Graduate Faculty of the College of Medicine and to the Graduate School and was accepted as partial fulfillment of the requirements for the degree of Doctor of Philosophy.

August 1996

Mohan K. Raine
Dean, College of Medicine

Kenneth G. Holbrook
Dean, Graduate School

UNIVERSITY OF FLORIDA



3 1262 08554 7379